COURSE 1

UNIVERSALITIES: FROM ANDERSON LOCALIZATION TO QUANTUM CHAOS

BORIS L. ALTSHULER AND B. D. SIMONS

Massachusetts Institute of Technology
77, Massachusetts Avenue
Cambridge, MA 02139
USA

and

NEC Research Institute, Inc.
4, Independence Way
Princeton, NJ 08540
USA

photograph of lecturer

Contents

1. Introduction

The problem of quantum localization of a particle in a random potential first raised by Anderson [1] has proven to be surprisingly rich. In spite of the collective effects of a considerable number of scholars the problems associated with Anderson localization are still not exhausted and the subject continues to generate new ideas. As a result of past developments there are now rather elegant and sophisticated theoretical constructions and a good understanding of certain experimental aspects of the problem. At the same time there remains a number of well formulated outstanding problems.

The goal of this course is to create a guide for a student or physicist from outside the field that would enable them to become acquainted with the basic concepts and ideas without going through too many theoretical details. In doing so we have concentrated on developments which occurred after 1979 when the scaling theory of localization was proposed. The wide scope of this review does not allow us to make a very comprehensive and detailed discussion. At the same time we have attempted to make the material useful from a theoretical point of view and have tried to highlight the important technical developments and difficulties. However, we hope that these lectures complement the existing full scale reviews which contain more material than a first-time reader can perhaps appreciate. Throughout the course we have tried to point out sources where more information can be found. Very often these sources are not the original papers and therefore we must apologize for the incompleteness of our list of references. Perhaps the most complete list of references in this field can be found in the review of Kramer and MacKinnon [2]. Considering this course as part of a whole book we have completely omitted critical discussion of the experimental situation, and instead have restricted ourselves to the mention of only the most illustrative experiments.

We begin with a brief introduction to the concept of impurity bands in metals. The following chapter is devoted to a qualitative description of the interplay between quantum interference and disorder. In section 3 we discuss the basic arguments in favor of the scaling theory of localization and its major consequences. Section 4 is concerned with the study of the set of phenomena known collectively as weak localization. We address corrections to the conductivity and other physical processes due to quantum interference and interaction between electrons in disordered conductors. The discussion is based on diagrammatic perturbation theory. Sections 5 and 6 discuss the effective field theory of disordered metals and the metal-insulator transition. We have chosen the supersymmetric version of this approach since most of the very recent developments have been made using this technique. In the remainder of the course we apply the knowledge developed in the study of disordered conductors to the general problem of quantum chaos. In view the novelty of this developing field we have taken the liberty of making the discussion somewhat more technical and less qualitative than the previous sections. Nevertheless, we hope that the important results remain easily accessible.

Before beginning our discussion we wish to acknowledge A. V. Andreev, D. E. Khmelnitskii, and N. Taniguchi for helping to make this manuscript more readable.

1.1. Impurity States

We begin by recalling the behavior of a single electron in a solid. In a perfect crystalline potential the energy levels broaden into bands of Bloch states which obey the Schrödinger equation $\hat{H}(\boldsymbol{p})\psi_0(\boldsymbol{r}) = E(\boldsymbol{p})\psi_0(\boldsymbol{r})$ where, for free electrons, the Hamiltonian $\hat{H}(\boldsymbol{p}) = \hat{\boldsymbol{p}}^2/2m$.* In these lectures we will be concerned with how states are modified by the presence of a disorder potential, $V(\boldsymbol{r})$ which can originate from a variety of sources such as defects, impurities, composition, dislocations, or vacancies.

$$\left[\hat{H}(\boldsymbol{p}) + V(\boldsymbol{r})\right]\psi_\alpha(\boldsymbol{r}) = E_\alpha\psi_\alpha(\boldsymbol{r}). \tag{1.1}$$

We will focus on the electronic properties of materials in which the configuration of the disorder potential is frozen or "quenched." Such an assumption is justified when the typical time scale for the migration of defects is much slower than the electron dynamics. The different impurity configurations form a statistical ensemble from which it is possible to define averages.

To illustrate the very basic ideas let us recall the electronic properties of semiconductors. In clean crystalline semiconductors the electronic Fermi level lies in a gap between a filled valence band and an empty conduction

* Here, and except for some final expressions, we take $\hbar = 1$

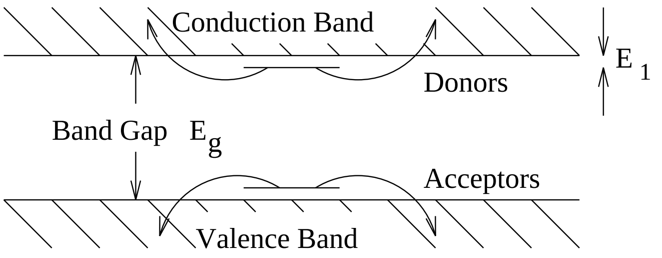

Fig. 1. Donor and acceptor levels in a semi-conducting band structure.

band. As a result, electrons are confined to the valence band by a gap in energy E_g and the low temperature properties are insulating. However, at temperatures $kT \sim E_g$, a substantial number of electrons occupy states in the conduction band.

The addition of impurities which provide states in the band gap can modify this picture drastically. In particular, impurity states with energies that lie just below the bottom of the conduction band (donors) can donate electrons to this band even at $kT \ll E_g$; impurities that create vacant electronic states just above the top of the valence band (acceptors) attract electrons and create holes in the band again at temperatures $kT \ll E_g$ (see fig. 1). This situation is realized by single impurity states with radii large in comparison to the bare lattice constant, and therefore with an energy small as compared to E_g.

An estimate of the effective ionization energy for a single impurity center with change $\mathcal{Z}e$ can be found from the effective Schrödinger equation

$$\Big[-\frac{\hbar^2}{2m}\boldsymbol{\nabla}^2-\frac{\mathcal{Z}e^2}{\kappa r}\Big]\Psi(r)=E\Psi(r), \tag{1.2}$$

where m denotes the effective mass, and κ the dielectric constant. The energy spectrum is hydrogenic with

$$E_\alpha=-\frac{e^2}{a^2\alpha^2}=-\frac{13.6\text{eV}}{\alpha^2}\Big(\frac{m}{m_0\kappa^2}\Big), \qquad \alpha=1,2,\cdots \tag{1.3}$$

where $a=\kappa\hbar^2/m\mathcal{Z}e^2=0.53\mathring{A}\ (\kappa m_0/m)$ denotes the effective Bohr radius. This formula is correct when $E_\alpha \ll E_g$, and $a \gg a_B = 0.53\mathring{A}$ which implies that $\kappa m_0/m \gg 1$. For GaAs $\kappa=12.5$, $m=0.066m_0$, $a=190a_B=100\mathring{A}$, and $E_1=5.67\text{meV}\approx 60K$. Similarly, for Si and Ge the ionization energy is $E_1=5.8\text{meV}$ and 6.1meV respectively. Therefore, for $T \geqslant 60K$ the conduction band is heavily occupied, while for $T \ll 60K$ and light enough doping nearly all the donor electrons are confined to the impurity sites.

For a single impurity the ground state wavefunction is localized and decays exponentially into the bulk, $\psi_0(|\boldsymbol{r}|) = (\sqrt{\pi a^3}/|\boldsymbol{r}|)\exp[-|\boldsymbol{r}|/a]$. As a result, at $kT \ll E_1$ the system should display insulating behavior. For a finite concentration of impurities, $N_{\rm imp}$ there is a weak but finite exponential overlap of different wavefunctions. This overlap can in principle delocalize the wavefunctions. If this happens the material is metallic, i.e. it has non-zero conductivity at $T = 0$.

1.2. Impurity Bands

For a vanishingly small impurity concentration $N_{\rm imp} \to 0$, the overlap of different impurity centers can be neglected and the total wavefunction can be expressed as the sum of degenerate states, $\Psi(\boldsymbol{r}) = \sum_\alpha A_\alpha \psi(\boldsymbol{r} - \boldsymbol{r}_\alpha)$. Since a is typically large as compared with the lattice spacing even a weak impurity concentration can generate substantial overlap of the states. As a consequence, levels are split and the states broaden into impurity bands. However, the underlying disorder causes the band to behave in a manner very different from bands formed by a regular crystalline lattice.

In discussing the properties of disordered metals the nature of the spectrum will play an important role. Consider the density of states (DoS)

$$\nu(E) = \frac{1}{L^d}\sum_\alpha \delta(E - E_\alpha), \tag{1.4}$$

where L^d denotes the volume and E_α labels the eigenenergies of the band. In a crystal, the quantum numbers are labeled by the crystal momentum and band index, $\alpha = \{\boldsymbol{p}, n\}$. If the DoS is constant in momentum space, then

$$\nu(E) = s\sum_n \int (\,\mathrm{d}p)\; \delta(E - E_n(\boldsymbol{p})), \tag{1.5}$$

where the factor of s accounts for spin-degeneracy. (Hereafter we adopt the shorthand $(\,\mathrm{d}p) = \mathrm{d}\boldsymbol{p}/(2\pi)^d$.) In three dimensions the DoS can be evaluated for free electrons giving $\nu(E) = (s/2\pi^2)mp_E$, where $p_E = \sqrt{2mE}$. The square root van Hove singularities of the DoS is a generic feature of *clean* three-dimensional systems.

In a first approximation, the impurity band can be modeled as donors forming a superlattice with spacing $b = N_{\rm imp}^{-1/d}$. This compares with the effective Bohr radius a which sets the characteristic size of the impurity states. The degree of overlap between the different impurities depends on the dimensionless parameter $N_{\rm imp}a^d = (a/b)^d$. For $N_{\rm imp}a^d \ll 1$ there is an exponentially small overlap between the wavefunctions and the states are stable towards delocalization. For $N_{\rm imp}a^d \geqslant 1$ different wavefunctions become strongly overlapping and extended.

For small overlap, it suffices to consider the interaction between nearest neighbors. The total wavefunction is given by the superposition of different impurities, $\Psi(\boldsymbol{r}) = \sum_i A_i \psi(\boldsymbol{r} - \boldsymbol{r}_i)$ with $\sum_i |A_i|^2 = 1$. The total energy is given by $E = E_1 \sum_i |A_i|^2 + I \sum_{\langle ij \rangle} A_i A_j^*$ where $I \propto \mathrm{e}^{-b/a}$ represents the overlap integral and $\langle ij \rangle$ denotes nearest neighbors. Expressed in second quantized notation, the tight-binding Hamiltonian for the impurity band can be written as

$$H = E_1 \sum_i c_i^\dagger c_i + I \sum_{\langle ij \rangle} c_i^\dagger c_j, \tag{1.6}$$

where $c_i^\dagger$ and c_i denote operators that create and annihilate electrons at site i, and for simplicity spin indices are suppressed. The Hamiltonian is diagonalized by the Bloch transformation $A_i = N_{\rm imp}^{-1/2} \exp[\mathrm{i}\boldsymbol{p} \cdot \boldsymbol{r}_i]$, and the spectrum obeys the dispersion relation $E(\boldsymbol{p}) = E_1 + 2I[\cos(bp_x) + \cos(bp_y) + \cos(bp_z)]$. The width of the impurity band $W_{\rm im} = 12I \propto \exp[-b/a]$ decreases exponentially fast with the dimensionless parameter while the effective mass $m_{\rm eff} = 1/2b^2 I \propto (1/b^2)\exp[b/a]$ increases. For one electron per impurity the resulting band is exactly half-filled and metallic.

However, this metallic phase is untenable for the following reasons: Firstly the band is exponentially narrow giving rise to very long tunnelling time between impurity centers. As a consequence the electron motion becomes quickly dephased. Secondly strong Coulomb interaction between electrons can lead to a Mott-Hubbard metal-insulator transition in which a gap in energy of order $e^2/\kappa a$ opens at the Fermi level [3]. In these lectures we will not consider the question of interaction and the Mott-Hubbard transition. Instead we will focus on the third manner in which metallic behavior can be destroyed — disorder.

1.3. Anderson Model

In its present form, Eq. (1.6) is too naive. The model suggests that however small the bandwidth all states are extended. More than 30 years ago, Anderson proposed a variant of the tight-binding model which incorporates disorder and admits the possibility of a transition to localization [1]. Since then this model has stood as a paradigm for a single-particle description

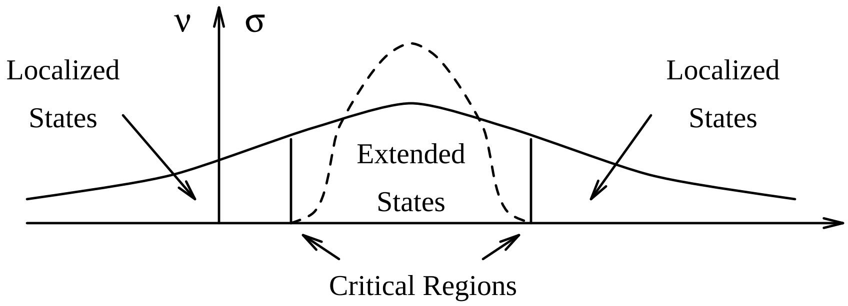

Fig. 2. Schematic diagram showing the variation of the DoS ν (solid line), and conductivity σ (dashed line) as a function of energy. Note that the DoS does not show singular behavior at the mobility edge while the conductance vanishes.

of disordered electronic systems. The Anderson model has the form

$$H = \sum_i W_i \, c_i^\dagger c_i + \sum_{ij} I_{ij} \, c_i^\dagger c_j , \tag{1.7}$$

where, in principle, both W_i and I_{ij} are random. In his original paper, Anderson proposed a model in which non-zero elements $I_{ij} = I$ occurred only for nearest neighbors ij, and W_i was chosen randomly from the interval $[-W/2, W/2]$. An alternative to this model was studied by Lloyd in which the elements W_i are chosen from the Cauchy distribution, $P(W_i) = W/(W_i^2 + W^2)$. Finally Lifshitz [4] studied a model in which disorder was incorporated in the off-diagonal elements alone.

The Anderson model has two characteristic energy scales, I and W which can be combined into the dimensionless ratio, W/I. For W/I larger than some critical value $(W/I)_c$ Anderson proposed that all states are localized. Below this value there is a mobility edge and all states are extended (see fig. 2). In the vicinity of the critical region the conductivity falls rapidly to zero, whereas the DoS shows no critical behavior. In particular, there are no square-root singularities either at the band edge or at the mobility edge. Instead, the there is a gradual decay of the DoS into localized tail states.

The nature of the tail states can be considered by invoking an argument due to Lifshitz [4] based on "optimal fluctuations." Suppose all "on-site" energies take the minimum value, $W_i = -W/2$. In this case the edge of the spectrum is bounded at $E_e = -W/2 - 12I$. The DoS close to the band edge, $\nu(E = E_e + \delta E)$ is dominated by states strongly localized in regions of size L where the on-site energies are anomalously small. The typical number of sites in such regions is $N = (L/b)^3$, and the energy of the states there differ from E_e only by the quantum zero point energy $\delta E \sim I/mL^2$. The typical number of states at energy $E_e + \delta E$ is therefore given by $N = (\delta E/I)^{-3/2}$. Taking the probability of finding N sites with on-site energies within a width I of $-W/2$ to be $P(N) = (I/W)^N$, the DoS can be estimated,

$$\frac{\nu(E_e + \delta E)}{\delta E} \sim N_{\rm imp} \left(\frac{I}{\delta E}\right)^{5/2} \exp\left[-\left(\frac{I}{\delta E}\right)^{3/2} \ln\left(\frac{W}{I}\right)\right]. \tag{1.8}$$

The van Hove singularities present in the clean system are destroyed by disorder and replaced by an exponential decay. This simple argument, generalizes to dimension d with $\nu(E_e + \delta) \sim \exp[\text{Const.}\ \delta E^{-d/2}]$ [5].

Turning to the extended states, consider a region far from the mobility edge for weak disorder, $I \gg W$. In the first approximation, we can assume that the states belong to an ideal band. The effect of impurities is to generate scattering centers characterized by a mean-free path, l and a mean-free time τ between collisions. Generally, $l = (S_{\rm imp} N_{\rm imp})^{-1}$ where $S_{\rm imp}$ is the scattering cross-section. A typical estimate gives $S_{\rm imp} = (b\ \delta E/E)^2$ where now δE denotes the fluctuation in energy, and b the width of the center. For $b = N_{\rm imp}^{-1/3}$, $E \sim I$, and $\delta E \sim W$ we find $l \sim b(I/W)^2$. The Fermi-momentum is comparable to the inverse spacing $k_F \sim 1/b$ giving,

$$k_F l \approx \left(\frac{I}{W}\right)^2. \tag{1.9}$$

This suggests that when $k_F l \gg 1$ the system behaves as a good metal, while for $k_F l \sim 1$ there is a mobility edge beyond which the system is insulating.

2. Quantum Interference Effects in Disordered Conductors

The phenomenon of Anderson localization is quantum mechanical. To understand how it appears it is instructive to discuss the manifestations of quantum interference in good metals with disorder. In recent years the fabrication of nanostructure semi-conducting devices has enabled direct measurements of such quantum interference effects. In such devices it is typical for electrons to propagate without inelastic collision with phonons or other electrons over distances, L_ϕ large in comparison to the sample size L. Bridging the gap between the atomic scale and the macroscopic they have become known as "mesoscopic." This phase coherence has a dramatic effect on transport properties and leads to the phenomena of "weak localization."

The characteristic of mesoscopic structures is the sensitivity of transport and spectral properties to small changes in the microscopic details such as geometry, or configuration of impurities, as well as to external magnetic fields. This sensitivity is a consequence of the quantum coherence of the electron motion. Understanding quantum transport phenomena in such devices therefore calls for a statistical approach. As with the Anderson model, from a theoretical point of view it is natural to treat each sample as one member of an ensemble prepared under identical macroscopic conditions. It is a remarkable feature of mesoscopic systems that this form of averaging is equivalent to averaging over some interval of energy (or external field) in one given sample. This equivalence implies an "ergodicity" which is crucial to understanding mesoscopic phenomena.

2.1. Waves in Random Media

Perhaps the most striking manifestation of quantum coherence effects in mesoscopics is the phenomena of universal conductance fluctuations (UCF). For weak disorder, the average conductance of a metallic grain is $\langle G\rangle \gg e^2/h$. Nevertheless, the fluctuation or variance of the conductance has the surprising property of being independent of microscopic details of the sample (size, geometry, morphology, etc.) [6, 7],

$$\langle(\delta G)^2\rangle \equiv \langle G^2\rangle - \langle G\rangle^2 \sim (e^2/h)^2. \tag{2.10}$$

Compare this result with the following naive estimate. If a sample of size L is separated into a set of statistically independent samples of a size l_c, we would estimate

$$\frac{\langle(\delta G)^2\rangle}{\langle G\rangle^2} \propto \left(\frac{l_c}{L}\right)^d. \tag{2.11}$$

Instead, taking $\langle G\rangle = \sigma L^{d-2}$, where σ denotes the usual residual conductivity, Eq. (2.10) implies that

$$\frac{\langle(\delta G)^2\rangle}{\langle G\rangle^2} \propto \left(\frac{e^2}{\hbar\sigma}\frac{1}{L^{d-2}}\right)^2. \tag{2.12}$$

The gross overestimate suggests that *non-locality* effects are crucial in governing the transport properties in mesoscopic samples. Eq. (2.10) and Eq. (2.12) are valid for the residual conductance at $T = 0$. We remark that if, as a result of finite temperature of for other reasons (see below), the coherence length L_ϕ becomes smaller than L, the "local" estimation of Eq. (2.11) with $l_c = L_\phi$ is indeed correct.

A qualitative explanation for these results can be given using Feynman's path integral formulation of quantum mechanics. The amplitude for propagation of a particle between two points is given by the sum of classical amplitudes connecting the two points. Classical mechanics involves only the most probable path. For a free particle, the dominant paths lie within a straight tube connecting the end points with a radius comparable to the de Broglie wavelength, $\lambda_F = 1/k_F$. For a disordered sample we can assume that each impurity presents a target of cross-section $S_{\rm imp} \sim \lambda_F^2$. The Feynman paths can themselves be presented as a random configuration of tubes which connect different impurities or scattering centers. The average length of each straight line segment defines the mean free path, $l = (S_{\rm imp} N_{\rm imp})^{-1}$, which can be estimated by comparing the volume of the tube, $S_{\rm imp}^2 l$ with the average volume per impurity, $N_{\rm imp}^{-1}$. Conceptually, this compares with the scattering of waves in random media.

Consider then the probability of a particle injected at the source B (fig. 3) to propagate to a detector at C in a good conductor ($\lambda_F \ll l$). Scattering from different impurities, a particle may travel between B and C following one of many paths. Let us focus on two possible paths each having a probability amplitude $A_{1,2} = \sqrt{W_{1,2}}\exp[{\rm i}\varphi_{1,2}]$. The total probability is given by

$$W \equiv |A_1 + A_2|^2 = W_1 + W_2 + 2\sqrt{W_1 W_2}\ \cos(\varphi_1 - \varphi_2). \tag{2.13}$$

where the first two terms represent the sum of probabilities for the particle to pass either way, and the last term describes the interference between the two trajectories.

Typically different paths have lengths that differ substantially implying a statistical independence of φ_1, and φ_2 ($|\varphi_1 - \varphi_2| \gg 2\pi$). Averaging over a random distribution of phases produces the classical result $\langle W \rangle = W_1 + W_2$. On the other hand, consider the fluctuation in the amplitude. Since $\langle \cos^2(\varphi_1 - \varphi_2)\rangle = 1/2$, the latter differs from the classical value by an interference term,

$$\langle W^2 \rangle = (W_1 + W_2)^2 + 2\ W_1\ W_2. \tag{2.14}$$

From this observation we can draw two important conclusions: Firstly $\langle W^2 \rangle \neq \langle W \rangle^2$ because of fluctuations, and secondly that non-locality originates from interference.

2.2. Aharonov-Bohm Oscillations

2.2.1. hc/e

Since magnetic fields give rise to additional phase factors $\int \boldsymbol{A} \cdot d\boldsymbol{r}$, where $\boldsymbol{A}$ denotes the vector potential, they can be used to monitor the effect of quantum coherence. This is illustrated most clearly by the Aharonov-Bohm geometry in which electrons emitted at a source O pass through

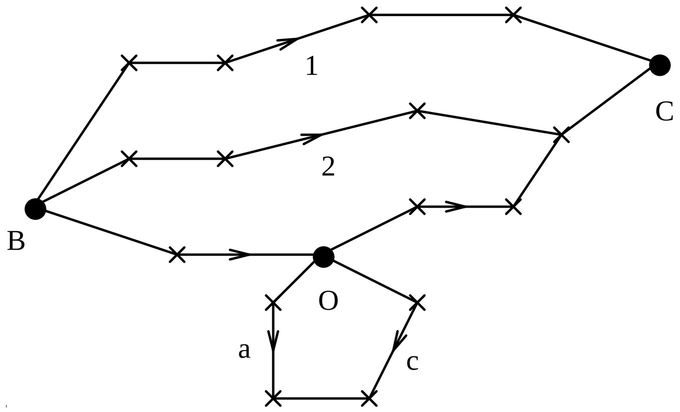

Fig. 3. Two typical trajectories between sites B and C in a disordered conductor.

one of two narrow slits to a detector at X (fig. 4). The superposition of amplitudes from each trajectory interfere and modify the total amplitude at X. Suppose a magnetic field is applied in such a way that the two paths encircle an Aharonov-Bohm flux, ϕ in opposite directions. The phase shift experienced by each particle is given by the line integral over the canonical momentum,

$$\varphi = \int \left(\boldsymbol{p} - \frac{e}{c}\boldsymbol{A}\right) \cdot \mathrm{d}\boldsymbol{r}. \tag{2.15}$$

This produces a phase difference between the two paths 1 and 2 of $\varphi_1 - \varphi_2 = (\varphi_1 - \varphi_2)_0 - 2\pi\phi/\phi_0$, where $\phi_0 = hc/e$ denotes the flux quantum. A change of flux induces a corresponding shift in the interference pattern, $W(\phi) \propto \cos^2(\pi\phi/\phi_0)$.

A similar situation arises if a uniform magnetic field is applied to the disordered metal. In this case an additional phase difference is induced between paths 1 and 2 of $\delta\varphi(H) = \varphi_1(H) - \varphi_2(H)$. Eq. (2.15) shows $\varphi(H) - \varphi(0) = 2\pi\phi/\phi_0$ where ϕ denotes the total flux enclosed by the two trajectories. It is straightforward to verify that $\langle W(H)^2\rangle$ is unchanged by the magnetic field and equal to the expression given in Eq. (2.14). However, since $\langle\cos(\delta\varphi(0))\ \cos(\delta\varphi(H))\rangle \to 0$ for $\phi/\phi_0 \gg 1$, the connected part of the autocorrelator is strongly affected by the magnetic field,

$$\langle W(H)\ W(0)\rangle_c = \begin{cases} 2\ W_1\ W_2 & \phi \ll \phi_0, \\ \to 0 & \phi \gg \phi_0. \end{cases} \tag{2.16}$$

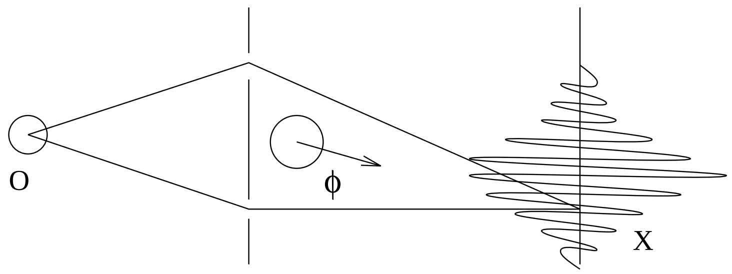

Fig. 4. Geometry of the two-slit experiment with Aharonov-Bohm flux.

The conductance, $G(H)$ is also a random function, and accordingly we can expect

$$\langle G(H)\ G(0)\rangle_c \sim \begin{cases} (e^2/h)^2 & H \ll H_c, \\ \to 0 & H \gg H_c. \end{cases} \tag{2.17}$$

where $H_c = \phi_0/A$ denotes the field required to drive a flux ϕ_0 through a sample with area A. The magnetic length $L_H = \sqrt{\hbar c/eH}$ plays the role of the coherence length L_ϕ and Eq. (2.11) can be rewritten,

$$\langle G(H)\ G(0)\rangle \propto \left(\frac{L_H}{L}\right)^d \propto \left(\frac{H_c}{H}\right)^{d/2}. \tag{2.18}$$

Therefore in the Aharonov-Bohm geometry we would expect a changing field to give rise to fluctuations in the measured conductance with a typical period of hc/e, together with aperiodic fluctuations with a typical amplitude e^2/h. This kind of magnetoconductance was observed experimentally by Webb et al. [8].

2.2.2. $hc/2e$

Even earlier, Sharvin and Sharvin observed oscillations of the magnetoconductance of a long metallic hollow cylinder with a period of half the size [9]. The latter originates from the interference of time-reversed paths and, as we will see, contributes directly to the average conductance.

The absence of interference effects in the average transmission probability between two points B and C was a consequence of the random phase of the different contributing paths. One way of ensuring trajectories add with uniform phase is to incorporate a self-intersection (fig. 3). Each path of this kind can be assigned an amplitude A_c or A_a according to whether the passage occurred in clockwise or anti-clockwise manner. In the absence of a magnetic flux, these two amplitudes are coherent for any realization of the random potential. Thus their interference can not be neglected. The probability to find the particle at O becomes,

$$|A_c|^2 + |A_a|^2 + 2\mathrm{Re}\ A_c A_a^* = 4|A_c|^2, \tag{2.19}$$

a factor of 2 larger than the classical value. This implies a reduced probability of finding it at the destination and therefore a decrease of the conductance. This picture gives qualitative understanding of the phenomenon of "weak localization" (for more details see Refs. [10–16]). The same interference effects have been long appreciated in the subject of light propagation in random media [17]. The interference of time-reversed paths is responsible for enhanced back-scattering observed in experiment.

By inducing a phase of opposite sign in each trajectory, a magnetic field serves to destroy the coherence and the weak localization effect. As a consequence, in contrast to the classical expectation, a magnetic field has the effect of enhancing the conductivity. The origin of the $hc/2e$ oscillations in the Aharonov-Bohm geometry is now clear. Time-reversed paths that encircle the flux pick up an additional phase of $2 \times 2\pi\phi/\phi_0$. It was this effect, predicted in Ref. [18], which was later observed in the experiment of Sharvin and Sharvin [9].

2.3. Variations in Random Potential

In speaking of a statistical ensemble we have assumed that each realization of the random potential generates a different member. To verify this assumption we should estimate how many impurities must be shifted to create a new realization [19, 20]. Consider a typical diffusion path that an electron takes through the system. For a mean free path, l and system size, L, an electron typically undergoes L^2/l^2 collisions in traversing the path. To find the probability that a given impurity participates in one of these collisions it is necessary to divide this number by the total number of impurities $n_{\mathrm{tot}} = N_{\mathrm{imp}} L^d$. As a result a shift of one impurity will change the conductance by

$$\delta G \sim \frac{e^2}{h}\left(\frac{L}{l}\right)^2 \frac{1}{N_{\mathrm{imp}} L^d} \equiv \frac{e^2}{h}\frac{1}{n_0}. \tag{2.20}$$

For this to be of the order of e^2/h it is necessary to move $n_0 = n_{\mathrm{tot}} l^2/L^2$ ($n_{\mathrm{tot}} \gg 1$) impurities. A shift of $\delta n_{\mathrm{imp}} < n_0$ impurities leads to

$$\delta G \sim \frac{e^2}{h}\left(\frac{\delta n_{\mathrm{imp}}}{n_0}\right)^{1/2}. \tag{2.21}$$

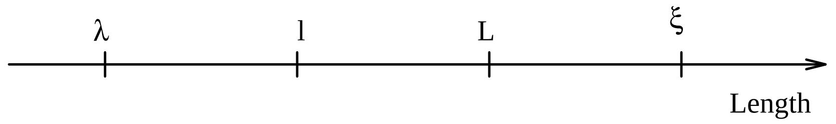

Fig. 5. Relevant length scales for diffusion.

We remark that in two-dimensions, n_0 is independent of L.

All of these theoretical predictions are found to be in good agreement with the experimental results of Prober et al. [21].

2.4. Diffusion

In this section we will recall some basic ideas of the semi-classical description of electrons in good conductors ($k_F l \gg 1$). We will concentrate on the "diffusive regime" where $l \ll L \ll \xi$, with ξ denoting the localization length (fig. 5) which, in principle, can be infinite.

Although, we have seen previously that non-locality is crucial to account for the behavior on short scales $r \leqslant k_F$, longer length scales can afford a local description. The erratic or "chaotic" motion of electrons in a solid means that the position and momentum of a single particle at any instant is random. It is therefore useful to characterize the motion by a distribution function $n(\boldsymbol{p}, \boldsymbol{r}, t)$ which gives the probability for finding a particle in a certain element of phase space. Integrating over momenta one can express the local density and current as

$$\rho(\boldsymbol{r}, t) = \int (\,\mathrm{d}p)\; n(\boldsymbol{p}, \boldsymbol{r}, t), \qquad \boldsymbol{j}(\boldsymbol{r}, t) = \int (\,\mathrm{d}p)\; \frac{\boldsymbol{p}}{m} n(\boldsymbol{p}, \boldsymbol{r}, t). \tag{2.22}$$

The distribution function obeys a classical Boltzmann equation from which a diffusion equation for the density can be derived [22],

$$\Big(\frac{\partial}{\partial t} + \boldsymbol{v} \cdot \boldsymbol{\nabla} + e\boldsymbol{E} \cdot \frac{\partial}{\partial \boldsymbol{p}}\Big) n(\boldsymbol{p}, \boldsymbol{r}, t) = \frac{\bar{n} - n(\boldsymbol{p}, \boldsymbol{r}, t)}{\tau}. \tag{2.23}$$

Suppose a system is taken out of equilibrium by the creation of a density fluctuation at $t = 0$, $\rho(\boldsymbol{r}, t = 0) = \rho_0(\boldsymbol{r})$. The result is a relaxation which for $t, r \to \infty$ can be expressed as a diffusion current

$$\boldsymbol{j}_D(\boldsymbol{r}, t) = -D\; \boldsymbol{\nabla}\rho(\boldsymbol{r}, t), \tag{2.24}$$

with a diffusion constant D. The conservation law for particle number implies the local continuity relation,

$$\boldsymbol{\nabla} \cdot \boldsymbol{j} = -\frac{\partial \rho}{\partial t}, \tag{2.25}$$

which together with Eq. (2.24) leads to the diffusion equation,

$$\frac{\partial \rho}{\partial t} = D \boldsymbol{\nabla}^2 \rho. \tag{2.26}$$

Now suppose an electric field is used to drive an Ohmic current,

$$\boldsymbol{j}_E = \boldsymbol{\sigma} \cdot \boldsymbol{E}. \tag{2.27}$$

Without leads (e.g. inside a capacitor) an equal and opposite diffusion current is induced to maintain charge neutrality. For a uniform electric field, the electrochemical potential $\mu + e\boldsymbol{E} \cdot \boldsymbol{r} = \text{const}$. For a charge density ρ_0 the diffusion current is equal to $\boldsymbol{j}_D = -e^2 D\nu(\mu)\boldsymbol{E}$ where we have used $\boldsymbol{\nabla}\rho = e\nu(\mu)\boldsymbol{\nabla}\mu$, with $\nu(\mu) \equiv e\ (\partial \rho_0/\partial \mu)$. Combining this with Eq. (2.27) we obtain the Einstein relation,

$$\sigma = e^2 \nu D. \tag{2.28}$$

This equation is readily generalized to tensor diffusion constants, and to spin currents and densities.

The diffusion equation ensures conservation of the total particle number (as can be verified by the integration of Eq. (2.26) over the volume of the system). Without inelastic processes, Eq. (2.26) is valid for the density of particles with a given energy. Therefore, the density $\rho(\boldsymbol{r}, t; E)$, and not just its energy integral, is conserved.

In a one particle language, if $\rho(\boldsymbol{r}, 0) = \delta(\boldsymbol{r})$, $\rho(\boldsymbol{r}, t)$ is the probability of finding a particle at $\boldsymbol{r}$ after a time t. The Boltzmann equation allows the diffusion constant to be determined as a function of the mean free path,

$$D = \frac{v_F l}{d} = \frac{v_F^2 \tau}{d}. \tag{2.29}$$

As a result, the Drude formula for the conductivity becomes equivalent to the Einstein relation.

$$\frac{Ne^2\tau}{m} = \sigma = e^2 \nu D. \tag{2.30}$$

2.5. Thouless Approach

In the early 1970's Thouless proposed a different approach to quantum transport [23, 24]. The Einstein relation allows the conductance to be expressed in the form

$$G = \sigma L^{d-2} = e^2 \left(\nu L^d\right) \frac{D}{L^2} = \frac{e^2}{\hbar} \frac{E_c}{\Delta}, \tag{2.31}$$

where the Thouless energy $E_c = \hbar D/L^2$ describes the typical inverse diffusion time, and $\Delta = (\nu L^d)^{-1}$ is the mean spacing between energy levels. We can then define a dimensionless conductance g where

$$\langle G \rangle = \frac{e^2}{\hbar} N_T \equiv \frac{e^2}{\hbar} g. \tag{2.32}$$

Physically, g denotes the average number of levels inside an energy window of width E_c.

To determine E_c (or D) from the exact solution of a quantum problem, Thouless proposed to study the sensitivity of energy levels to a change of boundary conditions. Extended states would be expected to show a strong dependence while localized states would show little, or no dependence. Consider then the response of the wavefunction to the imposition of a quasi-periodic boundary condition, $\psi(x, y = L) = \psi(x, y = 0) \exp[\mathrm{i}\varphi]$. The energy levels disperse as a function of φ. Properly averaged, perturbation theory shows [24] that the dissipative conductance is related to the curvature of the level dispersion through the relation $E_c \sim \overline{\partial^2 E_i(\varphi)/\partial \varphi^2}|_{\varphi=0}$, where the eigenvalues are denoted by $E_i(\varphi)$. This suggests that the transport properties do not depend explicitly on the high energy scales $\hbar/\tau$ and E_F, but only on $\Delta \propto L^{-d}$ and $E_c \propto L^{-2}$.

Our previous discussion suggested that conductance fluctuations are universal, $\delta G_{\mathrm{rms}} \propto e^2/h$. Together with Eq. (2.32) this implies that, while $g = N_T \gg 1$, the fluctuations in the Thouless number, the number of energy levels inside some interval E_c, $\delta N_T \sim 1$. By contrast a naive estimate based on the assumption of an uncorrelated spectrum would suggest $\delta N_T \sim \sqrt{N_T}$. This surprising result suggests a "rigidity" of the spectrum consistent with strong repulsion between the energy levels. This phenomena is characteristic of random matrix ensembles where $\langle(\delta N)^2\rangle \propto \ln N$ [25]. For open systems with a level width comparable to E_c, the logarithm is irrelevant and the fluctuation is comparable to unity. Later we will argue that this coincidence is not accidental but is a natural consequence of the chaotic dynamics of the electrons. This result has important ramifications implying a universality of spectral statistics.

3. Scaling Theory of Localization

The work of Thouless in the 1970's [26] motivated the development by Abrahams, Anderson, Licciardello, and Ramakrishnan [27] of a one-parameter scaling theory of localization which since then has formed the basis of the majority of approaches to quantum transport in disordered conductors. The ideas expressed in these studies are now widely accepted.

The central idea behind this approach is to suppose that the transport properties of a sample of size $(2L)^d$ is determined by one of size L^d. The eigenstates in the former are described by a linear combination of the states that make up the 2^d samples of the latter. The admixture of the states depends on their overlap at the interface and the average DoS. Recognizing that the overlap integral is related to the sensitivity of the sample to a change in boundary conditions, Thouless argued that a single parameter, the dimensionless conductance, controls the nature of the eigenstates as the sample size is doubled. (This idea can be applied to the Anderson model when the analogous quantity is set by the ratio I/W.)

This notion is embodied in the Gell-Mann Low equation for the scaling of the dimensionless conductance with system size,

$$\frac{1}{g}\frac{\mathrm{d}g}{\mathrm{d}\ln L} = \beta(g), \tag{3.33}$$

where $\beta(g)$ denotes the scaling function. The crucial point is that the scaling is universal, independent of $k_F l$ and the initial value of the conductance. Although it does, as we will see later, depend on certain symmetries.

On the metallic side, when the wavefunctions are extended, the conductance obeys Ohm's law,

$$g = \frac{\hbar\sigma}{e^2}L^{d-2}. \tag{3.34}$$

For samples large enough to have a well-defined mean-free path, the conductivity σ is an intensive quantity and the β-function takes the asymptotic form $\beta(g) = d-2$. On the insulating side, all states are localized near the Fermi energy. Transport occurs between well separated localized states with an amplitude which is suppressed by the exponentially small overlap, and $g \propto \mathrm{e}^{-L/\xi}$ where ξ denotes the localization length ($\xi \ll L$). This non-ohmic behavior implies that $\beta(g) = \ln(g/g_c)$ (calculation shows that $g_c \sim \pi^2$).

Scaling theory implies a continuous evolution of the conductance with increasing L from its initial value of g_0 at $L \sim l$ (which is determined by the strength of the random potential) approaching either the metallic or

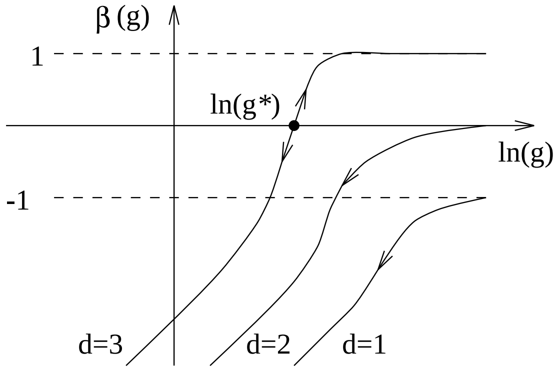

Fig. 6. The scaling function $\beta(g)$ for dimensions 1, 2, and 3.

insulating asymptotes at large L. Which of these is favored depends on the strength of the disorder potential (g_0), and the dimensionality. Interpolating smoothly between the asymptotic values the behavior of $\beta(g)$ is shown in fig. 6 for dimensions 1, 2, and 3.

In one-dimension $\beta(g) < 0$ for all values of g and so the RG flow converges rapidly on the localized phase with increasing length. This is consistent with the result that all states are localized in one-dimension [28, 29].

In three-dimensions the asymptotic regimes of the β-function are of opposite sign. This has a profound implication for transport. If the initial value of the conductance lies on the positive part of the curve scaling is towards the metallic Ohmic regime. On the other hand, if it is on the negative side scaling is towards the insulating localized regime. The critical value g^*, at which $\beta(g^*) = 0$, represents an unstable fixed point, and defines the mobility edge.

In the vicinity of g^*, $\beta(g)$ depends linearly on g

$$\beta(g) = \frac{1}{\nu}\Big(\frac{g - g^*}{g^*}\Big), \tag{3.35}$$

where $1/\nu g^*$ denotes the slope of the curve near g^*. Using Eqs. (3.33) and (3.35) we can evaluate the function $L(g)$ (which is inverse to $g(L)$, the length dependent conductance). Integration from g_0 ($L(g_0) \approx l$) to $g \approx 1$ ($L(1) \approx \sigma^{2-d}\hbar/e^2$), we find $g(L) = \sigma L$ where

$$\sigma \sim \frac{g^*}{l}\Big(\frac{g_0 - g^*}{g^*}\Big)^{\nu}. \tag{3.36}$$

On approaching the mobility edge the conductivity vanishes with a critical exponent ν.

On the localized side of the fixed point, at large enough length scales, there is crossover to the insulating regime in which states are exponentially localized,

$$g(L) = g_c \, \mathrm{e}^{-L/\xi}, \qquad \xi \approx l |(g_0 - g^*)/g^*|^{-\nu}, \tag{3.37}$$

implying a divergence of the localization length ξ with the same exponent. More details can be found in the review by Ramakrishnan [30].

A smooth interpolation suggests that, in two-dimensions $\beta(g) < 0$ implying that all states are localized. Whether or not this assumption is correct requires consideration of higher orders in $1/g$. In the next section we will develop one of the tools for addressing this question.

4. Perturbation Theory of Disordered Metals

In section 2 we examined qualitatively the effects of interference in quantum transport. In this section we will develop and make use of a formal diagrammatic approach† to make the theory quantitative. To provide a brief introduction (and fix our notation) we will begin with an elementary discussion of the Green function method.

4.1. Green Functions

The retarded Green function of a particle is defined by the equation

$$\Big[E + \mathrm{i}0 - H(\boldsymbol{r})\Big] \; G^R(\boldsymbol{r}, \boldsymbol{r}'; E) = \delta(\boldsymbol{r} - \boldsymbol{r}'), \tag{4.38}$$

and the advanced counterpart is given by the hermitian conjugate, $G^A(\boldsymbol{r}, \boldsymbol{r}'; E) = \big(G^R(\boldsymbol{r}, \boldsymbol{r}'; E)\big)^*$. Eq. (4.38) has the solution

$$G^{R,A}(\boldsymbol{r}, \boldsymbol{r}'; E) = \sum_\alpha \frac{\psi_\alpha(\boldsymbol{r}) \; \psi^*_\alpha(\boldsymbol{r}')}{E - E_\alpha \pm \mathrm{i}0}, \tag{4.39}$$

where $\psi_\alpha(\boldsymbol{r})$ represent the eigenstates of the Hamiltonian $H = -\boldsymbol{\nabla}^2/2m + V(\boldsymbol{r})$ with $V(\boldsymbol{r})$ denoting the potential. Analytical properties ensure that the retarded and advanced Green function vanish for $t < 0$ and $t > 0$ respectively.

† For more details see Ref. [31]

For a free particle ($V=0$) the wavefunctions are plane waves ($\alpha=\boldsymbol{p}$) and Eq. (4.38) is satisfied by

$$G^{R,A}(\boldsymbol{r},\boldsymbol{r}';t)=\Big(\frac{m}{2\pi\mathrm{i}\hbar t}\Big)^{d/2}\,\mathrm{e}^{\mathrm{i}m(\boldsymbol{r}-\boldsymbol{r}')^2/2\hbar t}\,\theta(\pm t). \tag{4.40}$$

Physically, $G^R(\boldsymbol{r},\boldsymbol{r}';t)$ represents the probability of a particle injected at position $\boldsymbol{r}$ to propagate to a position $\boldsymbol{r}'$ after a time t. The propagator can equally be expressed by the Feynman path integral

$$G^R(\boldsymbol{r},\boldsymbol{r}';t)=\int_{\boldsymbol{r}(0)=\boldsymbol{r}}^{\boldsymbol{r}(t)=\boldsymbol{r}'}\mathcal{D}\boldsymbol{r}(t)\;\exp\Big[\mathrm{i}\int_0^t\Big(\frac{\dot{\boldsymbol{r}}^2}{2m}-V(\boldsymbol{r})\Big)dt'\Big]. \tag{4.41}$$

4.2. Random Potential

Till now, we have required no formal definition of a statistical ensemble of impurity configurations. We therefore introduce the functional, $P\{V(\boldsymbol{r})\}$ which defines the probability distribution for the random potential $V(\boldsymbol{r})$. The ensemble average of the functional $A\{V(\boldsymbol{r})\}$ is then defined by the integral,

$$\Big\langle A\{V(\boldsymbol{r})\}\Big\rangle=\int\mathcal{D}V(\boldsymbol{r})\;P\{V(\boldsymbol{r})\}\;A\{V(\boldsymbol{r})\}. \tag{4.42}$$

Usually we will make the following assumptions about the disorder potential:

(a) that it has a vanishing average $\langle V(r)\rangle=0$;

(b) that the average is stationary under translation $\langle V(\boldsymbol{r}_1)V(\boldsymbol{r}_2)\rangle=W(\boldsymbol{r}_1-\boldsymbol{r}_2)$; and

(c) that it belongs to a Gaussian distribution

$$P\{V(\boldsymbol{r})\}=\frac{1}{\mathcal{Z}}\exp\Big[-\frac{1}{2}\int\mathrm{d}\boldsymbol{r}_1\,\mathrm{d}\boldsymbol{r}_2V(\boldsymbol{r}_1)K(\boldsymbol{r}_1-\boldsymbol{r}_2)V(\boldsymbol{r}_2)\Big], \tag{4.43}$$

where $\int K(\boldsymbol{r}_1-\boldsymbol{r}')\;W(\boldsymbol{r}'-\boldsymbol{r}_2)\;\mathrm{d}\boldsymbol{r}'=\delta(\boldsymbol{r}_1-\boldsymbol{r}_2)$, and $\mathcal{Z}$ provides the normalization.

The latter assumption has the advantage that all higher order correlation functions of V can be reduced to products of two-point correlators through the cumulant expansion,

$$\langle\exp[\mathrm{i}\phi]\rangle=\exp[-\langle\phi^2\rangle/2]. \tag{4.44}$$

For purposes of calculation it is often convenient to go further and assume that the impurity potential is δ-correlated white-noise, $W(\boldsymbol{r}_1-\boldsymbol{r}_2)=$

$\gamma\ \delta(\boldsymbol{r}_1-\boldsymbol{r}_2)$. In particular, we will be concerned with the limit of weak disorder, $\lambda_F \gg r_0 \gg b$ where $b = N_{\rm imp}^{-1/d}$ denotes the typical distance between impurities and r_0 denotes the correlation length of the potential. Defining $V(\boldsymbol{r}) = U\sum_i \delta(\boldsymbol{r}-\boldsymbol{r}_i)$ we will apply the limiting distribution: $N_{\rm imp}\to\infty$, $U\to 0$ such that $\gamma \propto N_{\rm imp}|U|^2 \to \text{Const}$.

4.3. Diagrammatics

To determine the impurity averaged Green function we require an expansion which allows ensemble averaging. In principle it is possible to form an expansion in the disorder potential V. Adopting a "matrix" notation (in which it is assumed that all internal coordinates are summed) we have‡

$$G^R = G_0^R + G_0^R\ \sum_{n=1}^{\infty}(V\ G_0^R)^n. \tag{4.45}$$

For a δ-correlated impurity potential averaging requires the consideration of all possible pairings of the potential V. This idea can be most simply illustrated in the form of a graph or diagram. Representing each bare Green function in Eq. (4.45) as a thin solid line, and each impurity scattering amplitude by a cross, the exact Green function G^R, denoted by a thick solid line, can be represented by the diagram shown in fig. 7. Ensemble averaging generates all possible pairings of the impurities which are denoted by dotted lines.

Different contributions to the average Green function can be classified according to whether or not they are separable. In fact, an expansion in V is insufficient to determine the leading order contributions to the average Green function in $(E_F\tau)^{-1}$. Instead it is necessary to collect all non-separable diagrams into the "self-energy" operator Σ^R and construct the following "Dyson equation" for the Green function (see fig. 8a),

$$G^R = G_0^R + G_0^R\sum_{n=1}^{\infty}(\Sigma^R G_0^R)^n = G_0^R + G_0^R\Sigma^R G^R. \tag{4.46}$$

‡ For example, the first order term in the expansion in space or momentum representation is given by,

$$G^R(r_1,r_2) = G_0^R(r_1,r_2) + \int \mathrm{d}r' G_0^R(r_1,r')\ V(r')\ G_0^R(r',r_2),$$

$$G^R(p_1,p_2) = G_0^R(p_1,p_2) + \int (\mathrm{d}p')(\mathrm{d}p'')G_0^R(p_1,p')\ V(p',p'')\ G_0^R(p',p_2).$$

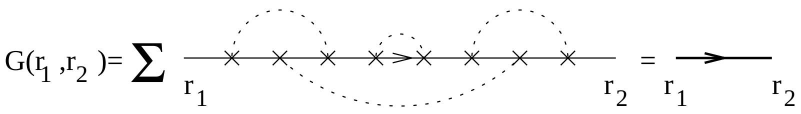

Fig. 7. Diagrammatic representation of the average Green function. The bare Green function is denoted by a thin solid line while the exact average Green function is shown as a thick line.

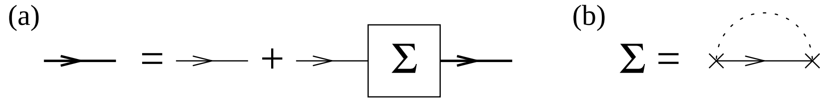

Fig. 8. Diagrammatic representation of (a) the Dyson equation, and (b) the corresponding self-consistent Born approximation to the self-energy.

It is then straightforward to derive the final expression,

$$G^R = \frac{1}{(G_0^R)^{-1} - \Sigma^R}. \tag{4.47}$$

In this way we can now perform a systematic expansion in Σ and be sure of retaining all relevant terms in G^R.

With a δ-correlated impurity potential, the leading order contribution to the self energy is given by the self-consistent Born approximation (fig. 8b)

$$\Sigma^R = \gamma \int (\,\mathrm{d}p) G_0^R(\boldsymbol{p}). \tag{4.48}$$

Although formally divergent, Re Σ^R can be absorbed into an irrelevant renormalization of the energy and can be neglected. Using the following expression for the DoS

$$\nu(E) = \frac{1}{L^d} \sum_\alpha \delta(E - E_\alpha) = -\frac{1}{\pi} \int \mathrm{d}\boldsymbol{r} \ \mathrm{Im}\ G^R(\boldsymbol{r}, \boldsymbol{r}; E), \tag{4.49}$$

we find

$$\mathrm{Im}\ \Sigma^R = -\frac{1}{2\tau}, \qquad \tau = \frac{1}{2\pi\nu\gamma}, \tag{4.50}$$

where we have introduced the parameter τ which defines the mean free time. The average Green function is therefore given by [31]

$$G^{R,A}(\boldsymbol{p};E)=\frac{1}{\epsilon-\xi_p\pm\mathrm{i}/2\tau}, \tag{4.51}$$

where $\epsilon=E-E_F$, and $\xi_p=\boldsymbol{p}^2/2m-E_F$. Higher order terms show that corrections are smaller by a factor $1/E_F\tau$. Fourier transforming, we obtain

$$G^{R,A}(\boldsymbol{r};E)=G^{R,A}(\boldsymbol{r};E|V=0)\,\mathrm{e}^{-\boldsymbol{r}/2l}, \tag{4.52}$$

$$G^{R}(\boldsymbol{r};E|V=0)=i\pi\nu\begin{cases}\frac{\sin(k_F|\boldsymbol{r}|)}{k_F|\boldsymbol{r}|} & d=3,\\ J_0(k_F|\boldsymbol{r}|) & d=2,\end{cases} \tag{4.53}$$

where $l=v_F\tau$. Physically, τ represents the typical decay time of a plane-wave state in which a particle typically moves a distance l.

4.4. *Conductivity*

In section 2 we saw that quantum coherence effects are manifest not in the average one-particle properties but rather in two-particle correlators. To observe the interference effects we will examine the frequency dependence of the conductivity. That latter can be expressed in linear response through the Kubo-Greenwood formula

$$\sigma_{\alpha\beta}(\omega)=\frac{\mathrm{i}e^2}{\pi m^2\omega}\int(\mathrm{d}p)\int\mathrm{d}E\,\left[n_F(E)-n_F(E+\omega)\right] \times\left\langle p_\alpha G^A(\boldsymbol{p};E)\;p_\beta\;\mathrm{Im}\;G^R(\boldsymbol{p};E+\omega)\right\rangle, \tag{4.54}$$

where $n_F(E)$ denotes the Fermi-Dirac distribution function. Omitting terms which are regular in ω, and using $v_\alpha=\partial\xi_p/\partial p_\alpha$ we obtain

$$\sigma_{\alpha\beta}(\omega)=\frac{e^2}{2\pi\omega}\int(\mathrm{d}p)\int\mathrm{d}E\,\left[n_F(E)-n_F(E+\omega)\right] \times\left\langle v_\alpha G^A(\boldsymbol{p};E)\;v_\beta G^R(\boldsymbol{p};E+\omega)\right\rangle. \tag{4.55}$$

Diagrammatically $\sigma_{\alpha\beta}(\omega)$ can be represented as the "bubble" shown in fig. 9.

4.4.1. *Drude Conductivity*

A first approximation is to replace each of the bare Green functions in Eq. (4.54) by their ensemble averages in Eq. (4.51) (see fig. 9b). The momentum integration can be exchanged for an energy integration $(\mathrm{d}p)=$

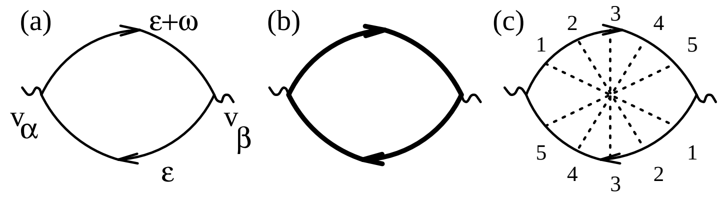

Fig. 9. Bubble graph for the conductivity: (a) before averaging; (b) the leading contribution after averaging; and (c) the first quantum correction. The impurity lines in (c) represent the maximally crossed diagram of the Cooperon.

$\nu\,\mathrm{d}\xi_p\,\mathrm{d}\Omega/4\pi$ where $\mathrm{d}\Omega$ denotes the angular integration over $\boldsymbol{p}$. ξ_p integration gives

$$\int \mathrm{d}\xi_p\ \langle G^A(\boldsymbol{p};E)\rangle\ \langle G^R(\boldsymbol{p};E+\omega)\rangle = 2\pi\frac{\tau}{(1-\mathrm{i}\omega\tau)}, \tag{4.56}$$

while the angular integration averages the velocity,

$$\int v_\alpha v_\beta \frac{\mathrm{d}\Phi}{4\pi} = \delta_{\alpha\beta}\frac{v_F^2}{d}. \tag{4.57}$$

Finally, after setting the Fermi level and temperature to zero $n_F(E) - n_F(E+\omega) = \theta(E)\theta(\omega - E))$ the energy integration contributes a factor ω. Piecing together the different contributions we obtain the classical Drude formula [32]

$$\sigma_{\alpha\beta}(\omega) = \frac{e^2 D\nu}{1-\mathrm{i}\omega\tau}\delta_{\alpha\beta}. \tag{4.58}$$

Similarly, for $T \gg \omega$, $n_F(E) - n_F(E+\omega) \approx -\omega(\partial n_F/\partial E)$ and, upon energy integration, we obtain the same result.

Although we have included only the single-particle average Green function we have obtained the correct Drude form for the conductivity. It may seem surprising that our neglect of impurity lines which connect different Green functions should not affect the average conductivity. To understand this result it is necessary to examine the "vertex corrections." Consider the first vertex correction shown in fig. 10. It gives a contribution

$$I_\alpha^{\mathrm{I}} = N_{\mathrm{imp}}\int (\,\mathrm{d}q) v_\alpha |V(\boldsymbol{q})|^2 G^A(\boldsymbol{p}-\boldsymbol{q};E)\ G^R(\boldsymbol{p}-\boldsymbol{q};E+\omega). \tag{4.59}$$

Thus for isotropic scattering $N_{\mathrm{imp}}|V(\boldsymbol{q})|^2 = \gamma$, angular integration causes I_α^{I} and similar terms to vanish [32]. This explains the coincidence of the

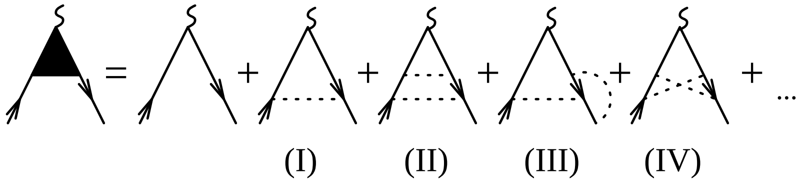

Fig. 10. Different contributions that renormalize the vertex. (I) and (II) denote the first two in a series of ladder diagrams. Diagrams (III) and (IV) give a negligible contribution to the vertex correction.

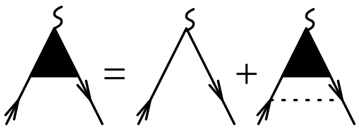

Fig. 11. Dyson equation for the vertex renormalization from ladder diagrams.

result with the Drude formula of classical conductivity. Presently, we will examine the first quantum correction.

4.4.2. Density Correlator and the Ladder Approximation

The diagrammatic technique can also be used to calculation the density correlator

$$R(\boldsymbol{q},\omega) = \left\langle G^A(\boldsymbol{p};E)\ G^R(\boldsymbol{p}+\boldsymbol{q};E+\omega)\right\rangle . \tag{4.60}$$

The first vertex correction in fig. 10 vanished because of its vector nature. However with a scalar coupling, for $|\boldsymbol{q}|l \ll 1$ and $\omega\tau \ll 1$ the contributions from diagram (I),

$$\begin{aligned}\zeta(\boldsymbol{q},\omega) &= \gamma \int (\,\mathrm{d}p)\langle G^A(\boldsymbol{p},E)\rangle\langle G^R(\boldsymbol{p}+\boldsymbol{q},E+\omega)\rangle,\\ &= 1+\mathrm{i}\omega\tau - D\boldsymbol{q}^2\tau,\end{aligned} \tag{4.61}$$

and (II) are not small, but are the first two in a series of important diagrams. Writing a corresponding Dyson equation, the ladder series in fig. 11a can be summed leading to the vertex correction

$$D(\boldsymbol{q},\omega) = \frac{1}{1-\zeta(\boldsymbol{q},\omega)} = \frac{1}{(-\mathrm{i}\omega + D\boldsymbol{q}^2)\tau}. \tag{4.62}$$

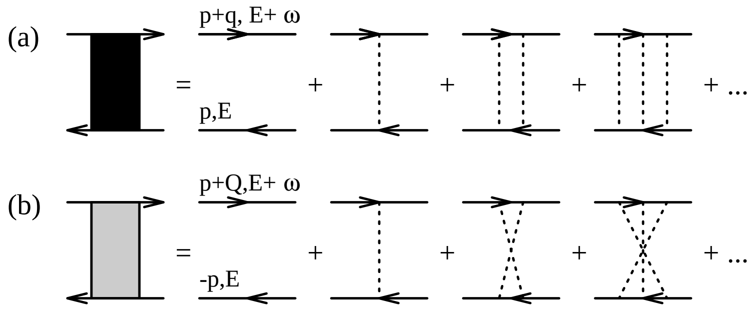

Fig. 12. Ladder diagram for the (a) the diffusion and (b) the Cooperon channel.

The contribution from the remaining diagrams are small. The crossed diagram (III) gives

$$\begin{aligned} I^{\mathrm{III}} &= \gamma^2 \textstyle\int (\,\mathrm{d}q_1)(\,\mathrm{d}q_2)\langle G^A(\boldsymbol{p}-\boldsymbol{q}_1-\boldsymbol{q}_2;E+\omega)\rangle \\ &\times\langle G^R(\boldsymbol{p}-\boldsymbol{q}_1-\boldsymbol{q}_2;E)\rangle\langle G^A(\boldsymbol{p}-\boldsymbol{q}_2;E+\omega)\rangle\langle G^R(\boldsymbol{p}-\boldsymbol{q}_1;E)\rangle. \end{aligned} \tag{4.63}$$

With the first pair of Green functions the poles are always close regardless of the values of $\boldsymbol{p}$, $\boldsymbol{q}_1$, and $\boldsymbol{q}_2$. However, with the latter pair, the poles are separated by $\max\{1/\tau, \xi_{\boldsymbol{p}-\boldsymbol{q}_1}-\xi_{\boldsymbol{p}-\boldsymbol{q}_2}\}$. Geometrical consideration shows the angle of scattering $\cos\theta \sim 1/ql$ where q is the typical momentum transfer. As a result, the angular integration brings a factor of $1/k_Fl$ which we assume to be small. Similarly, it is easy to show that the contribution from diagram (IV) is also diminished by the same factor.

Therefore, to leading order in $1/k_Fl$, the ladder series leads to the density correlator

$$R(\boldsymbol{q},\omega) = \gamma^{-1}\zeta(\boldsymbol{q},\omega)D(\boldsymbol{q},\omega) = \frac{2\pi\nu}{-\mathrm{i}\omega + D\boldsymbol{q}^2}. \tag{4.64}$$

When the Green functions are both retarded or advanced the corresponding correlator takes simply the disconnected value. These results determine the density response function

$$\begin{aligned} \Pi(\boldsymbol{q},\omega) &= \int (\,\mathrm{d}p)\int \frac{\mathrm{d}E}{2\pi}\Big[n_F(E)-n_F(E+\omega)\Big] \\ &\qquad\qquad \times\Big\langle G^A(\boldsymbol{p};E)\ \mathrm{Im}\ G^R(\boldsymbol{p}+\boldsymbol{q};E+\omega)\Big\rangle, \end{aligned} \tag{4.65}$$

$$= \nu\frac{D\boldsymbol{q}^2}{-\mathrm{i}\omega + D\boldsymbol{q}^2}. \tag{4.66}$$

We remark that the approximations used in deriving this equation are incidental. The form of this equation is a consequence of particle conservation and the diffusive nature of the propagation of density fluctuations. The expression for the diffusion propagator $D(\boldsymbol{q},\omega)$ in the retarded-advanced "particle-hole" channel is also a consequence of the conservation of particles with a given energy, and hence is valid only for times short as compared to the inelastic relaxation time. The propagator is a Green function of the diffusion equation

$$\left[\frac{\partial}{\partial t} - D\boldsymbol{\nabla}^2\right] D(0,\boldsymbol{r};0,t) = \frac{1}{\tau}\delta(\boldsymbol{r})\delta(t), \tag{4.67}$$

with the boundary conditions $\partial_\perp D = 0$ ($D = 0$) for closed (open) geometry. The diffusion propagator or "diffuson" describes the low energy and long wavelength density fluctuations in the disordered conductor.

4.4.3. Maximally Crossed Diagrams

The Drude formula describes the classical motion of an electron scattered by impurities. It appears to be a good approximation for $k_F l \gg 1$ since the interference between different scattering processes is suppressed due to the large distance between consecutive collisions. However, our earlier consideration of Feynman paths suggests the existence of an important quantum correction to the conductivity coming from the interference of self-intersecting time-reversed paths (see fig. 3). Such contributions were first identified diagrammatically by Langer and Neal [33].

The correction to the conductivity can be estimated in the following way. For paths contained with a tube of cross-section λ_F^2 the relative magnitude of the correction is given by

$$\frac{\delta\sigma}{\sigma} = \frac{\delta D}{D} \sim -\int_\tau^{t_c} v_F \lambda_F^2 P(t) dt, \tag{4.68}$$

where $P(t) = (Dt)^{-d/2}$ denotes the classical return probability density of diffusion after a time t, and $t_c = \hbar/E_c$ denotes the Thouless time (after which a particle has typically left the system). (The effective dimensionality is specified by the number of dimensions with a length $L \geqslant \sqrt{\hbar D/E_c}$). Integrating Eq. (4.68) we obtain

$$\frac{\delta\sigma}{\sigma} \sim -\frac{1}{\hbar\nu_d D}\frac{2}{2-d}(L_0^{2-d} - l^{2-d}), \tag{4.69}$$

where $L_0 = \sqrt{Dt_c}$, and ν_d denotes the number of states per unit length, area, or volume for $d = 1$, 2, or 3 respectively.

Looking for the same contribution diagrammatically, it is natural to examine the usual diffuson ladder after a time-reversal of one line (see fig. 12b). The resulting diagram no longer involves the momentum difference, but the sum $\mathbf{Q}$,

$$C(\mathbf{Q},\omega) = \frac{1}{(-\mathrm{i}\omega + D\mathbf{Q}^2)\tau}. \tag{4.70}$$

In contrast to the density correlator, $C(\mathbf{Q},\omega)$ is described by a two-particle Green function in the "particle-particle" channel. As such it is closely related to the Cooper channel of superconductivity from which it derives the name "Cooperon." In this case the diffusion-like pole occurs at small ω and small *total* momentum transfer.

Such diagrams are not diminished by angular integrations and contribute to the conductivity (fig. 9b). To order $1/k_F l$ we obtain the correction [34]

$$\delta\sigma = -\frac{De^2\tau}{2\pi}\int(\,\mathrm{d}Q)C(\mathbf{Q},\omega). \tag{4.71}$$

The integration over the Cooperon modes depends sensitively on the dimensionality. The Cooperon propagator $C(\boldsymbol{r},0;t,0)$ satisfies the diffusion equation

$$\left[\frac{\partial}{\partial t} - D\boldsymbol{\nabla}^2\right]C(\boldsymbol{r},0;t,0) = \frac{1}{\tau}\delta(\boldsymbol{r})\delta(t), \tag{4.72}$$

with the boundary conditions $\partial_\perp C = 0$ ($C = 0$) for closed (open) geometry. For a confined geometry, the different modes are quantized and the integration is in principle replaced by a summation. For a lateral dimension a with $D/a^2 \ll \omega$, D/L^2, only the lowest mode $\mathbf{Q} = 0$ need be considered. For dimensions $d \geqslant 2$ the integral diverges and must be cut off by an upper length scale, $|\mathbf{Q}| = \pi/L_0$ where L_0 can be set by the sample size L, the diffusion length $L_\omega = \sqrt{D/\omega}$, or the dephasing length L_ϕ. Integrating we obtain the weak localization corrections to the conductivity

$$\delta\sigma_d \sim \frac{e^2}{2\pi\hbar}\frac{1}{d-2}\left(\frac{-\mathrm{i}\omega}{D}\right)^{d/2-1}, \tag{4.73}$$

which leads to the result

$$\delta\sigma_d = \begin{cases} -\frac{e^2}{\pi\hbar}(L_0 - l) & d = 1, \\ -\frac{e^2}{\pi^2\hbar}\ln\left(\frac{L_0}{l}\right) & d = 2, \\ \frac{e^2}{2\pi^2\hbar}\left(\frac{1}{L_0} - \frac{1}{l}\right) & d = 3. \end{cases} \tag{4.74}$$

This result is in accord with the scaling theory. In particular, it implies that the first quantum correction to the scaling function in two-dimensions is equal to

$$\beta(g) = -\frac{1}{\pi^2 g}, \tag{4.75}$$

supporting the conjecture that for $d = 2$ all states are localized.

In the absence of spin-flip processes the electron phase breaking occurs as a result of inelastic processes. We shall consider such processes presently. We note here that all characteristic times of inelastic processes increase with decreasing temperature. If we set $1/\tau_\phi = AT^p$, Eq. (4.74) gives the temperature dependence of the anomalous negative correction to the conductivity [35].

Diffuson and Cooperon modes of diffusion provide a powerful way of treating diagrammatic perturbation theory. For the remainder of this section we will consider how this technology can be applied. In doing so we will visit various problems which have been extensively reviewed in the literature and our discussion will be deliberately brief. For a more lengthy discussion of coherence effects in disordered conductors we refer to reviews, for example, by Bergmann [11], Lee and Ramakrishnan [12], Altshuler et al. [15, 36, 37], Chakravarty and Schmid [13], Aronov and Sharvin [14] and Kramer and MacKinnon [2].

4.4.4. Spin Scattering

So far we have assumed impurity scattering to be spin independent. Scattering from magnetic impurities and spin-orbit interaction lead to a spin-dependent interaction of the form

$$\int (\mathrm{d}p)(\mathrm{d}p')\psi^*_\alpha(\boldsymbol{p})U_{\alpha\beta}(\boldsymbol{p},\boldsymbol{p}')\psi_\beta(\boldsymbol{p}'), \tag{4.76}$$

where the Greek subscripts denote the spin of the electron, and

$$U_{\alpha\beta}(\boldsymbol{p},\boldsymbol{p}') = U\delta_{\alpha\beta} + U_{\mathrm{s}}\boldsymbol{S}\cdot\boldsymbol{\sigma}_{\alpha\beta} + U_{\mathrm{so}}[\boldsymbol{p}\times\boldsymbol{p}']\cdot\boldsymbol{\sigma}_{\alpha\beta}. \tag{4.77}$$

$\boldsymbol{S}$ denotes the spin of the magnetic impurities, and U_{s} and U_{so} respectively denote the strength of the potential of the magnetic impurities and the spin-orbit interaction.

Spin dependent scattering modifies the average single-particle Green function only through the mean free time,

$$\frac{1}{\tau_{\mathrm{tot}}} = \frac{1}{\tau} + \frac{1}{\tau_{\mathrm{s}}} + \frac{1}{\tau_{\mathrm{so}}}, \tag{4.78}$$

where

$$\frac{1}{\tau_{\rm s}} = \pi\nu S(S+1)U_{\rm s}^2, \qquad \frac{1}{\tau_{\rm so}} = \pi\nu\overline{U}_{\rm so}[\boldsymbol{p}\times\boldsymbol{p}']^2, \tag{4.79}$$

with the bar denoting the angular average. $1/\tau_{\rm s}$ and $1/\tau_{\rm so}$ give a temperature independent contribution to the scattering time.

For the two-particle Green function in the particle-particle channel we have the same ladder approximation discussed earlier. For arbitrary values of τ and $\tau_{\rm so}$ the resulting integral equation is non-trivial, however, for $\tau_{\rm so} \gg \tau \sim \tau_{\rm tot}$ the electron momentum changes many times during the spin exchange. Thus the solution to the integral equation is determined by the kernel $\overline{U_{\alpha\nu}(\boldsymbol{p},\boldsymbol{p}')U_{\delta\nu}(\boldsymbol{p}',\boldsymbol{p})}$ averaged over all directions of momenta. In this case the spin-dependent equation for the Cooperon takes the form

$$\begin{aligned} C_{\alpha\beta\gamma\delta}(\mathbf{Q},\omega) &= \delta_{\alpha\beta}\delta_{\gamma\delta}\zeta(\mathbf{Q},\omega) \\ &\quad + \overline{U_{\alpha\nu}(\boldsymbol{p},\boldsymbol{p}')U_{\delta\nu}(\boldsymbol{p}',\boldsymbol{p})}\zeta(\mathbf{Q},\omega)C_{\mu\beta\gamma\nu}(\mathbf{Q},\omega), \end{aligned} \tag{4.80}$$

where ζ is given by Eq. (4.61) [38, 39, 15].

The coefficients can be separated into different contributions according to the total spin. Generally

$$C_{\alpha\beta\gamma\delta}(\mathbf{Q},\omega) = \sum_{J=0,1}\sum_{M=-J}^{J} c^{(J,M)} a_{\alpha\beta}^{JM}(a_{\gamma\delta}^{JM})^*, \tag{4.81}$$

where $a_{\alpha\beta}^{JM}$ denote the Clebsh-Gordon coefficients,

$$a^{00} = \mathrm{i}\sigma_y, \qquad a^{10} = \sigma_x, \qquad a^{1,\pm1} = \frac{\mathbf{1}\pm\sigma_z}{2}, \tag{4.82}$$

with σ representing the Pauli spin matrices.

Since only the diagonal contribution to the Cooperon enters the quantum correction to the conductivity let us consider the combination $C_{\alpha\beta\beta\alpha}$. Using Eqs. (4.81) and (4.82) we find $a_{\alpha\beta}^{JM}(a_{\beta\alpha}^{JM})^* = (-1)^J$. Moreover, since the coefficients $C^{(J,M)}$ turn out to be independent of M, we can write

$$C_{\alpha\beta\beta\alpha} = -C_{\alpha\beta}^{(0)}(\tau_{\rm s}) + 3C_{\alpha\beta}^{(1)}(\tau_{\rm s},\tau_{\rm so}), \tag{4.83}$$

where we remark that the spin-orbit interaction can not affect the singlet channel.

For magnetic impurities, random spin exchange occurs on a time scale $\tau_{\rm s}$ and the wavefunction becomes incoherent. As a consequence, for $\omega\tau_{\rm s} \ll 1$ the quantum correction to the conductivity has a weak dependence on frequency and is determined solely by $\tau_{\rm s}$ [38]. This contrasts with the diffuson propagator which, according to the particle conservation law, retains a pole even for $\tau_s \neq 0$.

The dependence on spin-orbit scattering is richer. τ_{so} does not enter the singlet $J = 0$ channel but affects only the triplet $J = 1$ channel. In the absence of spin-orbit scattering $C^{(0)}$, $C^{(1)}$, and the conductivity decrease with decreasing frequency or temperature. However, for strong spin-orbit scattering, $\omega\tau_{so} < 1$ the effect is reversed and the conductivity increases [39].

4.4.5. Anomalous Magnetoconductance

We now turn to the effect of a magnetic field on electron diffusion in a disordered conductor. Classically, we would anticipate a strong effect when $\omega_c\tau \geqslant 1$, where $\omega_c = eH/mc$ denotes the cyclotron frequency. Quantum mechanically, our consideration of Feynman paths suggests that quantum coherence effects will be suppressed when interfering paths enclose a flux of order unity. The corresponding phase coherence length can be estimated to be $\sqrt{\phi_0/H} = \sqrt{\hbar c/eH}$. Using $D \propto \hbar k_F l/m$ we find that this condition holds when $\omega_c\tau \sim (1/k_F l)(\tau/\tau_\phi)$, a value much smaller than unity. Therefore quantum effects show up at much weaker fields than classical effects.

Let us examine the effect of magnetic field on the diffuson and Cooperon propagators. The diffusion equation for $D(\boldsymbol{q},\omega)$ depends on the momentum difference $\boldsymbol{q} = \boldsymbol{p}_1 - \boldsymbol{p}_2$ whereas for $C(\mathbf{Q},\omega)$, the dependence is on the momentum sum $\mathbf{Q} = \boldsymbol{p}_1 + \boldsymbol{p}_2$. Consequently, the diffusion equation for the former is independent of magnetic field, while the Cooperon modes couple to the magnetic field with an effective charge $2e$.

$$\left[-\mathrm{i}\omega + D\left(-\mathrm{i}\boldsymbol{\nabla} - \frac{2e}{c}\boldsymbol{A}(\boldsymbol{r})\right)^2 + \frac{1}{\tau_\phi}\right] C(\boldsymbol{r},\boldsymbol{r}';\omega) = \frac{1}{\tau}\delta(\boldsymbol{r}-\boldsymbol{r}'). \quad (4.84)$$

The Cooperons behave as particles obeying a Schrödinger equation in imaginary time with an effective mass $1/2D$ and energy $1/\tau_\phi$. Since the mass is $k_F l$ times smaller than the effective mass of the electron, the corresponding cyclotron frequency

$$\Omega_c = 4DeH/\hbar c, \quad (4.85)$$

will be $k_F l$ times larger. This accounts for the sensitivity of quantum corrections to the conductivity to changes in magnetic field.

Solving Eq. (4.84) in three dimensions we obtain,

$$C(\boldsymbol{r},\boldsymbol{r}';\omega) = \sum_{n,\alpha} \frac{\psi^*_{n\alpha}(\boldsymbol{r})\ \psi_{n\alpha}(\boldsymbol{r}')}{[-\mathrm{i}\omega + DQ_\parallel^2 + \Omega_c(n+1/2) + 1/\tau_\phi]\tau}, \quad (4.86)$$

where $\psi_{n\alpha}(\boldsymbol{r})$ is the wavefunction with band index α in Landau level n, and $Q_{\|}$ is the component of total momentum parallel to the magnetic field.

Using Eq. (4.71) in the form

$$\delta\sigma(\omega) = -\frac{De^2\tau}{2\pi}C(\boldsymbol{r}=\boldsymbol{r}',\omega), \tag{4.87}$$

the sum over α and n can be readily performed and gives the result

$$\sigma_d(H) - \sigma_d(0) = \frac{e^2}{2\pi^2\hbar} f_d(\Omega_c\tau_\phi) L_H^{d/2-1}, \quad L_H = \left(\frac{eH}{hc}\right)^{-1/2}, \tag{4.88}$$

where L_H denotes the magnetic length. The particular functional form of $\sigma(H)$ is dependent on the dimensionality. In two dimensions [39]

$$f_2(x) = \ln x + \frac{\Gamma'(1/2+1/x)}{\Gamma(1/2+1/x)} = \begin{cases} x^2/24 & x \ll 1, \\ \ln x & x \gg 1, \end{cases} \tag{4.89}$$

where $\Gamma(x)$ denotes the Γ-function. The same asymptotics can be obtained using simple arguments. A diffusing particle returning after a time t typically encloses an area Dt. The dephasing of time-reversed paths modifies the previous estimate for the conductivity in Eq. (4.68) [10],

$$\frac{\delta\sigma}{\sigma} \sim -v_F\lambda_F^2 \int_\tau^{t_c} \frac{dt}{Dt}\left[1 - \cos\left(\frac{Dt}{L_\phi^2}\right)\right]. \tag{4.90}$$

Integration leads to directly to the asymptotics in Eq. (4.89).

In three dimensions summation gives the result [40]

$$f_3(x) = \sum_{n=0}^{\infty}\Big[2\Big((n+1+1/x)^{1/2} - (n+1/x)^{1/2}\Big) \\ -(n+1/2+1/x)^{-1/2}\Big], \tag{4.91}$$

$$= \begin{cases} x^{3/2}/48 & x \ll 1, \\ 0.605 & x \gg 1. \end{cases} \tag{4.92}$$

Thus, in the absence of spin-orbit scattering there is a magnetoconductance effect which suppresses weak localization and increases the conductivity. This effect is gradually destroyed by spin-orbit scattering. For strong spin-orbit scattering there is an anomalous magnetoconductance effect in which the conductivity is diminished by the magnetic field (see fig. 13).

4.4.6. Inelastic Processes

Although the interaction between electrons in metals is typically strong, a single particle description still proves to be remarkably successful. This

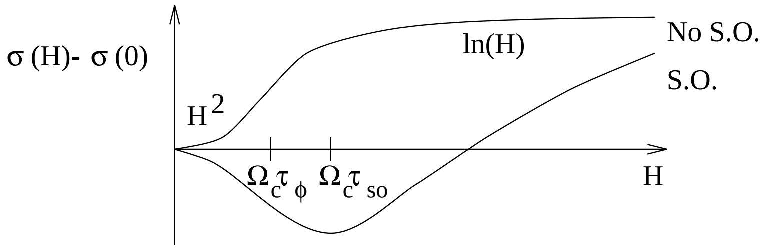

Fig. 13. Schematic diagram showing the magnetoconductance effect in two-dimensions.

can be attributed to the fact that the elementary excitations, which can no longer be thought of in terms of the bare electrons, can be described by weakly interacting quasi-particles — Landau's Fermi-Liquid. Its validity is based on the decay of electronic excitations being small as compared to the Fermi energy. For degenerate Fermi systems without disorder the inverse decay time associated with the electron-electron interaction, $\hbar/\tau_{\rm ee}$ is set by the phase volume to be of order $E^2/E_F \ll E$ where E is the excitation energy measured from the Fermi level E_F. Other inelastic scattering processes involve phonons with a typical relaxation time again set by the phase volume associated with the phonon DoS. For $\omega \sim E \sim T$, $\hbar/\tau_{\rm el-ph} \sim T^3/\theta_D^2$ where θ_D denotes the Debye frequency.

For disordered conductors this picture requires some modification. In this section we will examine how the relaxation times are affected by the presence of disorder. We will investigate two characteristic times; the energy relaxation time, $\tau_{\rm e}$ or the typical time for the an excitation to redistribute its energy as a result of inelastic processes; and the phase relaxation or typical dephasing time, τ_ϕ. The latter, as we have seen, can be determined directly from magnetoresistance measurements.

We first recall that the energy relaxation time associated with electron-electron interactions in a clean metal at zero temperature. Consider the inelastic scattering rate for the collision of an excited electron of energy E with another electron of energy E' involving an energy transfer ω (see fig.14). Using Fermi's Golden rule we find

$$\frac{\hbar}{\tau_{\rm e}(E)} \sim \int_0^E {\rm d}\omega \int_{-\omega}^0 {\rm d}E' \int ({\rm d}q)|U_q|^2 \times \int_{-1}^1 {\rm d}x\ \delta(\omega - qv_F x) \int_{-1}^1 {\rm d}x'\ \delta(\omega - qv_F x'), \tag{4.93}$$

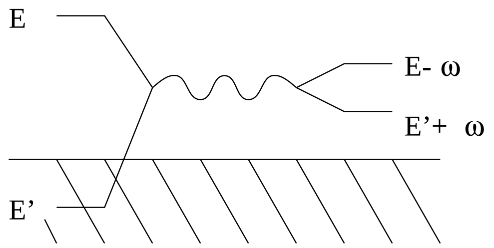

Fig. 14. Schematic diagram showing the relative energy configuration in the scattering.

where all energies are counted from the Fermi level, and $U_q = 4\pi e^2/(\boldsymbol{q}^2 + \kappa^2)$ denotes screened Coulomb interaction between electrons. The final terms represent the angular integrations of scattering; $\delta(\omega - \xi_p + \xi_{p-q}) = \delta(\omega - qv_F x)$ where $x = \boldsymbol{v} \cdot \boldsymbol{q}/v_F q$, $\boldsymbol{v} = \partial\xi_p/\partial\boldsymbol{p}$.

Integrating Eq. (4.93) we obtain

$$\frac{\hbar}{\tau_{\mathrm{e}}} \sim \int_0^E \omega \, \mathrm{d}\omega \int q^{d-1} \mathrm{d}q \frac{|U_q|^2}{(qv_F)^2} \propto \begin{cases} E^2/E_F & d = 3, \\ E^2 \ln(E/E_F) & d = 2. \end{cases} \tag{4.94}$$

The factor $1/qv_F$ can be interpreted physically as the typical time an electron, with velocity v_F, spends in an "interaction region" of dimension $1/q$.

In a disordered conductor, the typical interaction time is set by the diffusion time $\mathrm{Re}[-\mathrm{i}\omega + D\boldsymbol{q}^2]^{-1}$. This suggests that

$$\frac{\hbar}{\tau_{\mathrm{e}}} = \frac{\nu}{2\pi} \int_0^\infty \omega \, \mathrm{d}\omega \int (\mathrm{d}q) |U_q(\omega)|^2 \left[\mathrm{Re}\frac{1}{-\mathrm{i}\omega + D\boldsymbol{q}^2}\right]^2, \tag{4.95}$$

$$\propto \frac{1}{\nu}\left(\frac{E}{\hbar D}\right)^{d/2}, \tag{4.96}$$

a result confirmed by diagrammatic calculation [37]. Defining $L_E = \sqrt{\hbar D/E}$, we obtain

$$\frac{\hbar}{E\tau_{\mathrm{e}}} \equiv \Gamma_d(E) = \frac{1}{\nu E L_E^d} \sim \begin{cases} 1/\sqrt{E} & d = 1, \\ 1/\nu D \sim 1/\hbar(k_F l)(k_F a) & d = 2, \\ \sqrt{E} & d = 3, \end{cases} \tag{4.97}$$

where a denotes the sheet thickness. The quasi-particle picture can be justified when $\omega \sim E \gg \hbar/\tau_{\mathrm{e}}$, $\tau_\phi \sim \tau_{\mathrm{e}}$. Therefore, for sufficiently small excitation energies this picture holds for two and three dimensions. However, for sufficiently small energy scales Eq. (4.97) shows a breakdown of perturbation theory in one-dimension.

At finite temperature, an additional factor of $\coth(\omega/2T)$ is required in Eq. (4.96). As a result we obtain

$$\frac{1}{\tau_{\rm e}} \sim \frac{T}{\nu D^{d/2}} \int^{T} \frac{{\rm d}\omega}{\omega^2} \omega^{d/2}. \tag{4.98}$$

However, this expression is divergent for $d \leqslant 2$. To interpret this unphysical divergence and understand how to set the lower cut-off requires consideration of quasi-elastic scattering to which we now turn.

4.5. Quasi-Elastic Scattering

To what accuracy can the energy of a quasi-particle be measured in a time t? Consider a simplified model in which each inelastic process changes the energy of the quasi-particles randomly by an amount $\pm|\omega|$, assumed small. Given the mean time between inelastic collisions $\tau_{\rm in}$, the total uncertainty of the energy can be presented as a sum of quantum and classical contributions.

$$\Delta = \Delta_{\rm qu}(t) + \Delta_{\rm in}(t), \quad \Delta_{\rm qu}(t) = \hbar/t, \quad \Delta_{\rm in}(t) = \omega\left(\frac{t}{\tau_{\rm in}}\right)^{1/2}. \tag{4.99}$$

The latter diverges both as $t \to 0$ and $t \to \infty$, and takes its minimum when $\Delta_{\rm qu} \sim \Delta_{\rm in}$ or $t_{\rm min} = (\hbar^2 \tau_{\rm in}/\omega^2)^{1/3}$ and $\Delta_{\rm min} \sim \hbar/t_{\rm min}$. Comparing with the resolution time $\tau_{\rm E}$ for which $\Delta_{\rm in} = E$, we observe that $\tau_E = \tau_{\rm in}(E/\omega)^2 \gg t_{\rm min}$.

After a time t, the quasi-particle experiences a typical phase shift $\Delta\phi(t) \sim \Delta_{\rm in}(t)t$. Defining the dephasing time as $\Delta\phi(\tau_\phi) \sim 1$ we find $\tau_\phi \sim 1/\Delta_{\rm in}(\tau_\phi)$. This self-consistent equation has the solution $\tau_\phi \sim (\tau_{\rm in}/\omega^2)^{1/3} \sim t_{\rm min}$ [41]. Therefore, the phase breaking time τ_ϕ is also the shortest relevant inelastic time or inverse minimal uncertainty. If the energy transfer ω is smaller than $\hbar/\tau_\phi$ the scattering can not be considered as inelastic.

This suggests that the integral expression for $\tau_{\rm e}$ in Eq. (4.98) requires a lower cut off $\hbar/\tau_\phi$. As a result Eq. (4.98) leads to a self-consistent equation for τ_ϕ which has the solution

$$\frac{\hbar}{\tau_\phi} \propto \begin{cases} \left(\frac{T}{\nu D^{d/2}}\right)^{\frac{2}{4-d}} & d \neq 2, \\ \frac{T}{g} \ln\left(\frac{T\tau_\phi}{\hbar}\right) \propto T\frac{\ln g}{g} & d = 2, \end{cases} \tag{4.100}$$

where we have used to Einstein relation in Eq. (2.28) to define the dimensionless conductance $g = \sigma/(e^2/\hbar) = \hbar\nu D$. It follows from Eq. (4.100) that for $g \gg 1$, the inverse relaxation time $\hbar/\tau_\phi \ll T$, and the quasi-particles are well defined. In one dimension, $T\tau_\phi \propto T^{1/3}$ which implies a breakdown of the quasi-particle picture for $T\tau_\phi < 1$. For a conductivity per unit length of σ, the localization length is of order $\xi \sim \hbar\sigma/e^2$ ($g \sim 1$), and

$$L_\phi = \sqrt{D\tau_\phi} \propto \left(\frac{\hbar D}{T}\xi\right)^{1/3} \propto (L_T^2\xi)^2, \qquad \frac{T\tau_\phi}{\hbar} \propto \left(\frac{\xi}{L_T}\right)^{2/3}. \tag{4.101}$$

This implies that $\hbar/\tau_\phi \sim T$ when $L_T \sim L_\phi \sim \xi$. The conclusion is that near localization, the quasi-particles are badly defined. The whole picture seems unstable to electron-electron interaction. However, while L_ϕ, $L_T \ll \xi$ quasi-particles are well defined.

Substituting the phase relaxation time into the weak localization corrections to the conductivity in Eq. (4.74) (and incorporating the correct numerical prefactor) we obtain

$$\delta\sigma_d = \begin{cases} -0.55\frac{e^2}{\hbar}\left(\frac{\hbar^2\sigma_1 D}{e^2 T}\right)^{1/3} & d=1, \\ -\frac{e^2}{2\pi^2\hbar}\ln T & d=2. \end{cases} \tag{4.102}$$

Although we took into account τ_ϕ everything still depends on σ and D. The most impressive experimental confirmation of this temperature dependence of the conductivity can be found in Ref. [42].

How can we unambiguously obtain τ_ϕ? The average one-particle Green function depends on just one relaxation time which contains both elastic and inelastic times. In principle, although these are distinguished by the one-particle Green function, there is no way of treating it analytically. In contrast, the two-particle Green function serves as definition through the equation

$$C(\boldsymbol{q}=0, \omega=0) = \int \mathrm{d}\boldsymbol{r}\ C(\boldsymbol{r}, 0; \omega=0) = \frac{\tau_\phi}{\tau}, \tag{4.103}$$

where $C(\boldsymbol{q}, \omega) = [-\mathrm{i}\omega + Dq^2 + 1/\tau_\phi]^{-1}\tau$.

A second definition involves the formula for the quantum correction to the conductivity,

$$\delta\sigma(T) = -\frac{2e^2\tau}{\pi}DC(\boldsymbol{r}=\boldsymbol{r}') = \begin{cases} -\frac{e^2}{\pi\hbar}\sqrt{D\tau_\phi} & d=1, \\ -\frac{e^2}{\pi^2\hbar}\ln\frac{\tau_\phi}{\tau} & d=2, \\ \frac{e^2}{2\pi^2\hbar}\frac{1}{\sqrt{D\tau_\phi}} & d=3. \end{cases} \tag{4.104}$$

From a theoretical point of view, gauge invariance of σ_d favors the second definition over the first. Indeed from an experimental point of view, it is better to obtain τ_ϕ from the magnetoconductance.

4.6. Noise and Dephasing

For energy transfer $\omega \ll T$, we have $\coth(\omega/2T) \gg 1$. Therefore, from the point of view of a given electron, the effect of the other electrons can be thought of as a classical electromagnetic field, random in space and time — Nyquist noise. In the present section we will follow Ref. [43] and make use of the Schrödinger equation for the Cooperon in a random electromagnetic field to determine $C(\boldsymbol{r}, 0; \omega = 0)$ and estimate τ_ϕ using Eq. (4.103).

In a time-dependent electromagnetic field the Cooperon satisfies the diffusion equation (for a derivation, see Refs. [43, 37])

$$\left[\frac{\partial}{\partial t} + D\Big(-\mathrm{i}\boldsymbol{\nabla} - \tfrac{2e}{c}\mathcal{A}(\boldsymbol{r}, t, \theta)\Big)^2\right] C(\boldsymbol{r}, \boldsymbol{r}'; \theta, \theta'; t, t') = \tfrac{1}{\tau}\delta(\boldsymbol{r} - \boldsymbol{r}')\delta(t - t')\delta(\theta - \theta'), \tag{4.105}$$

where

$$\mathcal{A}(\boldsymbol{r}, t, \theta) = [\boldsymbol{A}(\boldsymbol{r}, \theta - t/2) + \boldsymbol{A}(\boldsymbol{r}, \theta + t/2)]/2. \tag{4.106}$$

Since the parameter θ does not involve time derivatives, we can deduce that $C(\theta, \theta') = C(\theta)\delta(\theta - \theta')$. Eq. (4.105) continues to describe the Schrödinger equation of a particle with charge $2e$ now propagating in a non-trivial effective vector-potential $\mathcal{A}$. The correlation function for the random function $\mathcal{A}$ can be derived from the correlator of $\boldsymbol{A}$.

An expression for the Cooperon propagator can be obtained from the Feynman path integral

$$C(\boldsymbol{r}, \boldsymbol{r}'; \theta; t) = \frac{1}{\tau}\int_{\boldsymbol{r}(t)=\boldsymbol{r}}^{\boldsymbol{r}(t')=\boldsymbol{r}'} \mathcal{D}\boldsymbol{r}(t) \exp\left[-\int_t^{t'} \mathrm{d}\tilde{t}\,\left(\frac{\dot{\boldsymbol{r}}^2}{4D} + \mathrm{i}\dot{\boldsymbol{r}}\cdot\mathcal{A}\right)\right]. \tag{4.107}$$

For Gaussian fluctuations of $\mathcal{A}$ the final term in the action is replaced by

$$\int \mathrm{d}\tilde{t}_1\,\mathrm{d}\tilde{t}_2\;\dot{r}_\alpha(\tilde{t}_1)\cdot\dot{r}_\beta(\tilde{t}_2)\Big\langle \mathcal{A}_\alpha(\boldsymbol{r}(\tilde{t}_1), \tilde{t}_1)\mathcal{A}_\beta(\boldsymbol{r}(\tilde{t}_2), \tilde{t}_2)\Big\rangle. \tag{4.108}$$

For a general correlator of $\mathcal{A}$ the path integral remains intractable. However, in the present case, translational invariance allows one of the time integrations to be performed by parts,

$$\frac{\partial}{\partial t}\exp[\mathrm{i}\boldsymbol{k}\cdot\boldsymbol{r}(t)] = \mathrm{i}\boldsymbol{k}\cdot\dot{\boldsymbol{r}}(t)\exp[\mathrm{i}\boldsymbol{k}\cdot\boldsymbol{r}(t)]. \tag{4.109}$$

We therefore require only the expression for the propagator of the fluctuating electromagnetic field. In the classical limit, the correlator $\langle A_\alpha(0,0)A_\beta(\boldsymbol{r}, t)\rangle_{\boldsymbol{k},\omega}$ is defined by the fluctuation-dissipation theorem. For simplicity we will assume that $D\kappa^2/\omega \gg 1$ where κ is the inverse Debye screening length. Moreover, if (as it usually is) $|\boldsymbol{k}|\delta_d \gg 1$ where the skin depth

$$\delta_d(\omega) = \begin{cases} c(2\pi\omega\sigma)^{-1/2} & d = 3, \\ c^2(2\pi\omega\sigma_\Box)^{-1} & d = 2, \end{cases} \tag{4.110}$$

and $\sigma_\Box$ denotes the sheet conductance, the correlator is given by

$$\langle A_\alpha(0,0)A_\beta(\boldsymbol{r},t)\rangle_{\boldsymbol{k},\omega} \approx \frac{2T}{\sigma_d}\frac{c^2}{\omega^2}\frac{k_\alpha k_\beta}{\boldsymbol{k}^2}. \tag{4.111}$$

Substituting the correlator we find that the Cooperon obeys the Schrödinger equation

$$\left[\frac{\partial}{\partial t} - D\frac{\partial^2}{\partial \rho^2} + U(\boldsymbol{\rho})\right] C(\boldsymbol{\rho},\boldsymbol{\rho}';t,-t) = \frac{1}{\sqrt{2}\tau}\delta(t)\delta(\boldsymbol{\rho}-\boldsymbol{\rho}'), \tag{4.112}$$

where $\boldsymbol{\rho}(t) = [\boldsymbol{r}(t) - \boldsymbol{r}(-t)]/\sqrt{2}$, and the effective "Coulomb interaction" is given by

$$U(\boldsymbol{\rho}) = \frac{2e^2T}{\sigma_d}\int(\,\mathrm{d}k)\frac{1-\cos(\sqrt{2}\boldsymbol{k}\cdot\boldsymbol{\rho})}{\boldsymbol{k}^2}. \tag{4.113}$$

Solving Eq. (4.112) we can obtain

$$C(\boldsymbol{r}=\boldsymbol{r}';\omega=0) = \int \mathrm{d}t\; C(\boldsymbol{\rho}=\boldsymbol{\rho}';t,-t), \tag{4.114}$$

which leads to the equations

$$\frac{\hbar}{\tau_\phi} \propto \frac{e^2T}{\sigma_d}L_\phi^{2-d}, \qquad D^{1-d/2}\tau_\phi^{2-d/2} \propto \frac{\sigma_d}{e^2T}, \tag{4.115}$$

and the solution

$$\tau_\phi \propto \left(\frac{\sigma_d}{e^2T}D^{d/2-1}\right)^{\frac{2}{4-d}}. \tag{4.116}$$

This compares with Eq. (4.100) and implies that the estimation based on the Golden rule with a proper low energy cut-off gives the same result as the straightforward calculation discussed in this section. Note that the only assumption was to neglect the frequency and momentum dispersion of the conductivity which is justified by the large relevant distance and time scales.

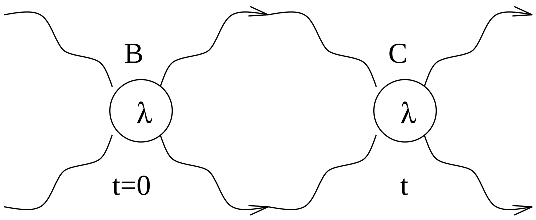

Fig. 15. Trajectories of two particles which interact at points B and C.

4.7. Effects of Electron-Electron Interaction

How does the electron-electron interaction manifest itself in measurable properties? Although, as we have seen, the average DoS, specific heat, magnetic susceptibility, etc. feel no correction due to weak localization effects, the electron interaction has a dramatic effect. Denoting each property by X we will argue that

$$\frac{\delta X(E)}{X} \propto \Gamma_d(E) \propto \begin{cases} 1/\sqrt{E} & d=1, \\ \ln \tau E & d=2, \\ \sqrt{E} & d=3, \end{cases} \tag{4.117}$$

where the typical excitation energy, $E \sim T$ and $\Gamma_d(E)$ is defined in Eq. (4.97).

The physical meaning of $\Gamma_d(E)$ can be found in terms of the semi-classical return probability. Consider a Fermi gas with weak short-ranged interactions. The parameters of Fermi-liquid theory such as mass renormalization rely on short length and large energy scales. As such their effects can be separated from that of disorder. Between each electron-electron interaction there is normal diffusion (see fig. 15). On time scales short as compared to $\hbar/E$ all interaction probabilities interfere constructively while at longer times there is a dephasing and loss of coherence. The properties of a Fermi-liquid is defined through an interaction constant, λ_0. In disordered metals, on time scales $t < \hbar/E$, the latter becomes renormalized by weak localization. The reason is that the probability amplitudes for two particles to interact interfere constructively at this time scale. The additional contribution to λ is determined by the probability to meet again at a time shorter than $\hbar/E$ (see fig. 15).

$$\lambda \sim \lambda_0\Big[1 + \int_\tau^{\hbar/E} \frac{v_F\,\mathrm{d}t}{k_F^{d-1}(Dt)^{d/2}}\Big] \sim \lambda_0\Big[1+\Gamma_d(E)\Big]. \tag{4.118}$$

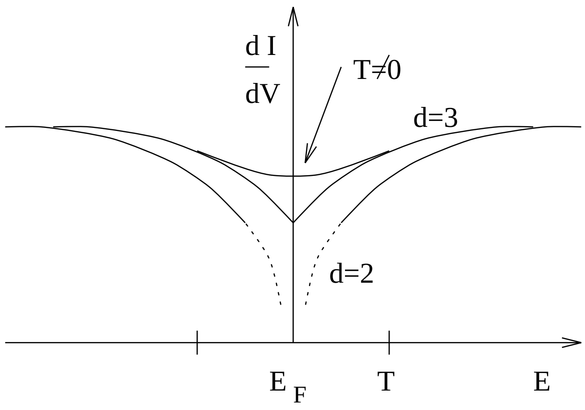

Fig. 16. Schematic diagram of the zero-bias anomaly or dip in the tunnelling DoS at the Fermi level. The smoothing of the cusp-like singularity at non-zero temperature is indicated.

Any physical quantity that depends on λ is therefore renormalized ($\delta X/X \propto \delta\lambda/\lambda \propto \Gamma_d(E)$) from which Eq. (4.117) can be deduced.

4.8. Zero-Bias Anomaly

Eq. (4.117) implies a singularity in the DoS which should manifest itself in the dependence of the resistance of a tunnelling contact on bias voltage. Taking the typical excitation energy to be of order the bias voltage eV, the change in the conductivity is proportional to the change in the DoS,

$$\frac{\delta G}{G} = \frac{\delta\nu(eV)}{\nu} = \Gamma_d(eV). \tag{4.119}$$

This produces a dip, or zero-bias anomaly [44] in the tunnel conductance as a function of gate voltage (see fig.16). This prediction has been confirmed by many experiments (see e.g. Dynes and Garno [45]).

A second interpretation of the zero-bias anomaly can be conceived in the following way [46]. The transfer of an electron from a tunnel junction or STM involves the creation of a wave-packet close to the tunnel contact. At first the wave-packet is strongly peaked and feels a Coulomb interaction energy which, if the interaction is short-ranged, has an energy

$$E_{\text{int}}(t) \sim \lambda \int \mathrm{d}\boldsymbol{r}\rho(\boldsymbol{r},t)^2. \tag{4.120}$$

For simple diffusion, the particle density is roughly constant over a radius $r(t)$ with a density $\rho(t) \sim r(t)^{-d}$. While $E < E_{\rm int}$ the particle remains "under the barrier." Therefore, the probability for a particle to tunnel onto the conductor is proportional to the action $\exp[-S_{\rm int}] \sim 1 - S_{\rm int}$ which is approximately equal to

$$S_{\rm int} \sim \lambda \int_{\tau}^{\min(1/eV,1/T)} \frac{v_F \, {\rm d}t}{k_F^{d-1}(Dt)^{d/2}} = \lambda \Gamma_d. \tag{4.121}$$

This concludes our very brief discussion of the influence of electron-electron interactions on the properties of disordered conductors. For more details including a more formal discussion of the diagrammatic approach, we refer to the review of Ref. [37].

5. Diffusion Modes and Fluctuations

Earlier we discussed the phenomenon of universal mesoscopic conductance fluctuations, and found a qualitative explanation based on level repulsion. The diffusion modes provide the means for quantitative theory to which we now turn.

5.1. Density of States Fluctuations

In contrast to the average, the fluctuation in the DoS depends on disorder. To examine its dependence we will determine the connected part of two-point DoS correlator

$$K(\Omega) = \Big\langle \nu(E - \Omega/2) \; \nu(E + \Omega/2) \Big\rangle_c . \tag{5.122}$$

Making use of Eq. (4.49), $K(\Omega)$ can be expressed through the product of retarded and advanced Green functions. The leading order (in $1/k_F l$) contribution from perturbation theory arises from the exchange of two diffuson and (for T-invariant systems) Cooperon ladders between two closed loops or tadpole diagrams (see Fig. 17). Substituting the propagators for the diffusion ladders in Eqs. (4.62) and (4.70), we obtain [47]

$$K(\Omega) = -\frac{s^2}{\pi^2 L^{2d}} {\rm Re} \sum_{\boldsymbol{q}} \frac{1}{[\Omega + {\rm i}D\boldsymbol{q}^2 + {\rm i}\gamma]^2}, \tag{5.123}$$

where s denotes the spin degeneracy and we have included some broadening, γ which might be due to, say, inelastic collisions.

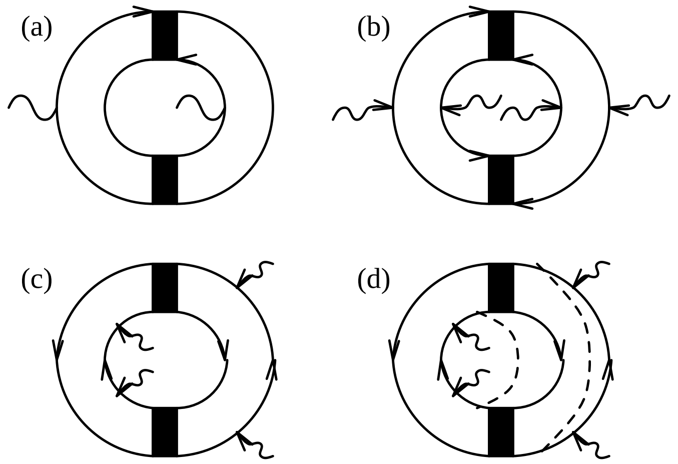

Fig. 17. Diagrams contributing to fluctuations in (a) the DoS and (b)-(d) the conductivity involving the exchange of diffuson ladders. In each case a similar Cooperon diagram can be drawn. In diagrams (b)-(d) the vertices carry vector indices.

For energy scales Ω much smaller than the Thouless energy $E_c = \hbar D/L^2$ we can focus on the lowest mode ($\boldsymbol{q} = 0$) for which

$$K(\Omega) = \frac{s^2}{\pi^2 L^{2d}} \frac{\gamma^2 - \Omega^2}{(\gamma^2 + \Omega^2)^2}, \tag{5.124}$$

This formula is correct for γ much greater than the average level spacing $\Delta = (\nu L^d)^{-1}$. For $\Omega > \gamma$ the formula reflects level repulsion whereas for $\Omega < \gamma$ it is determined predominantly by the correlation of the level with itself.

Eq. (5.124) has important implications for the rigidity of the spectrum. In particular, if we consider the fluctuation in the number of levels contained within some interval E of energy, which by convention is known as $\Delta_3(E)$, we find,

$$\Delta_3(E) = \int_{-E/2}^{E/2} \mathrm{d}E_1 \;\; \mathrm{d}E_2 K(E_1 - E_2) = \frac{s^2}{\pi^2} \ln\Big(\frac{E^2 + \gamma^2}{\gamma^2}\Big). \tag{5.125}$$

This compares with the result found for random matrix ensembles which gives [25]

$$\Delta_3(E) = \frac{2s^2}{\pi^2} \ln\Big(\frac{E}{\Delta}\Big). \tag{5.126}$$

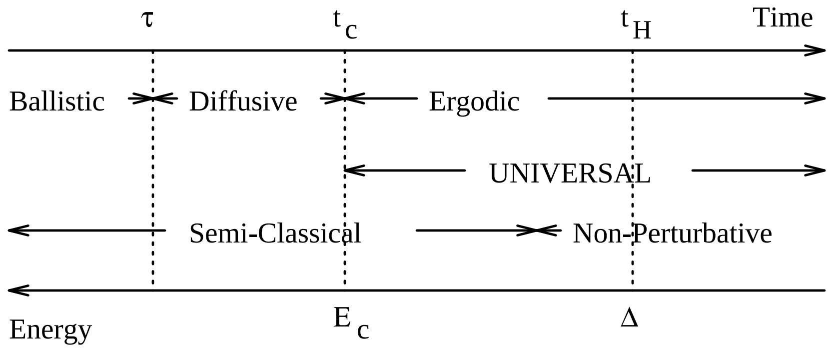

Fig. 18. Schematic phase diagram of a disordered metal resolved along time and energy scales.

The logarithmic dependence is characteristic of spectral rigidity which both random matrix ensembles and disordered metallic grains share. This coincidence is not accidental but closely related to the effective zero-dimensionality of the system when observed on time scales longer than the typical transport time, $t_c = \hbar/E_c$ (see fig. 18). Beyond t_c we can expect ergodic behavior in which the probability density of an injected particle is spread uniformly in phase space. Later we will have much to say about random matrix theory and its role in describing the behavior of disordered metals in confined geometries

5.2. Conductance Fluctuations

Conductance fluctuations can be treated similarly. Focusing on the connected average, the leading order contribution again comes from the exchange of two diffuson or Cooperon ladders between each conductance loop. The presence of two vector vertices on each loop increase the number of different contributions and they are shown in Fig. 17. Following Ref. [47], summing over diffuson and Cooperon modes, the total mean-square fluctuation in the static conductivity is given by

$$\langle \delta\sigma_{\alpha\gamma}\delta\sigma_{\nu\rho}\rangle = s^2\left(\frac{\sigma\tau^2}{\pi\nu V}\right)\sum_{\boldsymbol{q}}\int \frac{\mathrm{d}E_1\ \mathrm{d}E_2}{[4T\cosh(E_1/2T)\cosh(E_2/2T)]^2}$$
$$\times\left[\left|D(\boldsymbol{q}, E_1 - E_2)\right|^2\ \left(\delta_{\alpha\nu}\delta_{\gamma\rho} + \delta_{\gamma\nu}\delta_{\alpha\rho}\right)\right.$$

$$+\mathrm{Re}\Big(D(\boldsymbol{q}, E_1 - E_2)\Big)^2 \delta_{\alpha\gamma}\delta_{\nu\rho}\Big], \tag{5.127}$$

where $D(\boldsymbol{q}, E)$ is the diffusion pole defined in Eq. (4.62). At zero temperature this result can be greatly simplified by recognizing that the integrand is non-zero only when $E_1 = E_2 = 0$. In this case both terms contribute equally,

$$\Big|\tau D(\boldsymbol{q}, 0)\Big|^2 = \mathrm{Re}\Big(\tau D(\boldsymbol{q}, 0)\Big)^2 = \frac{1}{(D\boldsymbol{q}^2)^2}. \tag{5.128}$$

As a result, direct summation gives [12, 7, 48]

$$\langle \delta G_{\alpha\gamma} \delta G_{\mu\rho} \rangle = s^2 \Big(\frac{e^2}{\pi^3 \hbar}\Big)^2 b_d \Big(\delta_{\alpha\mu}\delta_{\gamma\rho} + \delta_{\alpha\rho}\delta_{\gamma\mu} + \delta_{\alpha\gamma}\delta_{\mu\rho}\Big), \tag{5.129}$$

where $b_1 = \pi^4/90$, $b_2 \approx 1.51$, and $b_3 \approx 2.0$. In particular, we remark that theory predicts a fluctuation in the conductance of $\mathrm{O}(e^2/\hbar)$ consistent with experiment (see, for example Ref. [49]).

Eqs. (5.124) and (5.129) describe T-invariant systems. Corresponding expressions for systems which violate T-invariance or depend on strong spin-orbit scattering can be found in Ref. [47].

5.3. Parameters of Perturbation Theory

Throughout we have assumed the smallness of the parameter $1/k_F l$. This semi-classical approximation ensures that particle propagation is diffusive. The weak localization correction to the conductivity gave

$$\frac{\delta\sigma_d(\Omega)}{\sigma_d} \approx \frac{1}{g^{d/2}} \Big(\frac{\Omega}{\Delta}\Big)^{d/2-1} \equiv \alpha_d(\Omega), \tag{5.130}$$

where $(\Omega/\Delta)^{d/2-1} \to \ln(1/\Omega\tau)$ in two dimensions. Similarly, higher mode corrections to $\Delta_3(E)$ can be shown to be proportional to $\alpha_d(E)$. Rather than $1/k_F l$, α_d plays the role of the parameter of the perturbation theory. This is witnessed by the infrared divergences of Eq. (5.123) in zero-dimensional metallic grains regularized only by the dephasing time. The conclusion is that for energy scales $\Omega < \Delta$, or equivalently for time scales $t > t_H = \Delta^{-1}$ perturbation theory fails (see fig. 18).

This concludes our discussion of the theory of weak localization. In this brief review we have been able to address only a few of its many successes. To learn more we would direct readers to reviews such as Refs. [2, 8, 11–16, 30, 36, 37]. In the following section we will return to the phenomena of strong localization and the scaling theory.

6. Field Theory of Localization

Although diagrammatic perturbation theory brings much insight we have also seen that the domain of its applicability is restricted. At the same time, the description of one-parameter scaling theory in terms of critical phenomena suggests that the problem of localization can be presented in the form of an effective field theory. In 1979 Wegner [50] proposed such a description of disordered conductors in the form of a non-linear σ-model. The effective action can be regarded as a Landau-Ginzburg functional for the low energy, long wavelength density fluctuations. Although the field theory seems highly non-trivial, it admits, under renormalization group, to a solid mathematical basis for the one-parameter scaling hypothesis. Soon after its introduction, several authors proposed a derivation of the σ-model model from a microscopic Hamiltonian. This lead to a number of important developments [51–58].

Conventional perturbation theory shows that the low energy, long wavelength properties of disordered metals are governed by diffusion modes which behave essentially as particles described by the propagator $\nu[D\boldsymbol{q}^2 - i\omega]^{-1}$. It is their interaction that drives the transition to localization. The field theoretic approach described below shows that the diffusion modes are precisely the Goldstone modes of a non-linear σ-model.

6.1. Supersymmetry Method

The basis of the field theoretic approach is the representation of correlation functions in the form of a functional or path integral over auxiliary fields. For this purpose different types of fields have been applied. The original calculation of Wegner [50] and subsequent works by Refs. [51, 53] relied on the use of commuting or bosonic fields. Subsequent developments by Efetov et al.[52] considered anticommuting Grassmann or fermionic fields. Both approaches make use of the replica trick [59, 60] in presenting averages over the random potential. Instead we will focus on a third approach which involves an equal number of bosonic and fermionic fields. As we will see presently, this approach, introduced by Efetov [57] circumvents the need for replicas. All three approaches can be developed largely in parallel and all yield the same results within a perturbative treatment. However, as a cautionary remark, Verbaarschot and Zirnbauer [61] have demonstrated that the analytic continuation called for in the replica approach apparently fails to account correctly for all contributions which are non-perturbative. Since such terms will be crucial to our later discussion of zero-dimensional systems or "quantum dots" we will focus on the "supersymmetry" approach

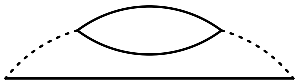

Fig. 19. Unphysical loops generated by the ensemble average.

of Efetov.§

6.1.1. Functional Integral

The field theoretic approach relies on finding a representation of Green functions which allows ensemble averaging. This is achieved by presenting bare Green functions in the form of functional or path integrals over auxiliary fields $\psi(\boldsymbol{r})$,

$$G^R(\boldsymbol{r},\boldsymbol{r}';E) = \frac{1}{\mathcal{Z}}\int \mathcal{D}\psi(r)\ \mathrm{e}^{-L(\psi)}\ \psi^\dagger(\boldsymbol{r})\ \psi(\boldsymbol{r}'), \tag{6.131}$$

$$L(\psi) = -\mathrm{i}\int \psi^\dagger(\boldsymbol{r})\Big[E - H(\boldsymbol{r}) + \mathrm{i}0\Big]\psi(\boldsymbol{r})\,\mathrm{d}\boldsymbol{r}, \tag{6.132}$$

where the field operators are defined in terms of the exact single-particle wavefunctions $\psi_k(\boldsymbol{r})$ of the full Hamiltonian H through the relations

$$\psi(\boldsymbol{r}) = \sum_k \Phi_k\,\psi_k(\boldsymbol{r}), \qquad \psi^\dagger(\boldsymbol{r}) = \sum_k \Phi_k^\dagger\,\psi_k^*(\boldsymbol{r}). \tag{6.133}$$

The representation of the advanced Green function follows accordingly.

The partition function $\mathcal{Z}$ plays a crucial role. Its presence generates unphysical loops (see, for example, fig. 19) that become connected with the main body of the diagram only after averaging. To proceed it is necessary to invoke some method of averaging that eliminates these loops. The method adopted by Wegner [50] is to replicate the fields $\psi \to \psi_n$, $n = 1, \cdots N$. Since such loops enter with a weight proportional to N, they are subsequently eliminated at the end of the calculation by analytic continuation $N \to 0$. The merit of this procedure is that it enables interaction effects to be treated. Its disadvantage is that the validity of the analytic continuation seems questionable [61].

The approach we adopt follows the supersymmetry method of Efetov [57, 58]. While complex or bosonic fields generate loops with a weight of one sign, fermionic or Grassmann fields contribute with the opposite sign. As

§ We remark that a detailed and technical account of the supersymmetry approach can be found in the contribution of Fyodorov to this volume.

a result, employing an equal number of bosonic and fermionic fields all loops are cancelled automatically. Mathematically, this can be seen as the cancellation of determinants arising from the Gaussian integration which defines the partition function: the bosonic fields bring the determinant to the denominator while the fermionic fields bring the same determinant to the numerator.

Since we will deal with the supersymmetry method explicitly in discussing metallic grains, we will employ the latter. Following Ref. [58] let us examine the first non-trivial average,¶

$$R(\boldsymbol{r},\boldsymbol{r}';\Omega)=\Big\langle G^A(\boldsymbol{r},\boldsymbol{r}';E-\Omega/2)\;G^R(\boldsymbol{r}',\boldsymbol{r};E+\Omega/2)\Big\rangle. \tag{6.134}$$

Making use of Eqs. (6.131) and (6.132) we can present R in the form of a functional integral. To do so, we introduce a $2\times2\times2$ component superfield Ψ. Taking our notation from Ref. [58] we define

$$\Psi=\begin{pmatrix}\Psi_{d=1}\\ \Psi_{d=2}\end{pmatrix}\equiv\begin{pmatrix}\psi^*\\ \psi\end{pmatrix},\qquad \psi_p=\begin{pmatrix}\psi_{p,g=1}\\ \psi_{p,g=2}\end{pmatrix}=\begin{pmatrix}\chi_p(\boldsymbol{r})\\ S_p(\boldsymbol{r})\end{pmatrix}, \tag{6.135}$$

where the subscripts d, p, and g index the conjugate components, advanced and retarded components, and the graded or Grassmann components respectively. $S(\boldsymbol{r})$ and $\chi(\boldsymbol{r})$ denote bosonic and fermionic fields respectively. Symmetry under T-invariance enforces the condition $\bar{\Psi}\equiv\Psi^\dagger\Lambda=(C\Psi)^T$ where $C=\Lambda C_0$ denotes the charge conjugation operator with

$$[C_0]_{gg'}=\begin{pmatrix}c_1 & 0\\ 0 & c_2\end{pmatrix}_{gg'}, \tag{6.136}$$

$$[c_1]_{dd'}=\begin{pmatrix}0 & -1\\ 1 & 0\end{pmatrix}_{dd'},\qquad [c_2]_{dd'}=\begin{pmatrix}0 & 1\\ 1 & 0\end{pmatrix}_{dd'}, \tag{6.137}$$

and $\Lambda=(-)^p$ is the matrix that breaks the symmetry between the advanced and retarded components.

With this definition, R can be expressed in the form,

$$\begin{aligned}R(\boldsymbol{r},\boldsymbol{r}';\Omega)=\Big\langle\int\mathcal{D}\Psi\;\mathrm{e}^{L_0(\Psi)+L_1(\Psi)}\Big(\Psi^\dagger(\boldsymbol{r})P(\mathrm{a},\mathrm{B})\Psi(\boldsymbol{r}')\Big)&\\ \times\Big(\Psi^\dagger(\boldsymbol{r}')P(\mathrm{r},\mathrm{B})\Psi(\boldsymbol{r})\Big)\Big\rangle&, \end{aligned}\tag{6.138}$$

$$L_0(\Psi)=\frac{\mathrm{i}}{2}\int\mathrm{d}\boldsymbol{r}\;\bar{\Psi}(\boldsymbol{r})\left[E-\frac{\Omega+i0}{2}\Lambda-\frac{\boldsymbol{p}^2}{2m}\right]\Psi(\boldsymbol{r}), \tag{6.139}$$

¶ We recall that random phase cancellation generates an average Green function which is independent of disorder

$$L_1(\Psi) = -\frac{\mathrm{i}}{2}\int \mathrm{d}\boldsymbol{r}\ \bar{\Psi}(\boldsymbol{r})\ V(\boldsymbol{r})\ \Psi(\boldsymbol{r}), \tag{6.140}$$

where $\bar{\Psi} = \Psi^\dagger\Lambda$, $V(\boldsymbol{r})$ denotes the random disorder potential, and the matrices $P(^{\mathrm{a}}_{\mathrm{r}}, \mathrm{B}) = (1 \pm \Lambda)(1-k)/4$, with $k = (-)^g$, project onto the advanced or retarded bosonic block. Since R is an autocorrelation in energy, the matrix Λ enters as a term which breaks symmetry between the advanced and retarded blocks. With this definition, integration of the fields Ψ is convergent.

6.1.2. Ensemble Averaging

Having brought the disorder potential to the exponent, the ensemble average over the δ-correlated white-noise impurity potential $V(\boldsymbol{r})$ can be performed straightforwardly. With $\langle V(\boldsymbol{r})V(\boldsymbol{r}')\rangle = 1/2\pi\nu\tau$ (see section 4), the ensemble average produces the the effective “four-fermion” interaction

$$\langle \mathrm{e}^{-L_1(\Psi)}\rangle = \mathrm{e}^{-L_{\mathrm{int}}(\Psi)}, \qquad L_{\mathrm{int}}(\Psi) = \frac{1}{16\pi\nu\tau}\int \mathrm{d}\boldsymbol{r}\ (\bar{\Psi}\Psi)^2. \tag{6.141}$$

Invariance under rotations of the supervectors in the superspace is broken only by the term $(\Omega + \mathrm{i}0)\bar{\Psi}\Lambda\Psi$. This might suggest that the “order parameter” can be identified as the DoS, $\langle\nu\rangle$ [50]

$$\left\langle \int \mathrm{d}\boldsymbol{r}\ \bar{\Psi}(\boldsymbol{r})\Lambda\Psi(\boldsymbol{r})\right\rangle \propto \left\langle \mathrm{Tr}\Big[G^R(E-\Omega/2) - G^A(E+\Omega/2)\Big]\right\rangle. \tag{6.142}$$

However, for the point of view of conventional critical phenomena, the problem of localization is peculiar in that the order parameter is finite on both sides of the transition. In this case the frequency can be interpreted as a symmetry breaking “external field”. We remark that a similar effective action controls the replica field theory [50, 56].

6.1.3. Hubbard-Stratonovitch Transformation

We now proceed by constructing a good mean-field theory. In Ψ^4 theories the symmetry can be broken by the existence of non-zero averages $Q \sim \langle\Psi\otimes\bar{\Psi}\rangle$. This can lead to Goldstone modes whose spectrum can be obtained by consideration of the long wavelength fluctuations of the collective field Q. The present situation is analogous — in this case we will see that the Goldstone modes are closely related to the diffusion modes of diagrammatic perturbation theory.

To find an effective theory of the long wavelength properties we must first separate the slow from the fast degrees of freedom. To do so, we first perform a Hubbard-Stratonovitch transformation with the introduction of

8×8 supermatrix fields $Q(\boldsymbol{r})$. A similar decomposition can be formed for the replica theory with n-component fields. Although straightforward, the extension of this decoupling to superfields is somewhat technical and we refer to Refs. [58, 62], or the lecture notes by Fyodorov [63] for a more detailed discussion. As a result of the transformation we obtain

$$\mathrm{e}^{-L_{\mathrm{int}}} = \int \mathcal{D}Q \exp\Big[-\frac{1}{2\tau}\int \Big(\bar{\Psi}Q\Psi + \frac{\pi\nu}{4}\mathrm{STr}\ Q^2\Big)\,\mathrm{d}\boldsymbol{r}\Big], \tag{6.143}$$

where the supertrace, STr serves as the trace operation for supermatrices and follows the convention STr $Q =$ Tr $Q_{FF} -$ Tr Q_{BB}. A comprehensive discussion of other supermatrix operations, such as the transpose, can be found in the book by Berezin [64] (or in Refs. [58, 62, 65]).

The symmetry properties of the Hamiltonian in turn induce symmetries of Q reflecting the algebraic structure of the dyadic product $\Psi \otimes \bar{\Psi}$. Taking our notation from Ref. [58], the compactness of the manifold and T-invariance lead to the symmetries,

$$\bar{Q} \equiv CQ^T C^T = Q, \qquad \bar{Q} = KQ^\dagger K, \tag{6.144}$$

where C is defined in Eq. (6.137),

$$[K]_{pp'} = \begin{pmatrix} \mathbf{1}_4 & 0 \\ 0 & k \end{pmatrix}_{pp'}. \tag{6.145}$$

Since the dependence on Ψ is now Gaussian, its integration can be readily performed. Our approximation will be to retain only the one type of coupling of the fields Ψ which does not decay rapidly with distance. As a result the correlator of Eq. (6.134) is expressed as

$$\begin{aligned} R(\boldsymbol{r},\boldsymbol{r}';\Omega) = &-\int \mathcal{D}Q\ \ \mathrm{e}^{-F[Q]} \\ &\times \mathrm{STr}\ [k\ P(\mathrm{a},\mathrm{B})\ \mathcal{G}(\boldsymbol{r},\boldsymbol{r})\ k\ P(\mathrm{r},\mathrm{B})\ \mathcal{G}(\boldsymbol{r}',\boldsymbol{r}')], \end{aligned} \tag{6.146}$$

$$F[Q] = \int \mathrm{d}\boldsymbol{r}\ \Big[\frac{\pi\nu}{8\tau}\mathrm{STr}\ Q^2 - \frac{1}{2}\mathrm{STr}\ (\ln\ \mathcal{G}^{-1})(\boldsymbol{r},\boldsymbol{r})\Big], \tag{6.147}$$

where $\mathcal{G}$ denotes the supermatrix Green function determined by

$$\Big[E - \frac{\Omega + \mathrm{i}0}{2}\Lambda - \frac{\boldsymbol{p}^2}{2m} - \frac{\mathrm{i}}{2\tau}Q(\boldsymbol{r})\Big]\mathcal{G}(\boldsymbol{r},\boldsymbol{r}') = \delta(\boldsymbol{r}-\boldsymbol{r}'). \tag{6.148}$$

6.1.4. Saddle-Point Equation

In the present form it is impossible to proceed further without approximation. Varying the effective action in Eq. (6.147) we obtain the saddle-point

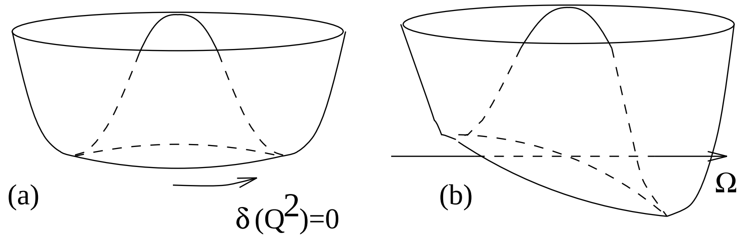

Fig. 20. Schematic representation of the saddle-point manifold for (a) $\Omega \to 0$ and (b) $\Omega > 0$. For $\Omega \to 0$ longitudinal fluctuations around the potential well generate massless Goldstone modes while the transverse fluctuations are massive. For $\Omega > 0$ longitudinal modes become massive.

equation

$$\mathrm{i}Q_{\mathrm{sp}} = \frac{1}{\pi\nu}\int \mathcal{G}(\boldsymbol{p},\boldsymbol{p})(\,\mathrm{d}p). \tag{6.149}$$

To leading order in $(E_F\tau)^{-1}$ Eq. (6.149) can be solved within a self-consistent Born approximation analogous to that used in section 4. Eq. (4.51) suggests the solution $Q_{\mathrm{sp}} = \Lambda$. However, a more careful analysis shows there to be a whole manifold of saddle-points spanned by unitary supermatrices T

$$Q_{\mathrm{sp}} = T\Lambda T^{-1}, \qquad Q_{\mathrm{sp}}^2 = 1. \tag{6.150}$$

The symmetry properties of Q in Eq. (6.144) induce the following constraints on T:

$$T^{-1} = KT^{\dagger}K, \qquad T^T = C^T T^{-1} C. \tag{6.151}$$

Qualitatively, the saddle-point can be compared with the potential shown in fig. 20. Fluctuations in the longitudinal ($\delta(Q^2) \equiv Q(\delta Q) + (\delta Q)Q \neq 0$) direction are massive and do not contribute significantly to the path integral. However, for $\Omega \to 0$ spatial fluctuations in the transverse direction are massless Goldstone modes. The unitary matrices $T(\boldsymbol{r})$ which generate the saddle-point manifold can be compared to the phase of the Landau-Ginzburg order parameter for BCS. The breaking of symmetry between the advanced and retarded blocks by Λ violates the supersymmetry and as a result causes the longitudinal modes to become massive. In this case, the saddle-point manifold shrinks to a point. It is the longitudinal fluctuations about this saddle-point which generates conventional perturbation theory.

Within the self-consistent Born approximation, the substitution of Eq. (6.150) into Eq. (6.148) gives the following expression for the supermatrix Green function (see for example Ref. [66, 67])

$$\mathcal{G}(\boldsymbol{r},\boldsymbol{r}') = \mathrm{Re}\ \langle G^A(\boldsymbol{r},\boldsymbol{r}')\rangle \mathbf{1} + \mathrm{i}\pi\nu f_d(\boldsymbol{r}-\boldsymbol{r}')Q((\boldsymbol{r}+\boldsymbol{r}')/2), \tag{6.152}$$

where

$$f_d(\boldsymbol{r}-\boldsymbol{r}') = \frac{\mathrm{Im}\ \langle G^A(\boldsymbol{r},\boldsymbol{r}')\rangle}{\mathrm{Im}\ \langle G^A(\boldsymbol{r},\boldsymbol{r})\rangle}, \tag{6.153}$$

and the impurity averaged Green function is given explicitly in Eq. (4.51).

6.1.5. Non-Linear σ-Model

Allowing longitudinal fluctuations around the saddle-point, an expansion of the action to leading order in $(E_F\tau)^{-1}$ generates the effective field theory

$$F[Q] = \frac{\pi\nu}{8}\int \mathrm{d}\boldsymbol{r}\ \mathrm{STr}\left[D(\boldsymbol{\nabla}Q)^2 + 2\mathrm{i}(\Omega+\mathrm{i}0)\Lambda Q\right], \tag{6.154}$$

$$R(\boldsymbol{r},\boldsymbol{r}';\Omega) = (\pi\nu)^2\int \mathcal{D}Q\ \mathrm{e}^{-F[Q]} \\ \times \mathrm{STr}\ [k\ P(\mathrm{a},\mathrm{B})\ Q(\boldsymbol{r})\ k\ P(\mathrm{r},\mathrm{B})\ Q(\boldsymbol{r}')], \tag{6.155}$$

with the constraint that $Q(\boldsymbol{r})$ remains on the saddle-point manifold defined in Eq. (6.150), and where $D = v_F^2\tau/d$ is the classical diffusion constant.

The effective field theory of long wavelength fluctuations in disordered metals is described by a functional non-linear σ-model of 8×8 supermatrix fields. In the replica formulation, the equivalent field theory is an O(N) non-linear σ-model. To interpret the behavior of this model it is useful to draw an analogy with ferromagnetism and at the same time understand the origin of the infrared divergences of perturbation theory.

To make the analogy it is convenient to introduce the new variables

$$t = \frac{8}{\pi\nu D}, \qquad H = -\mathrm{i}\widetilde{\Omega}, \qquad \widetilde{\Omega} = \frac{\Omega}{D}, \tag{6.156}$$

and rewrite $F[Q]$ in the form

$$F[Q] = \frac{1}{t}\int \mathrm{STr}\Big[(\boldsymbol{\nabla}Q)^2 - 2H\Lambda Q\Big]\,\mathrm{d}\boldsymbol{r}. \tag{6.157}$$

Reinterpreting the Q matrix as an N-component spin with fixed length $Q^2 = 1$, Eq. (6.157) coincides with the action of the O(N) non-linear σ-model of ferromagnetism, with t denoting the effective temperature (measured in units of the spin-wave stiffness) and H plays the role of the magnetic field.

LOCALIZATION	FERROMAGNETISM
Metallic Phase	Magnetic Phase
Insulating Phase	Paramagnetic Phase
Degree of Disorder $\hbar/k_F l$	Temperature T
Mobility Edge	Curie Point T_c
ΛQ	Magnetization
Diffusion Modes	Spin Waves
Diffusion Constant D	Spin-wave Stiffness
Frequency Ω	Magnetic Field H
Magnetic Field	Magnetic Anisotropy

Table 1
Glossary for the analogy between localization and ferromagnetism

For large magnetic fields the spin degrees of freedom can be expanded around their ferromagnetic configuration in which the "spin" Q is aligned with H. As a result we obtain the usual bare transverse spin-wave propagator $[\boldsymbol{q}^2 + H]^{-1}$. This compares with the form of the diffusion propagator $[D\boldsymbol{q}^2 - \mathrm{i}\Omega]^{-1}$. For small magnetic fields the Goldstone modes become important and the spin-wave theory becomes infrared divergent. A similar catastrophe is met in the disordered metal. Perturbation theory corresponds to including fluctuations only around a single-point in the saddle-point manifold (fig. 20). It is the inclusion of all points on the saddle-point manifold that saves the theory from infrared divergences. Later, we will explore this analogy further in discussing the critical behavior of the σ-model and the transition to localization. A summary of the correspondences between to the two problems is shown in table 1.

We emphasize that in contrast to ferromagnetism, the average "magnetization", $\langle \Lambda Q \rangle$ does not serve as useful order parameter for localization since it corresponds to the average DoS and shows no singular behavior at the transition. The physical origin of this result stems from the fact that on long time scales particle conservation admits only diffusion with a renormalization of the diffusion constant. The low energy fluctuations are therefore described by the diffusion modes which do not affect properties of one-particle Green functions such as the DoS.

Perturbation theory can be recovered by forming an expansion around the saddle-point Λ. Choosing the parametrization [58]

$$Q = W + \Lambda(1 - W^2)^{1/2}, \qquad W = \begin{pmatrix} 0 & Q^{RA} \\ Q^{AR} & 0 \end{pmatrix}, \tag{6.158}$$

and expanding to leading order in the unconstrained supermatrices W, we obtain [58]

$$F[Q] = \frac{\pi\nu}{8} \int \mathrm{d}\boldsymbol{r}\ \mathrm{STr}[D(\boldsymbol{\nabla} W)^2 - \mathrm{i}\Omega W^2]. \tag{6.159}$$

This yields the standard result for the diffusion propagator $R(\boldsymbol{k}, \Omega)$ shown earlier in Eq. (4.64).

This approach allows expansion to higher order and the construction of a theory of interacting diffusion modes. In this way it is possible to systematically reproduce the results of diagrammatic perturbation theory. In particular, it is possible to confirm that the diffusion mode interaction does not change the diffusive form of the density response function in Eq. (4.64) but simply brings about a change in the diffusion constant. Before examining the non-linear σ-model further, let us digress by discussing the influence of magnetic fields and spin-orbit scattering on the field theory.

6.1.6. Magnetic Fields

In the presence of a magnetic field, it is necessary to treat the canonical momentum $\hat{\boldsymbol{p}} - (e/c)\boldsymbol{A}(\boldsymbol{r})$, where $\boldsymbol{A}(\boldsymbol{r})$ denotes the vector potential. Since the latter violates time-reversal symmetry,

$$\frac{1}{2m} \int \mathrm{d}\boldsymbol{r}\ \psi^* \left[\left(\hat{\boldsymbol{p}} - \frac{e}{c}\boldsymbol{A} \right)^2 \psi \right] = \frac{1}{2m} \int \mathrm{d}\boldsymbol{r}\ \left[\left(\hat{\boldsymbol{p}} + \frac{e}{c}\boldsymbol{A} \right)^2 \psi^* \right] \psi, \tag{6.160}$$

the action takes the form of Eq. (6.139) but with a canonical momentum that includes the symmetry breaking matrix between conjugate elements, $\tau_3 = (-)^d$.

$$\boldsymbol{p} \to \boldsymbol{p} - \frac{e}{c}\tau_3 \boldsymbol{A}. \tag{6.161}$$

For weak magnetic fields we again obtain an effective theory expressed in the form of a functional non-linear σ-model but with the derivative in Eq. (6.155) exchanged for the covariant derivative

$$\boldsymbol{\nabla} Q \to \boldsymbol{\nabla} Q - \frac{\mathrm{i}e}{c}\ \boldsymbol{A}\ [Q, \tau_3]. \tag{6.162}$$

The appearance of the commutator has a natural interpretation in terms of the diffusion modes of perturbation theory. The components of the

Q matrix that commute with τ_3 describe the diffuson degrees of freedom which, as we have seen, are unaffected by the presence of a magnetic field. On the other hand, the components which do not commute reflect the Cooperonic degrees of freedom and the corresponding Goldstone modes acquire a mass (gap) in the presence of a magnetic field. For sufficiently strong fields these degrees of freedom are frozen out and as a result the symmetry of the Q matrices which contribute to $F[Q]$ obeys the further constraint, $[Q, \tau_3] = 0$.

Consideration of the Hall conductivity σ_{xy} in addition to σ requires a generalization of the σ-model. Eq. (6.155) involves only one constant D connected with σ by the Einstein relation. We understand, however, that this generalization should not affect the "equation of motion" which, in the zeroth order of approximation, has the form of a diffusion equation. The apparent contradiction was resolved by Pruisken et al. [68] who derived an additional contribution to $F[Q]$. Originally formulated within the replica approach, the new contribution has a counterpart in the supersymmetrical theory [69] and is given by

$$F[\sigma_{xy}] = \sigma_{xy} \int \mathrm{d}r \mathrm{STr}\Big(Q\ [\partial_x Q, \partial_y Q]\Big). \tag{6.163}$$

Since this term is topological (i.e. it takes the form of a full derivative), it has no effect on the equation of motion. This approach has been used as a justification for two-parameter scaling in the integer Quantum Hall Effect [70].

6.1.7. Spin-Orbit Scattering

In the presence of strong spin-orbit interaction the action acquires an additional term,

$$L_{\mathrm{so}} = \frac{1}{2}\Big\langle\Big(\int \mathrm{d}\boldsymbol{r}\ \bar{\Psi}(\boldsymbol{r})\ \boldsymbol{\sigma}[\boldsymbol{\nabla} U_{\mathrm{so}} \times \hat{\boldsymbol{p}}]\ \Psi(\boldsymbol{r})\Big)^2\Big\rangle, \tag{6.164}$$

where σ denote the Pauli spin matrices, and the average is performed over the impurities and over the Fermi surface. (To account for the spin degrees of freedom the superfields Ψ are required to carry an additional index.) The latter leads to a contribution to Eq. (6.155) of

$$F_{\mathrm{so}} = -\frac{\pi\nu}{4} \sum_{i=x,y,z} \frac{1}{\tau_{\mathrm{so}}^{(i)}} \mathrm{STr}\ [Q, \sigma_i]^2, \tag{6.165}$$

where $1/\tau_{\mathrm{so}} = 2\pi\nu\langle[\boldsymbol{\nabla} U_{\mathrm{so}}(\boldsymbol{r}) \times \boldsymbol{p}]_i^2\rangle$, and Q, a supermatrix quarterion, carries spin indices. Thus, while the singlet components of the supermatrix

	Orthogonal	Unitary	Symplectic
T-invariance	$\surd$	$\times$	$\surd$
Spin-rotation	$\surd$	$\surd$ or $\times$	$\times$
β	1	2	4

Table 2
Summary of the different university classes.

Q remain massless, the rest are frozen out. As a result, in addition to Eq. (6.150), the saddle-point manifold is described by the further constraint $[Q, \sigma_i] = 0$.

6.1.8. Universality Classes

The examples above can be separated into three universality classes according to the symmetry of the Hamiltonian. In the first case, T-invariance is conserved and the Q matrix obeys only the condition $Q^2 = 1$. Such systems are classified as orthogonal, the notation, as we will see, coming from random matrix theory. If T-invariance is broken by, say, a magnetic field the symmetry of the saddle-point manifold is bound by the further constraint that $[Q, \tau_3] = 0$. Such systems are classified as unitary. Finally, for systems which conserve T-invariance but display strong spin-orbit scattering we have the constraint $[Q, \sigma_i] = 0$. Such systems are termed symplectic. This classification is summarized in Table 2.

This concludes our derivation of the effective field theory describing the low energy, long wavelength density fluctuations in disordered conductors. In the next section we will make use of this model to examine the localization transition.

6.2. Renormalization Group and the $2 + \epsilon$ Expansion

To examine the critical properties of the supermatrix non-linear σ-model we again draw on the analogy of the model with the O(N) vector spin model. For the latter, a renormalization group procedure was proposed by Polyakov as a method of obtaining the critical behavior of the ferromagnetic transition in $2+\epsilon$ dimensions [71, 72]. In this approach, the unitary matrices which span the saddle-point manifold are factorized into slowly and rapidly varying contributions. The latter are integrated out to give an effective model and the process repeated. This leads to a set of renormalization group equations for the coupling constant.

A similar approach can be applied to the present case by separating the unitary supermatrix $T(\boldsymbol{r})$ in Eq. (6.150) into the product of slowly $\widetilde{T}(\boldsymbol{r})$ and rapidly $T_0(\boldsymbol{r})$ varying parts,

$$T(\boldsymbol{r}) = \widetilde{T}(\boldsymbol{r})T_0(\boldsymbol{r}). \tag{6.166}$$

To illustrate the renormalization procedure we will prepare the first step in the analysis. Substituting Eq. (6.166) into Eq. (6.157) we obtain [58]

$$F[Q] = \frac{1}{t}\int \mathrm{STr}\Big[\,(\boldsymbol{\nabla}Q_0)^2 + 2[Q_0,\boldsymbol{\nabla}Q_0]\cdot\boldsymbol{Y} + [Q_0,\boldsymbol{Y}]^2 \\ +2i\widetilde{\Omega}\widetilde{T}^{-1}\Lambda\widetilde{T}Q_0\Big]\,\mathrm{d}\boldsymbol{r}, \tag{6.167}$$

where $\widetilde{\Omega} = \Omega/D$, $Q_0 = T_0^{-1}\Lambda T_0$, and $\boldsymbol{Y} = \widetilde{T}^{-1}\boldsymbol{\nabla}\widetilde{T} = \boldsymbol{Y}^{-1}$.

Integration over the rapidly varying degrees of freedom is not straightforward. It is facilitated by a careful choice of gauge and dimensional regularization. For details of the renormalization procedure for the supermatrix model we refer to the review by Efetov [58] from which our notation is taken. Within the replica approach there are many more extensive reviews as well as some recent developments which can be found in Refs. [73, 74]. Here we present only the main results.

After performing the momentum shell integrations, $\lambda < k < k_0$ in $2-\delta$ dimensions and making the analytic continuation to $2+\epsilon$ one obtains the Gell-Mann-Low equation. The first point to note is that upon renormalization the value of $\Omega \propto \widetilde{\Omega}/t$ does not change. This reflects the particle conservation law discussed previously and holds in all orders of the renormalization group. Secondly it is observed that the first non-trivial corrections to the lowest-order β function appear in the fourth-loop. We remark that calculations to this order were first performed by Wegner [73]. Subsequently calculations by Hikami [74] produced even the five-loop corrections which we present below.

$$\frac{d\widetilde{t}}{d\ln\lambda} = \epsilon\widetilde{t} + \begin{cases} -2\widetilde{t}^2 - 12\zeta(3)\widetilde{t}^5 + O(\widetilde{t}^7) & \beta = 1, \\ -2\widetilde{t}^3 - 6\widetilde{t}^5 + O(\widetilde{t}^7) & \beta = 2, \\ \widetilde{t}^2 - (3/4)\zeta(3)\widetilde{t}^5 & \beta = 4. \end{cases} \tag{6.168}$$

where $\widetilde{t} \equiv t/16\pi = 1/2\pi^2 g$ (see Eq. (6.156)). We remark that $\beta_{\mathrm{orth}}(\widetilde{t}) = -\beta_{\mathrm{symp}}(-\widetilde{t}/2)$ and $\beta_{\mathrm{unit}}(\widetilde{t}) = \beta_{\mathrm{unit}}(-\widetilde{t})$.

This renormalization group equation is in accord with the one-parameter scaling hypothesis discussed in section 3. Moreover, Eq. (6.168) predicts the existence of a fixed point t^* at which $\beta(t^*) = 0$ in $d > 2$ for all three ensembles. Indeed, in the symplectic case, a transition is predicted to occur at $g^* = (3\zeta(3)/4)^{1/3}$ even for $d = 2$. For the orthogonal ensemble, the weak localization correction to the conductivity, which corresponds to the leading order expansion of Eq. (6.168), predicts a transition at $g^* = 1/\epsilon$. Higher orders produce a significant shift to $1/g^* = \epsilon - (3/4)\zeta(3)\epsilon^4$ when extrapolated to $d = 3$. It yields a critical exponent for the conductivity ($\sigma \propto (E - E_c)^s$) of

$$s = \nu\epsilon = 1 - 9/4\zeta(3)\epsilon^3 + O(\epsilon^4), \tag{6.169}$$

where ν is the localization length exponent ($\xi \propto (E_c - E)^{-\nu}$). Neglecting higher loop corrections this suggests $s = \nu \sim 0.4$ in $d = 3$ [73] violating the inequality $\nu \geqslant 2/d$ established by Chayes et al. [75] and compares to the figure $s = \nu \sim 1.5 \pm 0.2$ predicted numerically by MacKinnon and Kramer [76].

What conclusions can be drawn about the scaling theory and the field theoretic description of the critical properties of the localization transition? Despite the controversial debate over the correct exponents there remains overwhelming numerical evidence for the validity of the scaling theory. The inability of present analytical methods to accurately predict an exponent which agrees with the numerics can be due to many reasons. To mention two, it is certainly possible that the $2+\epsilon$ expansion converges too slowly. If so, the present field theory is valuable in that it presents a good qualitative description of the localization transition. A second and potentially more damaging explanation is that the high-order gradient terms neglected in the present non-linear σ-model are relevant to the fixed point, and ϵ expansion. The latter have been shown to acquire a positive anomalous dimension [77] (for a review see Ref. [78]). The conclusion is that the critical properties of the localization transition remains unresolved.

This completes our brief discussion of the field theory of disordered metals. By no means complete, we hope that the review gives some indication of the important role which the theory has played in understanding the phenomena of localization lending theoretical support to scaling theory as well as giving a systematic framework for the development of perturbation theory. Recently interest in this model has been reinvigorated because of its ability to describe phenomena of disordered metals in confined geometries. In the rest of these lectures we will focus on this limit and discuss some of the implications it has for quantum chaos.

7. Zero-Dimensional σ-Model

So far we have been concerned with quantum effects in transport phenomena of *open systems* where the size of the leads are of the order of the system

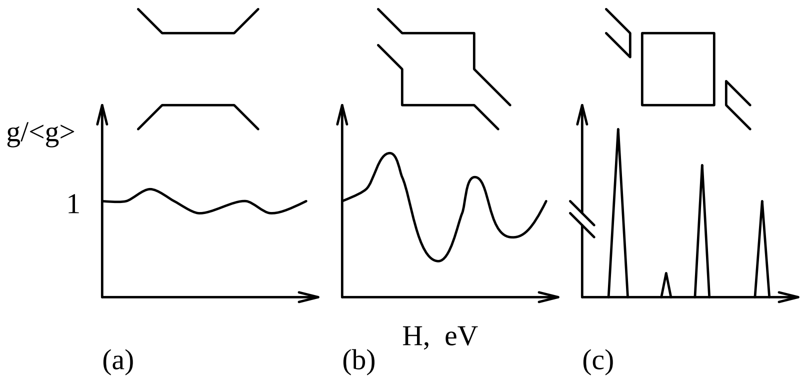

Fig. 21. Schematic diagram showing the relative fluctuation of the conductance as a function of Fermi energy, E_F or magnetic field, H for a system with (a) open leads with many channels, (b) open leads with a single channel, and (c) tunnel contacts.

size, L (see fig. 21). We have discussed how quantum interference leads to localization when the system size or degree of disorder is increased. We have also found that the sample to sample fluctuations of the conductance δg are of order unity, so that close to the insulating state they become of the same order as the average conductance, $\langle g \rangle$.

Another way to emphasize the quantum effects is to decrease the size of the leads without changing L or l. This clearly decreases $\langle g \rangle$ without changing the magnitude of the fluctuations $\delta g \sim 1$. As a result, the relative fluctuations of the conductance g as a function of Fermi energy E_F, or magnetic field will become increasingly pronounced as indicated in fig. 21. For a single channel lead $\delta g \sim \langle g \rangle$.

Indeed it is possible to go further and apply to the system tunnel contacts with very low transmittance (for a review see Kastner [79]). If Coulomb Blockade effects can be neglected, $g(E_F)$ is described by a series of resonance peaks (see fig. 21(c)). The location of the peaks is determined by the spectrum of the system while the widths are set by the escape rate $\hbar/\tau_{\rm esc}$. If the latter is smaller than the Thouless energy E_c, then E_c is irrelevant.

When the system was open there were two relevant energy scales, E_c and the mean level spacing Δ, which can be combined into the dimensionless ratio $g = E_c/\Delta$. Before we were concerned with the scaling theory for the renormalization of this dimensionless conductance. Now we will be interested with time scales $t \geqslant \hbar/\Delta \equiv t_H$ $(t \leqslant \tau_{\rm esc})$ when the individual levels are well resolved. In this case we have only one relevant energy scale

Δ (or, equivalently, one time scale, the Heisenberg time, t_H). Therefore, the statistical properties of the system should become universal after proper rescaling.

For the point of view of the non-linear σ-model, universality arises in the following way: on time scales $t \gg t_c$ the path integral becomes dominated by a single mode or "zero-mode" that does not involve g. Higher modes acquire a mass proportional to the dimensionless conductance. Treating only the zero-mode the functional integration becomes definite and the theory tractable. Evaluating this integral we also obtain a proper cut-off of the infrared divergences of the semi-classical perturbation theory (see section 5). In a pioneering work, Efetov [58] evaluated the integral and confirmed the conjecture long held [80] that the single-particle properties of weakly disordered metallic grains obey the same statistics as random matrix ensembles. It stands as perhaps the only example where the statistics of random matrix theory (RMT), believed by many to be the characteristic signature of quantum chaos, can be confirmed analytically from a microscopic Hamiltonian. As such it represents one of the triumphs of σ-model approach.

As a prelude to discussing the general phenomena of quantum chaos, we will first examine in some detail the "zero-dimensional" limit of the non-linear σ-model and discuss its relation to the theory of random matrix ensembles. In particular, we will focus on the spectral properties of an ensemble of weakly disordered metallic grains in the presence of Aharonov-Bohm flux. Our goal will be to determine spectral correlations both as a function of energy, and in response to an applied perturbation — in this case, the flux itself.

7.1. Aharonov-Bohm Flux

As a generalization of Efetov's original calculation, we will consider the problem of a disordered metallic grain threaded by an Aharonov-Bohm flux ϕ (fig. 22) described by the Hamiltonian

$$H(\phi) = \frac{\hbar^2}{2m}\Big(-\mathrm{i}\boldsymbol{\nabla} + \frac{2\pi}{L}\phi\, \boldsymbol{e}_\phi\Big)^2 + V(\boldsymbol{r}), \tag{7.170}$$

where $\boldsymbol{e}_\phi$ is the unit vector along the azimuthal direction. We will confine our attention to the regime in which all states are extended (i.e. $L \ll \xi$), and further assume that disorder is sufficiently weak that an effective description in terms of the non-linear σ model is justified. The relevant length and energy scales considered here were shown earlier in fig. 5.

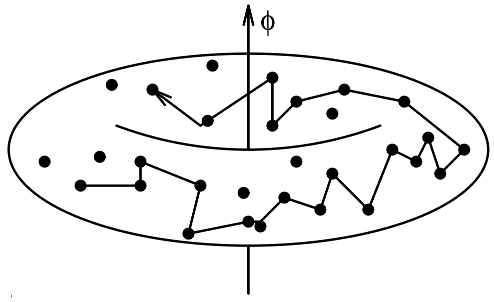

Fig. 22. Geometry of the metallic grain with Aharonov-Bohm flux considered in the text.

Following our study of perturbation theory in section 4, we will investigate the connected part of the dimensionless two-point DoS autocorrelator both as a function of energy and of magnetic flux,

$$k(\Omega,\bar{\phi},\phi) = \Delta^2\Big\langle \nu(E-\Omega/2,\bar{\phi}-\phi/2)\ \nu(E+\Omega/2,\bar{\phi}+\phi/2)\Big\rangle_c, \quad (7.171)$$

where $\Delta = (\nu L^d)^{-1}$ denotes the mean level spacing at the Fermi energy, and the subscript c denotes the connected part of the correlator. Using Eq. (4.49) k can be expressed as a product of retarded and advanced Green functions in the form,

$$k(\Omega,\bar{\phi},\phi) + \frac{1}{2} = \frac{\Delta^2}{2\pi^2}\ \mathrm{Re}\int \mathrm{d}\boldsymbol{r}\ \ \mathrm{d}\boldsymbol{r}'\ \Big\langle G^R(\boldsymbol{r},\boldsymbol{r};E-\Omega/2,\bar{\phi}-\phi/2)$$
$$\times G^A(\boldsymbol{r}',\boldsymbol{r}';E+\Omega/2,\bar{\phi}+\phi/2)\Big\rangle. \quad (7.172)$$

Proceeding as before the Green functions can be expressed as a functional integral over 8-component superfields Ψ in the form,

$$k(\Omega,\bar{\phi},\phi) + \frac{1}{2} = \frac{\Delta^2}{2\pi^2}\mathrm{Re}\int \mathrm{d}\boldsymbol{r}\ \ \mathrm{d}\boldsymbol{r}'\ \Big\langle \int \mathcal{D}\Psi\ \ \mathrm{e}^{-L[\Psi]}$$
$$\times\Big(\Psi^\dagger(\ \boldsymbol{r})P(\mathrm{a},\mathrm{B})\Psi(\boldsymbol{r})\Big)\ \Big(\Psi^\dagger(\boldsymbol{r}')P(\mathrm{r},\mathrm{B})\Psi(\boldsymbol{r}')\Big)\Big\rangle, \quad (7.173)$$

where the action is given by Eqs. (6.139) and (6.140) with the bare supermatrix Hamiltonian $\boldsymbol{p}^2/2m$ is replaced by

$$\frac{1}{2m}\Big(\mathrm{i}\boldsymbol{\nabla} - \frac{2\pi}{L}(\bar{\phi}+\phi\Lambda/2)\ \boldsymbol{e}_\phi\ \tau_3\Big)^2. \quad (7.174)$$

The violation of T-invariance is reflected in the action by the appearance of the matrix τ_3 which breaks the symmetry between the conjugate components of Ψ. In addition, the flux difference ϕ acquires a factor Λ required to break the symmetry between the retarded and advanced Green functions. Ensemble averaging over the disorder potential, decoupling the interaction and integrating over Ψ we arrive at the following expression

$$k(\Omega,\bar{\phi},\phi)+\frac{1}{2}=\frac{\Delta^2}{8\pi^2}\mathrm{Re}\int \mathrm{d}\boldsymbol{r}\ \mathrm{d}\boldsymbol{r}'\ \int \mathcal{D}Q\ \mathrm{e}^{-F[Q]}$$
$$\times\mathrm{STr}[\ \mathcal{G}(\boldsymbol{r},\boldsymbol{r}')P(\mathrm{a},\mathrm{B})]\ \mathrm{STr}[\ \mathcal{G}(\boldsymbol{r}',\boldsymbol{r})P(\mathrm{r},\mathrm{B})], \tag{7.175}$$

where $F[Q]$ and supermatrix Green function, $\mathcal{G}$ are defined by Eqs. (6.147) and (6.148) with the corresponding expression for the bare Hamiltonian shown in Eq. (7.174).

To leading order in $(E_F\tau)^{-1}$, and l/L the saddle-point equation for Q is unchanged and its solution is given by Eq. (6.150). Expanding to lowest order in the fluctuations we obtain the effective non-linear σ-model for k,

$$k(\Omega,\bar{\phi},\phi)=-\frac{1}{2}-\frac{1}{8}\int\frac{\mathrm{d}\boldsymbol{r}\ \mathrm{d}\boldsymbol{r}'}{L^{2d}}\int\mathcal{D}Q\ \mathrm{e}^{-F[Q]}\,\mathrm{STr}\ [P(\mathrm{a},\mathrm{B})Q(\boldsymbol{r})]$$
$$\times\mathrm{STr}\ [P(\mathrm{r},\mathrm{B})Q(\boldsymbol{r}')], \tag{7.176}$$
$$F[Q]=\frac{\pi\nu}{8}\int\mathrm{d}\boldsymbol{r}\ \mathrm{STr}\Big[\hbar D\Big(\boldsymbol{\nabla}Q-\mathrm{i}\frac{2\pi}{L}\boldsymbol{e}_\phi\ [\tau_3\ (\bar{\phi}+\phi\Lambda/2),Q]\Big)^2$$
$$+2\mathrm{i}\ (\Omega+\mathrm{i}0)\Lambda Q\Big]. \tag{7.177}$$

From our consideration of the magnetic field in the previous section we could have anticipated the form of the effective action. The only difference appears in the term proportional to $\Lambda\phi$.

The form of $F[Q]$ is natural. In the presence of magnetic flux the modes corresponding to the Cooperon degrees of freedom acquire a mass proportional to $\bar{\phi}^2$. For a sufficiently large field the Cooperon modes give a negligible contribution to k and the symmetry class is unitary. The symmetry breaking between retarded and advanced degrees of freedom generated by $\Lambda\phi$ gives a mass to both the diffuson and Cooperon degrees of freedom proportional to ϕ^2.

Gauge invariance of the functional integral under the transformation

$$Q(\boldsymbol{r})\to\mathrm{e}^{-\mathrm{i}n\pi\tau_3(\boldsymbol{e}_\phi\cdot\boldsymbol{r})/L}\ Q(\boldsymbol{r})\ \mathrm{e}^{\mathrm{i}n\pi\tau_3(\boldsymbol{e}_\phi\cdot\boldsymbol{r})/L}, \tag{7.178}$$

for n integer, reveals the periodicity of k in $\bar{\phi}$. We therefore restrict further consideration to fluxes $\bar{\phi}\in[0,\phi_0/4]$ and $|\phi|\ll\phi_0$. Relaxing the saddle-point condition $Q^2 = 1$, it is straightforward to recover the results of diagrammatic perturbation theory [65].

Instead, we will make use of the confinement of the particles which separates the higher modes from the lowest spatial mode by an energy of order $E_c = \hbar D/L^2$. For $g \equiv E_c/\Delta \gg 1$ and $\bar{\phi} \gg g^{-1/2}$ it suffices to retain only the zero-mode [81] which, up to the gauge invariance, corresponds to Q independent of position. In this zero-dimensional limit we obtain

$$k(\Omega,\phi) = -\frac{1}{8}\int d[Q]\; e^{-F[Q]}\;\mathrm{STr}\;[P(\mathrm{a},\mathrm{B})(Q-\Lambda)] \times \mathrm{STr}\;[P(\mathrm{r},\mathrm{B})(Q-\Lambda)], \tag{7.179}$$

$$F[Q] = \mathrm{i}\frac{\pi(\Omega+\mathrm{i}0)}{4\Delta}\mathrm{STr}\;(\Lambda Q) - \frac{\pi^3}{8}g\phi^2\;\mathrm{STr}\;[\Lambda, Q]^2, \tag{7.180}$$

where we have made use of the dimensionless conductance $g = E_c/\Delta$.

Although we have eliminated the spatial dependence of the theory and made the functional integral definite the result is still far from trivial. In fact, to proceed, we require an explicit parametrization of the saddle-point manifold, i.e., one that fulfills all the symmetry constraints on Q as well as satisfying the condition $Q^2 = 1$. Since Efetov's original work, different parametrizations have been proposed with different merits. Choosing the most suitable parametrization has become largely a matter of taste. For reasons which will become clear, we will focus on the former. We would, however, wish to draw attention to a parametrization by Altland et al. [65] which is particularly instructive since it separates the degrees of freedom which correspond to Cooperon and diffuson modes.

The construction of a suitable parametrization is somewhat laborious and we feel that it is inappropriate to reproduce the technical details here. Instead we will simply quote the form presented in Ref. [58] and refer to the papers by Refs. [62, 82, 65] for a more detailed discussion. Since they will be of use presently, we will present a parametrization for all three universality classes discussed above.

Following the notion of Ref. [58] the saddle-point manifold can defined by the following parametrization of Q. Separating the components of the RA block, the Q matrix can be expressed in the form

$$Q = U\begin{pmatrix} \cos\hat{\theta} & \mathrm{i}\sin\hat{\theta} \\ -\mathrm{i}\sin\hat{\theta} & -\cos\hat{\theta} \end{pmatrix} U^{-1}, \qquad U = \begin{pmatrix} u & 0 \\ 0 & v \end{pmatrix}, \tag{7.181}$$

where the BF blocks are defined by

$$\hat{\theta} = \begin{pmatrix} \theta_{11} & 0 \\ 0 & \theta_{22} \end{pmatrix}, \tag{7.182}$$

β	θ_{11}	θ_{22}	Limits
1	$\begin{pmatrix}\theta & 0\\ 0 & \theta\end{pmatrix}$	$\mathrm{i}\begin{pmatrix}\theta_1 & \theta_2\\ \theta_2 & \theta_1\end{pmatrix}$	$0<\theta<\pi, \quad \theta_1,\theta_2>0$
2	$\begin{pmatrix}\theta & 0\\ 0 & \theta\end{pmatrix}$	$\mathrm{i}\begin{pmatrix}\theta_1 & 0\\ 0 & \theta_1\end{pmatrix}$	$0<\theta<\pi, \quad \theta_1>0$
4	$\begin{pmatrix}\theta_1 & \theta_2\\ \theta_2 & \theta_1\end{pmatrix}$	$\mathrm{i}\begin{pmatrix}\theta & 0\\ 0 & \theta\end{pmatrix}$	$\theta>0, \quad 0<\theta_1<\pi, \quad 0<\theta_2<\pi/2$

Table 3
Elements of $\hat{\theta}$ for different symmetries.

with conjugate elements shown in table 3. In this parametrization the degrees of freedom of the Q-matrix are separated into the eigenvalues, $\hat{\theta}$ and unitary supermatrices. As we will see shortly, this form is particularly convenient since the Grassmann variables, which are contained entirely within the unitary supermatrices, disappear from the exponent.

The matrices u and v satisfy the conditions

$$\bar{u}u = 1, \qquad \bar{v}v = 1, \qquad \bar{v} = kv^{\dagger}k, \qquad \bar{u} = u^{\dagger}, \tag{7.183}$$

imposed by the symmetry of Q expressed in Eq. (6.151). Factorizing the matrices into commuting and anticommuting contributions we obtain

$$u = u_1u_2, \qquad v = v_1v_2, \qquad \bar{u}_1u_1 = \bar{u}_2u_2 = \bar{v}_1v_1 = \bar{v}_2v_2 = 1, \tag{7.184}$$

where

$$\begin{aligned} u_1 &= \begin{bmatrix} 1-2\eta\bar{\eta}+6(\eta\bar{\eta})^2 & 2\eta(1-2\bar{\eta}\eta) \\ -2(1-2\bar{\eta}\eta)\bar{\eta} & 1-2\bar{\eta}\eta+6(\bar{\eta}\eta)^2 \end{bmatrix}, \\ v_1 &= \begin{bmatrix} 1+2\kappa\bar{\kappa}+6(\kappa\bar{\kappa})^2 & 2\mathrm{i}\kappa(1+2\bar{\kappa}\kappa) \\ -2\mathrm{i}(1+2\bar{\kappa}\kappa)\bar{\kappa} & 1+2\bar{\kappa}\kappa+6(\bar{\kappa}\kappa)^2 \end{bmatrix}, \end{aligned} \tag{7.185}$$

and u_2, v_2, and η are defined in table 4 according to the symmetry of the Dyson ensemble with

$$M = \begin{pmatrix} m & m_1^* \\ m_1 & -m \end{pmatrix} \tag{7.186}$$

and m, χ, and ϕ real.

The elementary volume $[\mathrm{d}Q]$ can be written in the form,

$$[\mathrm{d}Q] = J_1J_2dR, \tag{7.187}$$

β	u_2	v_2	η
1	$\begin{pmatrix} \frac{(1-\mathrm{i}M)}{(1+\mathrm{i}M)} & 0 \\ 0 & \mathrm{e}^{\mathrm{i}\phi\tau_3} \end{pmatrix}$	$\begin{pmatrix} 1 & 0 \\ 0 & \mathrm{e}^{\mathrm{i}\chi\tau_3} \end{pmatrix}$	$\begin{pmatrix} \eta_1 & \eta_2 \\ -\eta_2^* & -\eta_1^* \end{pmatrix}$
2	$\begin{pmatrix} \mathrm{e}^{\mathrm{i}\phi\tau_3} & 0 \\ 0 & \mathrm{e}^{\mathrm{i}\chi\tau_3} \end{pmatrix}$	$\begin{pmatrix} 1 & 0 \\ 0 & 1 \end{pmatrix}$	$\begin{pmatrix} \eta_1 & 0 \\ 0 & -\eta_1^* \end{pmatrix}$
4	$\begin{pmatrix} \mathrm{e}^{\mathrm{i}\phi\tau_3} & 0 \\ 0 & \frac{(1-\mathrm{i}M)}{(1+\mathrm{i}M)} \end{pmatrix}$	$\begin{pmatrix} \mathrm{e}^{\mathrm{i}\chi\tau_3} & 0 \\ 0 & 1 \end{pmatrix}$	$\begin{pmatrix} \eta_1 & \eta_2 \\ -\eta_2^* & \eta_1^* \end{pmatrix}$

Table 4
Elements of the unitary supermatrices which define Q.

β	J_1	J_2
1	$2^{-}20(\lambda^2+\lambda_1^2+\lambda_2^2-2\lambda\lambda_1\lambda_2-1)^{-2}$	$\frac{2^{12}}{\pi^4}\frac{\mu^3\mu_1\mu_2}{(1+m^2+m_1^2)^3}$
2	$\frac{1}{2^8}(\lambda_1-\lambda)^{-2}$	$\frac{2}{\pi^2}\mu\mu_1$
4	$2^{-20}(\lambda^2+\lambda_1^2+\lambda_2^2-2\lambda\lambda_1\lambda_2-1)^{-2}$	$\frac{2^{12}}{\pi^4}\frac{\mu^3\mu_1\mu_2}{(1+m^2+m_1^2)^3}$

Table 5
Terms which enter the measure $\mathrm{d}Q$.

where

$$\begin{aligned} \mathrm{d}R = {} & \mathrm{d}\eta_1\,\mathrm{d}\eta_1^*\,\mathrm{d}\kappa_1\,\mathrm{d}\kappa_1^*\,\mathrm{d}\phi\,\mathrm{d}\chi\,\mathrm{d}\theta\,\mathrm{d}\theta_1 \\ & \times \begin{cases} \mathrm{d}\eta_2\,\mathrm{d}\eta_2^*\,\mathrm{d}\kappa_2\,\mathrm{d}\kappa_2^*\,\mathrm{d}m\,\mathrm{d}m_1\,\mathrm{d}m_1^*\,\mathrm{d}\theta_2 & \beta=1,4, \\ 1 & \beta=2, \end{cases} \end{aligned} \tag{7.188}$$

and J_1, J_2 are given in table 5 with

$$\begin{cases} \lambda=\cos\theta, \quad \lambda_1=\cosh\theta_1, \quad \lambda_2=\cosh\theta_2, & \beta=1, \\ \lambda=\cos\theta, \quad \lambda_1=\cosh\theta_1, & \beta=2, \\ \lambda=\cosh\theta, \quad \lambda_1=\cos\theta_1, \quad \lambda_2=\cos\theta_2, & \beta=4, \end{cases} \tag{7.189}$$

and $\mu_i=|1-\lambda_i^2|^{1/2}$.

Substituting the parametrization for Q into Eq. (7.180) and performing the Grassmann integration as well as the phase integrals over ϕ and χ we obtain the final result expressed in terms of the eigenvalues λ and λ_1.‖

$$k(\Omega,\phi)=\mathrm{Re}\int_1^\infty \mathrm{d}\lambda_1\int_{-1}^1\frac{\mathrm{d}\lambda}{2}\,\mathrm{e}^{-\mathrm{i}(\pi\Omega^+/\Delta)(\lambda-\lambda_1)-2\pi^3 g\phi^2(\lambda_1^2-\lambda^2)}\,. \tag{7.190}$$

Eq. (7.190) provides the exact non-perturbative expression for the connected part of the two-point DoS autocorrelator. Corrections to it are smaller by a factor of (l/L), $1/g$, and $(\Omega\tau)$.

Let us first consider the case $\phi=0$. In this case both integrations can be performed and as a result we obtain the expression [58]

$$k(\Omega,0)=-\frac{\sin^2(\pi\Omega/\Delta)}{(\pi\Omega/\Delta)^2}, \tag{7.191}$$

coinciding with the result found from RMT [25]. In fact, it is clear that whatever the origin of the T-violation, whether it be Aharonov-Bohm flux, or a weak uniform magnetic field, the result will not change. This allowed Efetov [58] to confirm the earlier conjecture made by Eliashberg and Gorkov [80] that (on time scales $t>t_c\equiv\hbar/E_c$) level statistics in weakly disordered metallic grains are universal and coincide with RMT. We remark that a similar conclusion can be shown to apply to orthogonal and symplectic ensembles. Does this interpretation extend to parametric correlations?

Eq. (7.190) shows the statistical correlations to depend on two microscopic parameters Δ and g. The former can be removed by the usual unfolding of the energy levels $\epsilon_i=E_i/\Delta$, or specifically, $\omega=\Omega/\Delta$. To remove the latter, let us consider the general rescaling

$$x^2=C(0)X^2,\qquad C(0)=\frac{1}{\Delta^2}\Big\langle\Big(\frac{\partial E_i}{\partial X}\Big)^2\Big\rangle, \tag{7.192}$$

where, in this case $X\equiv\phi$.

For the present problem, instead of estimating $C(0)$ it is more straightforward to determine the level velocity distribution directly. This can be achieved by invoking the general relation [83]

$$\Big\langle\delta\Big(V-\frac{\partial E_i}{\partial X}\Big)\Big\rangle=\lim_{X\to 0}Xk(\Omega=VX,X). \tag{7.193}$$

‖ Again we refer to Ref. [82] for a discussion of the Grassmannian integration. We remark that the contribution from the term of zeroth order in Grassmann variables due to the Parisi-Soulas-Efetov-Wegner theorem vanishes identically. This arises as a result of choosing the connected part of the correlator. Eq. (7.190) arises from the term of highest weight in Grassmann variables.

Applying Eq. (7.190) to Eq. (7.193) we find the velocity distribution to be Gaussian with variance,

$$C(0) = 4\pi g. \tag{7.194}$$

Compare this result to the estimate made in section 2. Eq. (7.194) is analogous to the Thouless formula for conductance but defined not through the average curvature but by the square of the level gradient. This result also compares with the findings of Akkermans and Montambaux [84] where the correspondence of $C(0)$ with the conductance was first proposed.

Applying Eq. (7.194) to Eq. (7.192) the utility of the rescaling is apparent. The conductance is absorbed into the definition of the dimensionless parameter x, and Eq. (7.190) takes the form,

$$k(\omega, x) = \mathrm{Re}\int_1^\infty \mathrm{d}\lambda_1 \int_{-1}^1 \frac{\mathrm{d}\lambda}{2}\, \mathrm{e}^{-\mathrm{i}\pi\omega^+(\lambda-\lambda_1)-(\pi^2x^2/2)(\lambda_1^2-\lambda^2)}\,. \tag{7.195}$$

In fact, the form of the zero-dimensional σ-model for parametric correlations does not rely on the nature of the perturbation. It therefore seems likely that the parametric dependence shown in Eq. (7.195) is as generic as the energy dependence. To establish whether this type of universality is a robust feature of spectral (or indeed wavefunction) statistics begs the question as to whether properties of random matrix ensembles be presented in the form of a zero-dimensional σ-model. In fact, such a theory was proposed by Weidenmüller and collaborators to address the question of scattering in compound nuclei [62]. In the next section we will briefly describe how such a theory can be constructed.

7.2. Random Matrix Theory

To establish the connection between the zero-dimensional non-linear supermatrix σ-model and RMT let us repeat the previous calculation for the Hamiltonian

$$H = H^{(0)} + X_\alpha \Phi^{(\alpha)}, \tag{7.196}$$

where $H^{(0)}$ is an $N\times N$ random real symmetric (orthogonal) matrix drawn from a Gaussian ensemble, and $\{\Phi^{(\alpha)}\}$ denote a set of matrices chosen, for simplicity, from the same ensemble. We will consider the generalization of the supermatrix approach to the study of m-point correlators. Although we at present unable to complete the analytical calculation for $m > 2$, we will consider the σ-model for arbitrary m since it will serve as a method of establishing certain useful identities.

Specifically, let us consider the m-point correlator of advanced and retarded Green functions,

$$S_m(\{E_\alpha, X_\alpha; \Sigma_\alpha\}) = \prod_{\alpha=1}^{m} \mathrm{Tr}\Big[\frac{1}{E_\alpha + \mathrm{i}\Sigma_\alpha 0 - H(X_\alpha)}\Big], \tag{7.197}$$

where the set $\{\Sigma_\alpha = \pm 1\}$ determines whether the resolvents in the product are advanced or retarded, and Greek indices have been used to label the parameters of the m-point function. It is straightforward to generalize the method here to account for the correlations of the off-diagonal components of the Green functions.

Finding an expression for $\langle S_m\rangle$ we can proceed in an manner analogous to the previous calculation: The only difference is that the fields Ψ have N components instead of a spatial dependence. Then

$$S_m(\{E_\alpha, X_\alpha; \Sigma_\alpha\}) = \int \mathrm{d}\Psi \ \mathrm{e}^{-L_0 - L_1} \prod_\alpha \left[\frac{\mathrm{i}}{2}\Psi^\dagger P(\alpha, \mathrm{B})\Sigma_\alpha \Psi\right], \tag{7.198}$$

where the action is specified by the two components,

$$L_0[\Psi] = -\frac{\mathrm{i}}{2}\bar{\Psi}[\hat{E} + \mathrm{i}\hat{\Sigma}0 - \hat{X}\hat{\Phi}]\Psi, \qquad L_1[\Psi] = -\frac{\mathrm{i}}{2}\bar{\Psi}\Phi\Psi, \tag{7.199}$$

and the supervectors Ψ now have $2 \times 2 \times m \times N$ components. In each case, the hats on the parameters $\hat{E}$, $\hat{\Sigma}$, $\hat{X}$, and $\hat{\Phi}$ indicate matrices in the α components (i.e. $\hat{\Phi} = \mathrm{diag}(\Phi^{(1)} \cdots \Phi^{(m)})$, etc.). The matrix $\hat{\Sigma}$ is simply the generalization of Λ to m-components and $\bar{\Psi} = \Psi^\dagger \hat{\Sigma}$.

Matrices $H^{(0)}$ belong to a Gaussian probability distribution which can be presented in terms of eigenvalues, λ_i and eigenvectors specified by the unitary diagonalizing matrices, U [25, 85]

$$\begin{aligned} P(H^{(0)})\,\mathrm{d}H^{(0)} &= C\exp\left(-\frac{\beta\pi^2}{4N\Delta^2}\mathrm{Tr}(H^{(0)})^2\right)\mathrm{d}H, \\ &= C\prod_{i<j}|\lambda_i - \lambda_j|^\beta \prod_i \left[\exp\left(-\frac{\beta\pi^2}{4N\Delta^2}\lambda_i^2\right)\mathrm{d}\lambda_i\right]\mathrm{d}U. \end{aligned} \tag{7.200}$$

The normalization constant C can be found in Ref. [25]. The Jacobian of the group transformation depends explicitly on the symmetry of the Dyson ensemble β and vanishes when two eigenvalues coincide. In the present case we require $\beta = 1$.

Ensemble averaging over the probability distribution function we generate an effective action with the quartic interaction

$$L_{\mathrm{int}} = -\frac{N\Delta^2}{4\pi^2}(\bar{\Psi}\Psi)^2, \tag{7.201}$$

which can be decoupled by the introduction of $4m \times 4m$ supermatrices Q. Performing the Gaussian integration over Ψ we obtain the result,

$$\left\langle S_m \right\rangle = \left(\frac{N}{2}\right)^m \int \mathrm{d}Q \ \mathrm{e}^{-F[Q]} \prod_\alpha \mathrm{STr}\ [\mathcal{G}P(\alpha, \mathrm{B})], \tag{7.202}$$

$$F[Q] = \frac{N}{4}\mathrm{STr}\ Q^2 - \frac{1}{2}\mathrm{STr}_N \ln \mathcal{G}^{-1}, \tag{7.203}$$

where the subscript N denotes an additional trace over the matrix components of the Hamiltonian, and $\mathcal{G}$ is represents the supermatrix Green function

$$\mathcal{G}^{-1} = \frac{\mathrm{i}N\Delta}{\pi}\Big[Q - \mathrm{i}\frac{\pi}{N\Delta}\Big(\hat{E} + \mathrm{i}\hat{\Sigma}0 + \hat{X}\hat{\Phi}\Big)\Big]. \tag{7.204}$$

As with the disordered grain, we proceed by expanding Eq. (7.203) around the saddle-point in Q. For energies E_α which have a center of mass that lies far from zero the saddle-point equation leads to Wigner's semi-circle law for random matrix ensembles [86]. Since our interest is in fluctuations we will assume that all energies are in the vicinity of the center of the semi-circle, $E_\alpha/\Delta \sim \mathrm{O}(N^0)$. The saddle-point equation is thus found by setting $X = 0$ and $E_\alpha = 0$ when we obtain the condition $Q_{\mathrm{sp}}^2 = 1$ found earlier.

To admit fluctuations we expand to leading order in E_α and X_α around the saddle-point**

$$\left\langle S_m \right\rangle = \left(\frac{\mathrm{i}\pi}{2\Delta}\right)^m \int \mathrm{d}Q \ \mathrm{e}^{-F[Q]} \prod_\alpha \mathrm{STr}\ [QP(\alpha, \mathrm{B})], \tag{7.205}$$

$$F[Q] = \mathrm{STr}_N\left[\mathrm{i}\frac{\pi}{2N\Delta}Q\Big(\hat{E} + \mathrm{i}\hat{\Sigma}0 + \hat{X}\hat{\Phi}\Big) - \frac{\pi^2}{4N^2\Delta^2}\Big(Q\hat{X}\hat{\Phi}\Big)^2\right]. \tag{7.206}$$

For matrices $\Phi^{(\alpha)}$ drawn randomly from a Gaussian distribution, the contribution from terms of higher order are small as $1/N$ and can be neglected. To compare with the previous calculation let us examine the product of advanced and retarded Green functions ($m = 2$) for a single perturbation, $\Phi^{(1)} = \Phi^{(2)} = \Phi_c$. Taking the average drift to be zero ($\mathrm{Tr}_N\Phi_c = 0$) we find

$$F[Q] = \mathrm{STr}\Big[\mathrm{i}\frac{\pi\Omega}{4\Delta}Q\Lambda - \frac{\pi^2}{16}\frac{1}{N^2\Delta^2}X^2\mathrm{Tr}_N\Phi_c^2\ (Q\Lambda)^2\Big], \tag{7.207}$$

where $\hat{E} = E + \Omega\Lambda/2$ and $\hat{X} = \bar{X} + X\Lambda/2$. As in the previous section, for matrices which obey unitary symmetry we require the additional constraint $[Q, \tau_3] = 0$, and for symplectic symmetry, $[Q, \sigma_i] = 0$. Thus, after

** $\mathrm{Tr}\ln[A - B] = \mathrm{Tr}\ln A - \mathrm{Tr}[A^{-1}B] - \frac{1}{2}\mathrm{Tr}[A^{-1}BA^{-1}B] - \cdots$

proper rescaling, Eq. (7.207) coincides with the zero-dimensional σ-model of Eq. (7.180). Performing the definite integration using the parametrization of Q defined in the previous section we obtain the universal correlators

$$k(\omega,x)=\mathrm{Re}\int_{-1}^{1}\mathrm{d}\lambda\int_{1}^{\infty}\mathrm{d}\lambda_1\int_{1}^{\infty}\mathrm{d}\lambda_2\frac{(1-\lambda^2)(\lambda-\lambda_1\lambda_2)^2}{(2\lambda\lambda_1\lambda_2-\lambda^2-\lambda_1^2-\lambda_2^2+1)^2}$$
$$\times\ e^{-(\pi^2x^2/4)(2\lambda_1^2\lambda_2^2-\lambda_1^2-\lambda_2^2-\lambda^2+1)-\mathrm{i}\pi\omega^+(\lambda-\lambda_1\lambda_2)}, \tag{7.208}$$

for $\beta=1$, Eq. (7.195) for $\beta=2$, and

$$k(\omega,x)=\mathrm{Re}\int_{1}^{\infty}\mathrm{d}\lambda\int_{-1}^{1}\mathrm{d}\lambda_1\int_{0}^{1}\mathrm{d}\lambda_2\frac{(\lambda^2-1)(\lambda-\lambda_1\lambda_2)^2}{(2\lambda\lambda_1\lambda_2-\lambda^2-\lambda_1^2-\lambda_2^2+1)^2}$$
$$\times\ e^{-2\pi^2x^2(\lambda_1^2+\lambda_2^2+\lambda^2-2\lambda_1^2\lambda_2^2-1)+2\pi\mathrm{i}\omega^+(\lambda-\lambda_1\lambda_2)}. \tag{7.209}$$

for $\beta=4$, where we have applied the rescaling of Eq. (7.192) with [87, 88]

$$C(0)=\frac{2}{\beta N^2\Delta^2}\mathrm{Tr}\ \Phi_c^2. \tag{7.210}$$

However, in this case we can go further and consider the m-point function for $\Phi^{(\alpha)}=\Phi_c$ for all α. Then Eq. (7.206) can be rewritten in the form

$$F[Q]=\mathrm{STr}\Big[\mathrm{i}\frac{\pi}{2}\sum_{\alpha}^{m}Q_{\alpha\alpha}\Big(\epsilon_\alpha+\mathrm{i}\Sigma_\alpha 0\Big)$$
$$+\frac{\pi^2}{16}\sum_{\alpha,\beta}^{m}(x_\alpha-x_\beta)^2Q_{\alpha\beta}Q_{\beta\alpha}\Big], \tag{7.211}$$

showing *all* higher-point correlators of eigenfunctions as well as eigenvalues to be universal under the same rescaling.

This completes the proof that, on time scales longer than the ergodic time $t_c=\hbar/E_c$, the properties of weakly disordered metallic grains are universal and coincide with random matrix ensembles. Moreover, the universal correlators which characterize these random Hamiltonians can be presented through a zero-dimensional supermatrix non-linear σ-model. Whether it is more convenient to use the σ-model or more conventional approaches to RMT is largely a matter of taste. At least for parametric correlation functions it seems that progress is more straightforward using the former. Later we will develop a useful connection between the parametric motion of the energy levels and the dynamical properties of a strongly interacting system of particles.

Although we have focussed on properties of disordered systems, the universality of the results in the ergodic regime suggest a wider generality.

In fact, RMT first appeared as a tool for studying complex quantum systems more than 40 years ago. In an attempt to reconcile the scattering properties of complex nuclei, Wigner [86] proposed a description in which the coupling between different resonances was treated as random. The remarkable success of this approach in describing properties of a still wider variety of complex systems demands explanation and is the subject of the next section.

8. Ergodicity, Universality, and Quantum Chaos

If the number of degrees of freedom exceeds the constants of motion classical dynamics becomes indeterminate or chaotic. Does this rigorous definition have a counterpart in quantum mechanics? After many years, this question is still the subject of inquiry and debate [89]. In this section we will review the insight disordered metals and RMT brings to this question.

The dynamics of particles propagating in a random potential is classically "non-integrable" or chaotic. At the same time we have seen that the low energy properties of quantum particles propagating in an irregular potential are controlled by diffusion modes. Is this a generic feature of the quantum mechanics of classically chaotic systems? And, if so, what role does the non-linear σ-model play in describing universal properties of "clean" non-integrable systems?

Previously, we identified several important time scales in disordered conductors (see fig. 18). At time scales longer than the mean free time, τ quantum particles propagate diffusively. Quantum interference effects in this regime give rise to the phenomena of weak localization. In section 2 an interpretation of the quantum dynamics and interference effects was offered in terms of semi-classical trajectories or Feynman paths. Although the particle propagation is diffusive, it becomes ergodic only after all the available phase space has been occupied. This occurs after the typical transport or Thouless time $t_c = \hbar/E_c$. At longer time scales still propagation becomes insensitive to spatial variations. This coincides with the limit in which only the zero-mode offers a substantial contribution to the σ-model. In the same limit we observed that the quantum statistical properties of the disordered conductor coincide exactly with the statistical properties of random matrix ensembles.

This circumstance is not accidental. In weakly disordered conductors ($g \gg 1$), at time scales comparable to the average level spacing, the perturbation applied through the irregular potential mixes strongly all states in the manner of a random matrix. The associated level repulsion implies

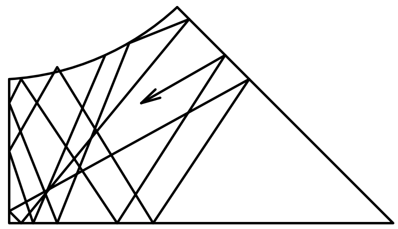

Fig. 23. Geometry of Sinai Billiard.

a rigidity of the spectrum.

8.1. Quantum Billiards

The utility of a disorder potential is that it offers a method of statistical averaging through the ensemble. In ballistic cavities it is no longer possible to speak of an ensemble yet at the same time it is easy to find configurations which display classical chaos (see the lecture notes of Smilansky [90]). Perhaps the simplest example is the "Sinai billiard" where particles, confined to a box, scatter from an excluded disk [91] (see fig. 23). In this ballistic example, it is clear that the typical transport time L/v_F falls short of the ergodic time. Classically, the Lyapunov exponent characterizes the typical rate of separation of unstable trajectories. Quantum mechanically, the ergodic time scale plays a similar role.

The time scale at which a wavepacket has become uniformly spread throughout the available phase space defines the ergodic time. Although for the billiard it is clearly larger than L/v_F, it is the transport time that sets the appropriate scale. At time scales longer than the ergodic time, t_c we would anticipate statistical properties which reflect the zero-dimensional structure. In this limit, we can again expect random matrix theory to provide a valid description. Of course, in general it is impossible to investigate the validity of this statement using analytical means. However, problems such as the Sinai billiard can be readily treated numerically and the spectral properties measured directly. In the next section we will compare numerical measurements made on two different types of system with the statistical properties of a random matrix Hamiltonian.

8.2. Numerics

As we have seen, it is usually impossible to verify the validity of the universal description of chaotic or non-integrable systems through analytical means. Instead emphasis is given to numerical methods. To illustrate the generality of the rescaling and universality we will compare statistical measures of two different non-integrable systems with results taken from random matrices. The first example is the lattice analogue of the problem studied in the previous section — the Anderson model with quasi-periodic boundary conditions which impose an Aharonov-Bohm flux.[††] The second example, which apparently has no classical analogue, involves the exact many-particle spectrum of several fermion confined to a ring interacting through a long-range pairwise potential and subject to quasi-periodic boundary conditions. In this case, although the Aharonov-Bohm flux apparently breaks the T-invariance of the one-dimensional ring, orthogonal symmetry is restored by inversion symmetry. We emphasize that in the latter case there is no disorder and no notion of ensemble averaging. In this case, statistical averaging is performed by averaging over a selected range of flux and energy.

Instead of analyzing the two-point correlator of DoS, or some other related quantity we will examine a different correlation function for which an analytical expression is unavailable. Our choice, which formally involves all higher moments, serves a useful purpose demonstrating the generality of the universal rescaling to arbitrary correlators. Comparison of the results for systems described above with exact analytical expressions can be found in Refs. [92, 93] (for other examples see also Refs. [94–96]).

While the gradient correlation function

$$c(x) = \left\langle \frac{\partial \epsilon_i}{\partial \bar{x}}(\bar{x}+x)\frac{\partial \epsilon_i}{\partial \bar{x}}(\bar{x}) \right\rangle, \tag{8.212}$$

is straightforward to obtain numerically, it does not as yet seem possible to access theoretically. However, the conclusions drawn from the study of the generating function suggests that all such correlators are equally universal. We can therefore compare $c(x)$ for different systems. Applying it to the Anderson model and the strongly correlated system described above we obtain the results shown in fig. 24. All the results collapse onto two different curves, one corresponding to unitary and the other to orthogonal symmetry.

For large x separations, a random phase argument suggests that the condition that level gradients be taken from the same level in Eq. (8.212)

[††] A non-zero transverse flux is applied to ensure unitary symmetry for all values of flux.

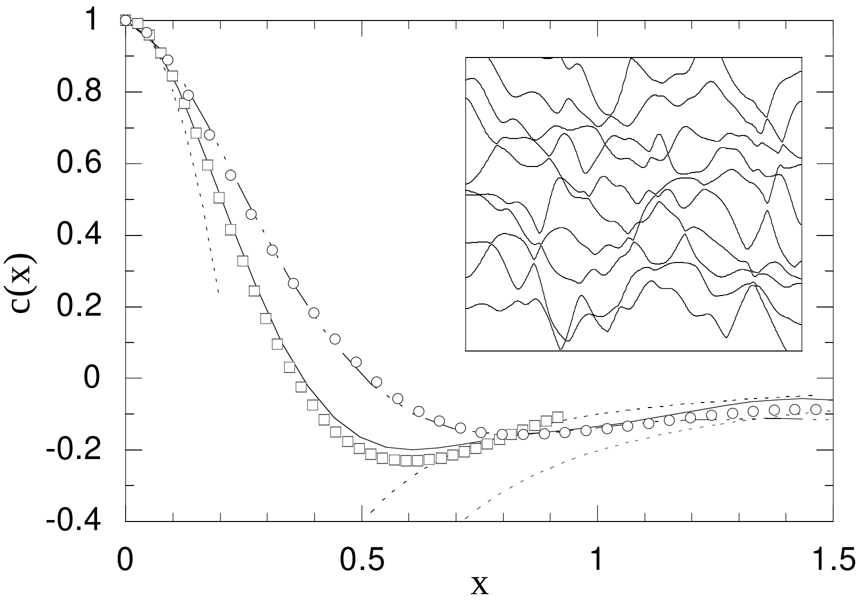

Fig. 24. Measurements of $c(x)$ taken from a single realization of a 150×150 random matrix Hamiltonian with unitary (solid curve) and orthogonal (dashed curve) together with data taken from numerical simulations of an Anderson model ($\square$) and a clean, strongly interacting, many-particle system of fermions on a ring ($\circ$) both subject to an Aharonov-Bohm flux. A typical spectrum of levels for the interacting system is shown inset. Theoretical predictions of perturbation theory and the second order expansion for unitary symmetry are shown dotted.

can be relaxed. This allows the correlator to be related to the two-point density correlator through the approximation [97, 81, 92]

$$\lim_{x\gg 1} c(x) = -\int_{-\infty}^{0}\int_{-\infty}^{0} \mathrm{d}\epsilon_1\,\mathrm{d}\epsilon_2 \frac{\partial^2}{\partial x^2} k(\epsilon_1-\epsilon_2, x) \sim -\frac{2}{\beta\pi^2 x^2}. \qquad (8.213)$$

For unitary ensembles, repulsion of the energy levels allows an estimate in the opposite limit [92]

$$c(x) = 1 - 2\pi^2 x^2 + \mathrm{O}(x^4). \qquad (8.214)$$

These estimates compare favorably with the numerical simulations shown in fig. 24.

8.3. Hard and Soft Chaos

In classical mechanics, an important distinction is drawn between soft and hard chaos. In integrable systems phase space separates into invariant tori on which particles move on closed orbits. Classical non-integrability leads to the destruction of invariant tori and the proliferation of open unstable trajectories. However, very often an intermediate regime of soft chaos is found in which some invariant tori persist as regions of order in a background of chaos.

The non-vanishing tunnelling probability for particles to depart from classical trajectories implies that such a distinction can not be drawn quantum mechanically. However, at time scales shorter than the typical tunnelling time, the presence of classically invariant tori show up as strong features in the statistical properties of the spectrum. Until the inverse tunnelling time becomes comparable with the mean spacing between levels, spectral rigidity is not completely developed. Between level crossings, the dispersion under a parametric perturbation would resemble an integrable decorrelated spectrum.

8.4. Periodic Orbit Theory

Semi-classics offers a more general approach to quantum chaos. The method is based on an approximation in which the path integral is expressed as a sum over classical periodic orbits [98, 99]. In this formulation, universality is a consequence of the domination of the sum by the longest trajectories. This approach is employed and discussed in some detail in this volume (see, for example Ref. [100, 90]) and we feel it is inappropriate to review the method here. However, it is instructive to compare the findings of this approach to the problem studied earlier — statistics of energy levels in a metallic grain with Aharonov-Bohm flux. To do so we will follow a recent calculation of Berry and Keating [101] who applied this technique to study the two-point density correlation function for the Sinai billiard (fig. 23) with quasi-periodic boundary conditions imposed by a flux $\varphi = \phi/\phi_0$.

Applying the Gutzwiller trace formula, the integrated DoS, $N(E,\varphi) = \sum_i \theta(E - E_i(\varphi))$ can be expressed as the sum over closed orbits,

$$N_\epsilon(E,\varphi) \equiv \bar{N} + \sum_j B_j(E)\, \mathrm{e}^{\mathrm{i}[S_j(E)/\hbar + 2\pi w_j \varphi] - \gamma T_j(E)/\hbar}, \tag{8.215}$$

where the sum is over both clockwise and anticlockwise traversals, the mean "Weyl staircase" $\bar{N} \equiv \langle N(E)\rangle$ is assumed to be independent of flux, T_j is the period of the orbit with winding number w_j, and B_j is a complex weight associated with each orbit [101]. Convergence is imposed by a regularization $\gamma \ll \Delta$. Asymptotically, the two-point correlator of $N(E,\varphi)$ is related to the gradient correlator of the energy levels $C(\varphi)$ defined in Eq. (8.212) through the relation [97]

$$C(\varphi) = \left\langle \frac{\partial N}{\partial \bar{\varphi}}(\bar{\varphi} + \varphi) \frac{\partial N}{\partial \bar{\varphi}}(\bar{\varphi}) \right\rangle_{E,\bar{\varphi}}. \tag{8.216}$$

Flux averaging preserves only those contributions to the double sum which have the same winding number. Consideration of Feynman paths in section 2 suggested that quantum interference strongly affects overlapping trajectories. As a first approximation we can proceed by retaining only the diagonal contributions to the sum [101].

$$C(\varphi) = 4\pi^2 \sum_j |B_j|^2 w_j^2 \cos(2\pi w_j \varphi)\, \mathrm{e}^{-2\gamma T_j/\hbar}. \tag{8.217}$$

We remark that the breaking of T-invariance suppresses any contribution from time-reversed paths.

The exponential proliferation of orbits with increasing period is compensated by the damping of the weight $|B_j|^2$. This compensation forms the basis of the classical sum rule of Hannay and Ozorio de Almeida [102],

$$\sum_j |B_j|^2 \cdots \to \frac{1}{2\pi^2} \int_0^\infty \frac{dT}{T} \cdots \tag{8.218}$$

The final assumption involves the distribution of winding numbers. The proliferation of long orbits suggests a Gaussian distribution of winding numbers with zero average and a variance $\langle w(T)^2 \rangle = \alpha T/T_0$ where T_0 is the period of the shortest orbit, and α is a constant specific to the geometry [103]. Averaging Eq. (8.217), and applying Poisson summation, we obtain [101]

$$\lim_{w_* \ll \varphi \ll 1/2} C(\phi) = -\frac{1}{\pi^2 \varphi^2}, \tag{8.219}$$

where $w_*^2 \sim \hbar/\Delta T_0 \gg 1$. $C(0)$ can be associated with the parameter w_*^2 and represents the square of the winding number of a typical trajectory with period Δ [101]. This result coincides with the leading order of diagrammatic perturbation theory [97], and under rescaling coincides with Eq. (8.213) shown above. We remark that, in their paper, Berry and Keating go further to estimate the off-diagonal contributions to the sum which they argue are negligible.

It is important to recognize that for $\varphi \gg W_*$ the semi-classical approach can be justified. On the other hand, this approach apparently does not give a satisfactory description of the numerics for $\varphi \leqslant W_*$. Many attempts to go beyond the leading order or diagonal approximation to treat tunnelling effects between classical trajectories have been made. Whether it is possible to treat high orders or non-perturbative effects produced by RMT or the non-linear σ-model within this approach remains an important open question.

To summarize the conclusions of this section, we have left aside the question of finding a precise definition of quantum chaos. Instead, we have tried to argue that the quantum analogue of classical chaos is manifest through a universal statistical description of spectral and wavefunction properties which can serve as an empirical definition of quantum chaos. In the remainder of these notes we will return to examine properties of the universal correlation functions themselves.

9. T-Violation and the Crossover Between Ensembles

In section 7 we examined the response of a disordered metal and a random matrix to the action of an external perturbation. However, in each case, a perturbation was considered which preserved the symmetry of the original Hamiltonian. Very often, the external perturbation violates the original symmetry of the Hamiltonian. In this section we will extend previous results of Pandey and Mehta [104] (see also Ref. [65]) and examine how parametric correlations in the presence of a symmetry breaking field affect the universality through the σ-model. Consider the dimensionless two-point density correlation function

$$k(\Omega, X_u; \bar{X}) =$$

$$\Delta^2\Big\langle \nu(E-\Omega/2\ ,\bar{X}-X_u/2)\ \nu(E+\Omega/2,\bar{X}+X_u/2)\Big\rangle_c, \tag{9.220}$$

in the crossover region between orthogonal and unitary symmetry [105]. In this interval, k depends on both the difference in the unitary parameters, X_u and the degree of symmetry breaking $\bar{X}$. As an example we could imagine a quantum dot experiment (see, for example Ref. [106]) in which the role of the symmetry breaking perturbation is played by the magnetic field. More abstractly, we could imagine the orthogonal random matrix model of Eq. (7.196) acted upon by an antisymmetric (unitary) perturbation such as Aharonov-Bohm flux or magnetic field.

To account for the additional parameter it is necessary to extend the rescaling in Eq. (7.192) in the manner [105]

$$x_u^2 = C_u(0;\bar{X}\to\infty)\bar{X}^2, \qquad \bar{x}^2 = C_u(0;\bar{X}\to\infty)\bar{X}^2, \tag{9.221}$$

where $C_u(0,\bar{X}) = \langle(\partial\epsilon_i(\bar{X})/\partial\bar{X})^2\rangle$. We remark that X_u is rescaled in the unitary limit while an orthogonal or symplectic perturbation would be rescaled in their respective limits.

A straightforward extension of the previous calculation yields the expression in Eq. (7.205) ($m=2$) with

$$F[Q] = \mathrm{STr}\Big[\mathrm{i}\frac{\pi}{4}\omega\Lambda Q - \frac{\pi^2}{8}[Q,\bar{x}\tau_3 + x_u\tau_3\Lambda/2]^2\Big], \tag{9.222}$$

and the constraint $Q^2=1$. This result compares with Eq. (7.177). Although the definite integration can be performed explicitly the results are somewhat technical and we feel do not warrant rewriting here. Instead we would direct interested readers to Ref. [105] and [67] where details of the calculation are presented. However, Eq. (9.222) demonstrates the universality of the two-point correlator of DoS depends, $k(\omega, x_u;\bar{x})$.

We remark that, for a set of independent perturbations indexed by the vector $\boldsymbol{x}=(x_1,x_2,\cdots x_n)$, we obtain the same expression for the action as Eq. (9.222) with $\bar{x}^2=\bar{\boldsymbol{x}}^2$, $x_u^2=\boldsymbol{x}_u^2$, and $|\bar{\boldsymbol{x}}||\boldsymbol{x}_u|\cos\theta = \bar{\boldsymbol{x}}\cdot\boldsymbol{x}_u$. In the present case, $\cos\theta=1$.

Using such results it is possible to determine the explicit expression for the distribution of level gradients as a function of the symmetry breaking parameter [105]. It is interesting to note that, in the orthogonal limit, the variance of the level gradient shows a logarithmic dependence on $\bar{x}$

$$\lim_{\bar{x}\ll 1}\Big\langle\Big(\frac{\partial\epsilon_i}{\partial x_u}\Big)^2\Big\rangle = -2\pi^2\bar{x}^2\ln(2\pi^2\bar{x}^2). \tag{9.223}$$

This dependence, which can be understood from a 2×2 random matrix suggests a divergence of the variance of the curvature distribution in the same limit [107].

10. Beyond Level Correlations

So far we have concentrated on universal level correlations in the spectrum of quantum chaotic systems. In the following section we will go beyond level correlations to explore the properties of the dimensionless density response functions

$$n_D(\epsilon_1, \epsilon_2; x_1, x_2) = \Delta^2 \Big\langle \mathrm{Tr}\Big[\delta(E_1 - H(X_1))\delta(E_2 - H(X_2))\Big]\Big\rangle, \quad (10.224)$$

$$n_C(\epsilon_1, \epsilon_2; x_1, x_2) = \Delta^2 \Big\langle \mathrm{Tr}\Big[\delta(E_1 - H(X_1))\delta(E_2 - H(X_2))^T\Big]\Big\rangle, \quad (10.225)$$

defined in the particle-hole (diffuson) and particle-particle (Cooperon) channel respectively, as well as wavefunction correlations. Here we have used the shorthand $\delta(E - H(X)) \equiv -(1/\pi)\ \mathrm{Im}\ G^R(E, X)$. Later we will explore the physical applications of such correlations. However, to begin we will discuss a useful relation which connects different types of parametric correlation function through a "continuity relation" for energy levels.

We remark that for perturbations which conserve the symmetry of the Hamiltonian the function n_C is trivial — for T-invariant ensembles, the transpose operation leaves the Green function unchanged and $n_C(\epsilon_1 - \epsilon_2, x_1 - x_2) = n_D(\epsilon_1 - \epsilon_2, x_1 - x_2)$ or $-n_D(\epsilon_1 - \epsilon_2, x_1 - x_2)/2$ according to whether the symmetry is orthogonal or symplectic respectively. For unitary ensembles the Green function is statistically independent of its transpose and n_C vanishes. However in the vicinity of the crossover between ensembles n_C can still assume a non-vanishing value which smoothly interpolates between these two limits.

10.1. Continuity Relation

Although the response functions n_D and n_C appear to be independent of the DoS correlator k, in the following we will show them to be connected by a form of continuity relation [67]. As usual, the results we derive apply generally to quantum chaotic systems, but for convenience we will develop these ideas using RMT. Our starting point will be the generalization of the random matrix Hamiltonian of Eq. (7.196) to two adjustable sets of parameters $\{\boldsymbol{X}_\alpha\}$, $\{Y_\alpha\}$,

$$H(\boldsymbol{X}_\alpha, Y_\alpha) = H^{(0)} + \sum_\alpha \left(\boldsymbol{X}_\alpha \cdot \boldsymbol{\Phi}^{(\alpha)} + Y_\alpha \Theta^{(\alpha)}\right), \quad (10.226)$$

where, as before, $H^{(0)}$ is a random matrix belonging to one of the Dyson ensembles, and $\{\boldsymbol{\Phi}^{(\alpha)}\}$, $\{\Theta^{(\alpha)}\}$ denote fixed traceless Hermitian matrices.

A vector notation is used to indicate that the perturbation, $\boldsymbol{X}$ is allowed to have an arbitrary number of components each corresponding to an independent "direction" of perturbation. Subscripts, $\alpha = 1, 2$ are used to index the different symmetry classes, orthogonal and unitary. Symplectic symmetry will be considered presently. The independence of the perturbations, which can be imposed without loss of generality, implies

$$\begin{aligned}
&\mathrm{Tr}\ [\Phi_i^{(\alpha)}\ \Phi_j^{(\gamma)}] = \delta_{ij}\ \delta_{\alpha,\gamma}\ \alpha\ N^2\Delta^2 C_{X_i}(0)/2,\\
&\mathrm{Tr}\ [\Theta^{(\alpha)}\ \Theta^{(\gamma)}] = \delta_{\alpha,\gamma}\ \alpha\ N^2\Delta^2 C_Y(0)/2,\\
&\mathrm{Tr}\ [\Phi_i^{(\alpha)}\ \Theta^{(\gamma)}] = 0,
\end{aligned} \tag{10.227}$$

where Greek superscripts are used to index the different vector components of $\boldsymbol{\Phi}$. In fact the orthogonality condition can be relaxed providing the two types of matrices are uncorrelated such that $\mathrm{Tr}\ [\Phi_i^{(\alpha)}\ \Theta^{(\gamma)}] = \mathrm{O}(N)$. In the following, we will use the perturbations along Y_α as a "probe" in a manner analogous to linear response. In the supersymmetrical path-integral formulation, the perturbation along Y acts as a source.

For some given choice of γ we proceed by defining the following unrescaled correlation function,

$$\begin{aligned}
A(E, E'; \boldsymbol{X}_\alpha, \boldsymbol{X}'_\alpha) &= \frac{\partial}{\partial Y_\gamma}\frac{\partial}{\partial Y'_\gamma}\Big|_{Y_\gamma = Y'_\gamma = 0} \int_{-\infty}^{E} dS \int_{-\infty}^{E'} dS' \\
&\times \Big\langle \mathrm{Tr}\Big[\delta(S - H(\boldsymbol{X}_\alpha, Y_\gamma))\Big]\ \mathrm{Tr}\Big[\delta(S' - H(\boldsymbol{X}'_\alpha, Y'_\gamma))\Big]\Big\rangle,
\end{aligned} \tag{10.228}$$

where the integrand is recognized as the generalized two-point function k. The utility of this definition can be seen by making use of the antiunitarity of the product, $U^\dagger(\partial U/\partial Y) = -(\partial U^\dagger/\partial Y)U$. It is then straightforward to show that

$$\frac{\partial}{\partial Y}\mathrm{Tr}\ \delta(E - H(Y)) = -\frac{\partial}{\partial E}\ \mathrm{Tr}\Big[\delta(E - H(Y))\ \frac{\partial H(Y)}{\partial Y}\Big]. \tag{10.229}$$

Interpreting the right hand side as the total level "current" this identity can be regarded as a "continuity relation" for the spectrum. We remark that higher derivatives contain several contributing terms. Applying this relation to Eq. (10.228) and taking the derivative of the Hamiltonian we find

$$\begin{aligned}
&A(E, E'; \boldsymbol{X}_\alpha, \boldsymbol{X}'_\alpha) = \\
&\Big\langle \mathrm{Tr}\Big[\delta(E - H(\boldsymbol{X}_\alpha, 0))\ \Theta^{(\gamma)}\Big]\ \mathrm{Tr}\Big[\delta(E' - H(\boldsymbol{X}'_\alpha, 0))\ \Theta^{(\gamma)}\Big]\Big\rangle_c.
\end{aligned} \tag{10.230}$$

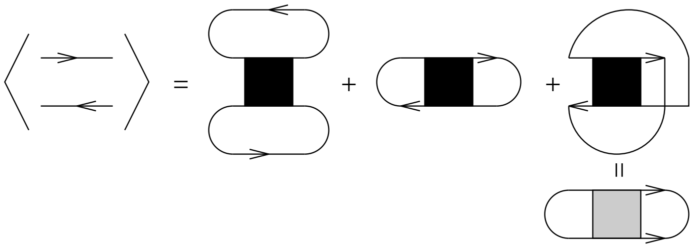

Fig. 25. Diagrammatic representation of two-particle average described in the text.

Averaging the kernel of A it is necessary to pair the matrix indices (see fig. 25). As a result we obtain [67]

$$\begin{aligned} N^2\Delta^2 \Big\langle \Big[\delta(E - H(\boldsymbol{X}_\alpha, 0))\Big]_{ij} \Big[\delta(E' - H(\boldsymbol{X}'_\alpha, 0))\Big]_{kl} \Big\rangle_c = \\ n_D(E - E', \boldsymbol{X}_\alpha, \boldsymbol{X}'_\alpha)\delta_{il}\delta_{jk} + n_C(E - E', \boldsymbol{X}_\alpha, \boldsymbol{X}'_\alpha)\delta_{ik}\delta_{jl} \\ + k(E - E', \boldsymbol{X}_\alpha, \boldsymbol{X}'_\alpha)\delta_{ij}\delta_{kl} + \mathrm{O}(N^{-1}). \end{aligned} \tag{10.231}$$

Had the matrices $\boldsymbol{\Phi}^{(\alpha)}$ and $\Theta^{(\gamma)}$ not been chosen "orthogonal", the residual term would not be smaller by a factor of N^{-1} but would instead contribute an amount comparable to the terms retained. We remark that, when dealing with disordered conductors we should identify the matrix indices with coordinates in space and make the substitution [66]

$$[\delta(E - H)]_{ij} \to (1/\pi)\mathrm{Im}\, G^R(\boldsymbol{r}_i, \boldsymbol{r}_j; E), \qquad \delta_{ij} \to f_d(\boldsymbol{r}_i - \boldsymbol{r}_j), \tag{10.232}$$

where f_d is given by Eq. (6.153).

Applying Eq. (10.231) to $A(E, E'; \boldsymbol{X}_\alpha, \boldsymbol{X}'_\alpha)$ we note that the vanishing of Tr $[\Theta^{(\gamma)}]$ causes the contraction of the first term to vanish. Assembling the remaining terms we obtain

$$\begin{aligned} A(E, E'; \boldsymbol{X}_\alpha, \boldsymbol{X}'_\alpha) = \\ \frac{\gamma C_Y(0)}{2}\Big[n_D(E - E'; \boldsymbol{X}_\alpha, \boldsymbol{X}'_\alpha) - (-)^\gamma n_C(E - E'; \boldsymbol{X}_\alpha, \boldsymbol{X}'_\alpha)\Big]. \end{aligned} \tag{10.233}$$

The minus sign that appears for unitary Θ is due to the antisymmetry of the perturbation under transpose. Combining Eq. (10.233) and Eq. (10.228) and applying the universal rescaling of Eq. (7.192) we obtain the general relation,

$$\frac{\partial}{\partial y_\gamma}\frac{\partial}{\partial y'_\gamma}\Big|_{y_\gamma = y'_\gamma = 0} k(\epsilon - \epsilon'; \boldsymbol{x}_\alpha, \boldsymbol{x}'_\alpha, y_\gamma, y'_\gamma) =$$

$$\frac{\gamma}{2}\frac{\partial}{\partial\epsilon}\frac{\partial}{\partial\epsilon'}\Big[n_D(\epsilon-\epsilon';\boldsymbol{x}_\alpha,\boldsymbol{x}'_\alpha)-(-)^\gamma n_C(\epsilon-\epsilon';\boldsymbol{x}_\alpha,\boldsymbol{x}'_\alpha)\Big]. \tag{10.234}$$

This is the principle relation which connects the three correlation functions k, n_D, and n_C. Subject to the conditions on the source described above, it applies quite generally, independent of the symmetry of $\boldsymbol{\Phi}^{(\alpha)}$ and the value of the parameters $\boldsymbol{X}_\alpha$ and $\boldsymbol{X}'_\alpha$. In particular, this relation holds even for the case in which the perturbation in X violates the symmetry of $H^{(0)}$ — the "crossover regime."

Defining $\omega=\epsilon-\epsilon'$, $y_o\equiv y_1-y'_1$, $\bar{y}\equiv(y_2+y'_2)/2$, $y_u=y_2-y'_2$ (and similarly $\boldsymbol{x}_o$, $\bar{\boldsymbol{x}}$, $\boldsymbol{x}_u$), and making use of $\gamma=1$ and 2 Eq. (10.234) can be inverted to give

$$\left[\frac{\partial^2}{\partial y_o^2}\pm\frac{1}{2}\left(\frac{\partial^2}{\partial y_u^2}-\frac{1}{4}\frac{\partial^2}{\partial\bar{y}^2}\right)\right]k(\omega;\boldsymbol{x}_\alpha,y_\alpha)\Big|_{y_\alpha=0}=\frac{1}{2}\frac{\partial^2}{\partial\omega^2}n_{\substack{D\\C}}(\omega;\boldsymbol{x}), \tag{10.235}$$

In the limiting cases Eq. (10.235) can be easily understood. Firstly, in the extreme unitary limit, k becomes independent of $\bar{y}$ and as a result $\partial^2k/\partial\bar{y}^2=0$. Moreover, since we are perturbing a unitary matrix, both the symmetric and antisymmetric perturbations act in a unitary direction. (In consequence, we should recognize that for the rescaling of Y_o a factor of $1/2$ (or $1/\beta$) must be included in the definition of $C(0)$.) Then we are at liberty to make the substitution $\partial^2/\partial y_o^2\to(1/2)\,\partial/\partial(y_o)^2$ in both equations. Finally, in the pure symmetry case, the dependence on the perturbations $\boldsymbol{y}$ (and $\boldsymbol{x}$) enters only through y_o^2, $\bar{y}^2$, and y_u^2 allowing us to drop the perturbation along Y altogether and write unambiguously the relation

$$2\frac{\partial k(\omega,x)}{\partial(x^2)}=\frac{\partial^2 n_D(\omega,x)}{\partial\omega^2}, \tag{10.236}$$

first reported in Ref. [108]. On the other hand Eq. (10.235) shows n_C to vanish. Applying Eq. (10.236) to Eq. (7.195) we obtain the universal expression for the density response function for unitary ensembles [109],

$$n_D(\omega,x)=\frac{1}{2}\mathrm{Re}\int_1^\infty d\lambda_1\int_{-1}^1 d\lambda\,\frac{\lambda_1+\lambda}{\lambda_1-\lambda}\times\mathrm{e}^{-\mathrm{i}\pi\omega^+(\lambda-\lambda_1)-(\pi^2x^2/2)(\lambda_1^2-\lambda^2)}, \tag{10.237}$$

Switching to the orthogonal limit consider the action of an antisymmetric perturbation. Since the eigenvalues are invariant under the transformation $Y_2\to-Y_2$ the level gradients must vanish at $Y_2=0$ for all eigenvalues. As a result the derivative $\partial^2/\partial Y_2\partial Y'_2|_{Y_2=Y'_2=0}k$ which makes up the second and third terms in Eq. (10.235) vanishes. Eq. (10.235) thus reduces to the relation in Eq. (10.236) and confirms the equivalence of n_D and n_C in this limit.

Previously we saw through the σ-model of Eq. (9.222) that statistical correlators depend on at most five independent parameters, ω, the modulus of the vectors, $x_\alpha \equiv |\boldsymbol{x}_\alpha|$, and the angle $\cos\theta = \bar{\boldsymbol{x}} \cdot \boldsymbol{x}_u/|\bar{\boldsymbol{x}}|\ |\boldsymbol{x}_u|$. (For a single unitary perturbation, $\theta = 0$.) It is therefore possible to abandon the source terms parametrized by y_α, and write the relation directly through derivatives on the original parameters. As a result we obtain,

$$\Big\{2\frac{\partial}{\partial(x_o^2)} \pm \Big[\frac{\partial}{\partial(x_u^2)} - \frac{1}{4}\frac{\partial}{\partial(\bar{x}^2)} - \frac{1}{2}\Big(\frac{1}{4\bar{x}^2} - \frac{1}{x_u^2}\Big)\cot\theta\frac{\partial}{\partial\theta}\Big]\Big\}k(\omega; x_\alpha, \theta)$$
$$= \frac{1}{2}\frac{\partial^2}{\partial\omega^2} n_{\substack{D\\C}}(\omega; x_\alpha, \theta). \tag{10.238}$$

Applying the relations above, n_D and n_C can be calculated from the general two-point density correlator. The results of this calculation can be found in Ref. [67]

Although we confined our discussion to the two-point correlators n_D, n_C, and k a similar approach can be applied to higher-point correlators. In particular, to develop the relation between the DoS fluctuations and the response functions we focussed on combinations of $G^R - G^A$. However, it is clear that the same consideration can be applied to separate combinations of Green functions such as $\langle \mathrm{Tr}\ G^R(1)\ \mathrm{Tr}\ G^A(2)\rangle$. Furthermore, it is possible to apply the same method to find integral relations between higher-point correlators.

10.2. Applications

Having determined the relation between two-point density correlator and the two types of density response function let us consider the implications for properties in the crossover region. In particular we will focus on three examples which are sensitive to n_C.

10.2.1. Dynamical Echo

Firstly, we will consider the diffusion propagator of a particle in a disordered metal and the phenomenon of "dynamical echo" recently discussed by Prigodin et al. [66]. Following Ref. [66] let us consider the conditional probability for a particle with energy E_F to propagate from a point $\boldsymbol{r}_1$ to a point $\boldsymbol{r}_2$ in a time t. This probability density $P(\boldsymbol{r}_{12}, t)$ can be expressed through the Fourier transform of the density response function $R(\boldsymbol{r}, \boldsymbol{r}'; \Omega)$

defined in Eq. (6.134),

$$P(\boldsymbol{r}_{12};\omega,\bar{x}) = \frac{1}{2\pi\nu}\Big\langle\, G^R(\boldsymbol{r}_1,\boldsymbol{r}_2;\epsilon_F+\omega/2,\bar{x}) \times G^A(\boldsymbol{r}_2,\boldsymbol{r}_1;\epsilon_F-\omega/2,\bar{x})\Big\rangle. \qquad (10.239)$$

where $\boldsymbol{r}_{ij} \equiv \boldsymbol{r}_i - \boldsymbol{r}_j$. Separating the statistical properties of the eigenvectors and eigenvalues as in Eq. (10.231) the ensemble average is obtained straightforwardly,

$$P(\boldsymbol{r}_{12};\omega,\bar{x}) = \pi\nu\Big[f_d(\boldsymbol{r}_{12})^2\ \Big(\frac{1}{2}+k(\omega,\bar{x})+n_C(\omega,\bar{x})\Big)+n_D(\omega)\Big], \qquad (10.240)$$

where $f_d(\boldsymbol{r})$ was defined previously in Eq. (6.153), and $\bar{x}$ denotes a rescaled symmetry breaking parameter which, as usual, can be attributed to an arbitrary perturbation such as Aharonov-Bohm flux or magnetic field. We remark that Eq. (10.240) coincides with the results obtained in Ref. [66] in all pure symmetry cases. However, in addition, the function $n_C(\omega,\bar{x})$ gives the correct dependence at arbitrary $\bar{x}$.

The presence of n_C is easily understood. It arises from the quantum interference between time-reversed paths or Cooperons. It contributes only to the return probability and so is regulated by the function $f_d(\boldsymbol{r})$. In fact this additional contribution to the return probability is the source of all weak localization effects.

Eq. (10.240) suggests that the probability to find the particle at a point $\boldsymbol{r}_2$ at a time t has a narrow peak at $\boldsymbol{r}_1 = \boldsymbol{r}_2$. This was first discussed in the limit $t \to \infty$ by Berry [110] and later by Heller [111]. The dynamics of this peak are complex: At $t \leqslant t_c$ it is determined by n_C, while for $t_c \ll t \leqslant t_H$ the time-dependent return probability is determined by k.

The phenomena can be understood qualitatively in the following way. Suppose a δ-function wavepacket is created at $t = 0$. An expansion of the wavepacket in terms of the exact eigenfunctions, ϕ_α gives $\psi(\boldsymbol{r},0) = \sum_\alpha c_\alpha\phi_\alpha(\boldsymbol{r})$ where $c_\alpha = \phi^*_\alpha(\boldsymbol{r}_1)$. To describe $\psi(\boldsymbol{r},t)$ we must consider the time-dependence $c_\alpha(t) = c_\alpha(0)\exp(\mathrm{i}E_\alpha h/\hbar)$. The phase dispersion of the terms in the series manifests itself in the broadening of the wavepacket. At $t > t_c$ we will end up with a uniform (in average) distribution.

The reason why the distribution does not remain uniform at all times is the spectral rigidity: At $t \sim t_H$ the phase coherence is recovered partially and the peak in the density distribution is developed. The stronger the level repulsion the more abrupt is the phenomenon. Qualitatively this dynamics is determined entirely by the Fourier transform of $k(\omega)$.

10.2.2. Oscillator Strengths

In experiment, such as the spectroscopy of diamagnetic hydrogen, it is typical to access not just the spectrum, but also the transition probabilities from an initial given state to excited states. In the case of optical transitions, these probabilities are known as oscillator strengths. Generally the oscillator strength can be defined as

$$W(\omega, \boldsymbol{x}) = 2\omega \sum_{\nu} |M_{0\nu}|^2 \delta(\epsilon_\nu(\boldsymbol{x}) - \epsilon_0 - \omega), \tag{10.241}$$

where $M_{0\nu} = \langle 0|\hat{M}|\nu\rangle$ is some non-universal matrix element between a reference ground state $|0\rangle \equiv \psi_0(\boldsymbol{r})$ and an excited state $|\nu\rangle$. For example, in the case of diamagnetic hydrogen, the operator $\hat{M} \equiv \hat{z}$ and $M_{0\mu}$ denotes the dipole matrix element.

Following Ref. [108] we will examine the connected two-point correlator

$$S(\omega, \boldsymbol{x}) = \Big\langle W(\epsilon - \omega, \bar{x} - x)\ W(\epsilon, \bar{x})\Big\rangle_c. \tag{10.242}$$

Representing the δ function in terms of Green functions, the correlation function can be expressed as

$$S(\omega, x) = \int d\boldsymbol{r}_1\ d\boldsymbol{r}_2\ d\boldsymbol{r}_3\ d\boldsymbol{r}_4\ B(\{\boldsymbol{r}_i\})\ R(\{\boldsymbol{r}_i\}), \tag{10.243}$$

where

$$B(\{\boldsymbol{r}_i\}) = 4\omega^2 \hat{M}\psi_0^*(\boldsymbol{r}_1))\ (\hat{M}\psi_0(\boldsymbol{r}_2))\ (\hat{M}\psi_0^*(\boldsymbol{r}_3))\ (\hat{M}\psi_0(\boldsymbol{r}_4)), \tag{10.244}$$

$$\begin{aligned} R(\{\boldsymbol{r}_i\}) = \frac{1}{\pi^2}\Big\langle &\mathrm{Im}\ G^R(\boldsymbol{r}_1, \boldsymbol{r}_2; \epsilon - \omega/2, \bar{x} - x/2) \\ &\times \mathrm{Im}\ G^R(\boldsymbol{r}_3, \boldsymbol{r}_4; \epsilon + \omega/2, \bar{x} + x/2)\Big\rangle_c. \end{aligned} \tag{10.245}$$

Eq.(10.245) is the coordinate representation of Eq. (10.231) and can be averaged in the same manner. As a result we obtain

$$S(\omega, x) = 2\pi\Big[S_0^2\Big(k(\omega, x) + n_D(\omega, x)\Big) + |S_1^2|\ n_C(\omega, x)\Big], \tag{10.246}$$

where

$$S_0 = \int d\boldsymbol{r}_1\ d\boldsymbol{r}_2\ (\hat{M}\psi_0^*(\boldsymbol{r}_1))\ f_d(\boldsymbol{r}_{12})\ (\hat{M}\psi_0(\boldsymbol{r}_2)), \tag{10.247}$$

$$S_1 = \int d\boldsymbol{r}_1\ d\boldsymbol{r}_2\ (\hat{M}\psi_0(\boldsymbol{r}_1))\ f_d(\boldsymbol{r}_{12})\ (\hat{M}\psi_0(\boldsymbol{r}_2)). \tag{10.248}$$

For diamagnetic hydrogen the Hamiltonian is antiunitary, invariant under a combination of T-reversal and inversion. As a result the symmetry is orthogonal and the wavefunctions can be chosen real. Hence $(S_1,\, n_C)$ and $(S_0,\, n_D)$ coincide respectively. However, if we apply an electric field in a direction which is neither parallel nor perpendicular to the magnetic field, the inversion symmetry is broken and with it the orthogonality of the Hamiltonian. The electric field then acts as a symmetry breaking parameter and n_C develops a non-trivial dependence.

10.2.3. Magnetoconductivity

Let us consider the conductivity defined in Eq. (4.54). In fact, this formula is valid only if Coulomb Blockade effects are negligible, i.e. when $e^2/C \ll \max(\Omega, \Delta)$ where C is the capacitance. The opposite case was discussed in detail in Refs. [112, 113]. Moreover, the relaxation processes that are neglected by Eq. (4.54) were shown in Ref. [114] to be of great importance for the conductivity of real systems. Nevertheless, it is important to understand the "free electron conductivity" in a quantum dot.

Proceeding with the Kubo formula for the conductivity in Eq. (4.54), and making use of Eq. (10.231), the vector nature of the vertex causes the diffuson contribution from n_D to vanish ($\hat{p}_\mu f_d(0) = 0$). The remaining contributions give

$$\langle \sigma_{\mu\nu}(\omega, \bar{x})\rangle = \sigma_0 \delta_{\mu\nu}\Big[1 + k(\omega, \bar{x}) + n_C(\omega, \bar{x})\Big], \qquad (10.249)$$

$$\sigma_0 = \frac{e^2 L^d}{\pi}\int d\boldsymbol{r}\, \frac{(\boldsymbol{r}\cdot\hat{e}_1)^2}{|\boldsymbol{r}|^2}\left|\frac{\partial f_d(|\boldsymbol{r}|)}{\partial |\boldsymbol{r}|}\right|^2 \int d\epsilon\, \frac{n_F(\epsilon+\omega) - n_F(\epsilon)}{\omega}. \qquad (10.250)$$

For unitary ensembles, the breaking of T-invariance destroys the Cooperon contribution and the average conductance becomes proportional to the two-point density correlator, $k(\omega, \bar{x})$. The average conductance depends only the correlation of the eigenvalues and is independent of the statistics of the matrix elements of the current operator. This result compares with the two-point correlator of oscillator strengths [108]. In particular, at large values of ω the result converges to the constant classical Drude value.

The Kubo formula in Eq. (4.54) can be applied to determine an expression for the rate of energy dissipation in a Hamiltonian with randomly distributed matrix elements in response to an external perturbation. Following Wilkinson [115] the effective conductivity can be expressed in the form

$$\sigma(\omega, x) \propto \frac{\partial H}{\partial y}\mathrm{Im}\ G^R(\epsilon+\omega, x)\frac{\partial H}{\partial y}\mathrm{Im}\ G^R(\epsilon, x)\Big]\Big|_{y=0}, \qquad (10.251)$$

where Y is some infinitesimal perturbation applied as a source along Θ

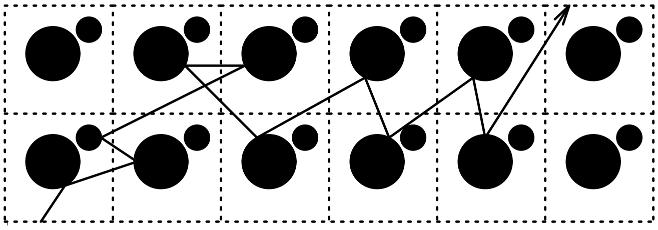

Fig. 26. Periodic array of chaotic cavities without a center of symmetry.

(Tr $\Theta = 0$). Averaging we obtain

$$\langle \sigma(\omega, \bar{x}) \rangle \propto \frac{1}{N^2 \Delta^2} \Big[\mathrm{Tr}\ \Theta_c^2 k(\omega, x) + \mathrm{Tr}\ (\Theta_c \Theta_c^T) n_C(\omega, \bar{x}) \Big], \qquad (10.252)$$

the matrix analogue of Eq. (10.249).

The same formula can be used to argue that the rate of energy dissipation in in response to a time dependent perturbation is equal to [115, 92]

$$\frac{\partial W}{\partial t} = \frac{\pi \beta}{2} \hbar C(0) \Big(\frac{\partial X}{\partial t} \Big)^2 . \qquad (10.253)$$

This represents a kind of "mesoscopic (sample to sample, or Fermi level to Fermi level) fluctuation-dissipation theorem" and gives to $C(0)$ the physical meaning of a generalized conductance. For the example of Aharonov-Bohm flux discussed earlier, Eq. (10.253) is confirmed straightforwardly.

10.2.4. Dielectric Response of a Periodic Irregular Structures

Antidot arrays and cavities offer the possibility of measuring the AC conductivity of periodic structures whose elementary cells are themselves chaotic (see fig. 26). This geometry was exploited in Ref. [109] to determine the dielectric response function of a periodic structure in the following way: The density response function defined in Eq. (4.65) can be related to the dielectric function through the relation,

$$\epsilon(\boldsymbol{q}, \Omega) = 1 - V(\boldsymbol{q}) \Pi(\boldsymbol{q}, \Omega), \qquad (10.254)$$

where $V(\boldsymbol{q})$ denotes the Coulomb potential. Moreover, the AC conductivity can be found from the continuity relation

$$\sigma(\Omega) = e^2 \lim_{\boldsymbol{q} \to 0} \frac{\mathrm{i}\Omega}{\boldsymbol{q}^2} \Pi(\boldsymbol{q}, \Omega). \qquad (10.255)$$

In the periodic crystal, the Schrödinger equation for the periodic part of the Bloch function can be presented as a chaotic cavity with quasi-periodic boundary conditions imposed by the quasi-momentum [81], $\varphi_\mu = Lk_\mu/2\pi$. Expressing the density response function through Green functions one obtains [109]

$$\Pi(\boldsymbol{q},\Omega) = -\nu - \delta_{\boldsymbol{q},2\pi\boldsymbol{\varphi}/L+\boldsymbol{G}} \frac{\mathrm{i}}{2\pi}\int_{-\Omega/2}^{\Omega/2} \mathrm{d}E \int \mathrm{d}\boldsymbol{r}\,\mathrm{d}\boldsymbol{r}' \times\Big\langle G^R(\boldsymbol{r},\boldsymbol{r}';E,\bar{\boldsymbol{\varphi}}-\boldsymbol{\varphi})\; G^A(\boldsymbol{r}',\boldsymbol{r};E,\bar{\boldsymbol{\varphi}})\Big\rangle, \tag{10.256}$$

where $\boldsymbol{G}$ denotes the reciprocal lattice vector and the average is taken over $\bar{\boldsymbol{\varphi}}$.

Making use of Eq. (10.231) we obtain

$$\mathrm{Im}\,\Pi(\boldsymbol{q},\omega) = -\pi\omega\nu n_D(\omega,x), \tag{10.257}$$

where $x = \sqrt{2}\widetilde{q}/\pi$ and $\widetilde{q}^2 = (\pi g/2)(\boldsymbol{q}L)^2$.

Asymptotically, in the limit of large $\widetilde{q}$ or $\widetilde{\omega} = \pi\omega$ we obtain

$$\Pi(\boldsymbol{q},\Omega) = \frac{2\nu\widetilde{q}^2}{-\mathrm{i}\widetilde{\omega} + 2\widetilde{q}^2}. \tag{10.258}$$

This demonstrates that, for $g \gg 1$, the diffusive result remains valid for $1/\sqrt{g}L \ll \max[|\boldsymbol{q}|, \sqrt{\Omega/D}] \leqslant 1/L$, and periodicity manifests itself only at scales larger than $\sqrt{g}L$ (as opposed to L).

Combining Eq. (10.257) with Eq. (10.255) we obtain the result

$$\mathrm{Re}\;\sigma(\Omega) = \nu e^2 D\; k(\omega), \tag{10.259}$$

consistent with the results of the previous section.

It is interesting to note [116] that, while the T-invariance is apparently broken by the quasimomentum, orthogonal symmetry can be restored by an inversion symmetry of the crystal [103]. This means that, depending on the symmetry of the elementary cell, all three types of response function can find application.

10.3. Wavefunction Correlations

The supersymmetry approach also allows the calculation of statistical properties of wavefunctions. Both conductance fluctuations in the Coulomb blockade regime [117, 118] and NMR of small metallic particles [119] have been studied using this approach. Perhaps the simplest example concerns the distribution of local density

$$P(v) = \Delta\Big\langle \sum_\alpha \delta(v - V|\psi_\alpha(\boldsymbol{r})|^2)\delta(E-E_\alpha)\Big\rangle. \tag{10.260}$$

As expected, where the zero-dimensional σ-model is applicable, results coincide with RMT and, in this case, yield the Porter-Thomas distribution

$$P(v) = \begin{cases} \mathrm{e}^{v/2}/\sqrt{2\pi v} & \beta = 1, \\ \mathrm{e}^{-v} & \beta = 2. \end{cases} \tag{10.261}$$

Indeed the σ-model approach has recently been used to determine how the distribution function interpolates between orthogonal and unitary in response to a perturbation which breaks T-invariance [120]. It is also evident from the form of the σ-model derived in section 7.2 that parametric correlations of wavefunction amplitudes, such as the oscillator strength correlator, are also universal.

The σ-model approach also offers the possibility of examining the spatial correlations of disordered conductors [121]. In Ref. [121] it was speculated that these studies apply equally to ballistic chaotic systems. This view is supported by recent experimental studies on microwave cavities [122, 123].

In conclusion, the zero-dimensional σ-model provides a convenient way of representing certain averages within RMT. Whether it is easier to determine results through the σ-model or through other RMT approaches depends very much on the problem at hand.

11. Level Dynamics and the Matrix Field Theory

The manifold of energy levels into which spectra separate have a form reminiscent of particle world lines with the eigenvalues playing the role of coordinates and the perturbation parameter acting as "time" (see, for example, fig. 24). Remarkably an interpretation of this kind is found to be exact. More than 30 years ago this notion lead Dyson [124] to a description of level statistics in terms of the Brownian motion of a classical one-dimensional Coulomb gas. Dyson envisaged each particle acted upon by some stochastic force and interacting with its neighbors. The Langevin equation describing the particle dynamics can be transformed into a many-particle Fokker-Planck equation. With this approach Dyson proved that Brownian motion of matrix elements implied the Brownian motion of eigenvalues.

There have been a number of related studies that associate the dispersion of a spectrum with the dynamics of interacting particles which lie outside the scope of this lectures (see, for example, Refs. [125–133]). In particular, we draw attention to the important work of Pechukas [125] (see also Refs. [126–128]) who demonstrated that the dispersion of the energy levels of a non-integrable Hamiltonian in response to an external perturbation can be expressed as a set of first order differential equations, later shown to be integrable [134]. Indeed the equilibrium statistical mechanics of the "Pechukas gas" becomes equivalent to random matrix theory if we accept a statistical hypothesis [89].

In Dyson's approach, no physical significance was attached to the fictitious time. In fact, as we will see, this time is intimately connected to the rescaled parameter of the perturbation, and the dynamics reproduce exactly the universal level correlations. In this section we will demonstrate that correlation functions derived previously describe the exact dynamical correlations of an interacting system of fermions.

We begin by establishing the connection (Brezin *et al.* [135]) between a matrix field theory and the Sutherland-Calogero-Moser class of Hamiltonians [136, 137]. The field theory

$$S[\Phi(\tau)] = \int_{-\infty}^{\infty} \mathrm{d}\tau \ \mathrm{Tr} \left[\frac{1}{4}\left(\frac{\partial\Phi(\tau)}{\partial\tau}\right)^2 + V(\Phi)\right], \tag{11.262}$$

$$\mathcal{Z} = \int \mathcal{D}\Phi(\tau)\, \mathrm{e}^{-S[\Phi(\tau)]}, \tag{11.263}$$

describes the free propagation of $N \times N$ Hermitian matrices, Φ in a Gaussian potential $V(\Phi) = \omega_0^2 \mathrm{Tr}\ \Phi^2$. We remark that for large N only planar diagrams contribute to $\mathcal{Z}$, and the logarithm of $\mathcal{Z}$ generates the sum of connected surfaces [138, 139]. For this reason, Eq. (11.263), with a generalized matrix potential, has formed the focus of attention for studies of string theory and two-dimensional quantum gravity.

The model of Eq. (11.263) describes the ordinary quantum mechanics of an $N \times N$ matrix Φ, governed by the Hamiltonian,

$$H = \mathrm{Tr}\left[-\frac{\partial^2}{\partial\Phi^2} + V(\Phi)\right]. \tag{11.264}$$

According to the symmetry of Φ, the Hamiltonian is invariant under global $SO(N)$, $SU(N)$, or $SU(N) \times SU(N)$ rotations for orthogonal, unitary, or symplectic ensembles respectively.

In the limit of large N, the N^2 degrees of freedom can be exchanged for the N eigenvalues of Φ and the problem reduced to a system of interacting fermions [135]. The diagonalization of $\Phi(\tau) = \Omega(\tau)\Lambda(\tau)\Omega(\tau)^\dagger$ can be viewed as a separation of the "radial" degrees of freedom specified by the diagonal matrix of eigenvalues, $\Lambda(\tau) = \mathrm{diag}(\lambda_1, \cdots \lambda_N)$, from the transverse or "angular" degrees of freedom of the unitary matrix $\Omega(\tau)$.

The integration measure can be determined from RMT [25],

$$\int \mathcal{D}\Phi \to \int \prod_i d\lambda_i \; \mathcal{D}\Omega \; J(\lambda_i), \qquad J(\lambda_i) \equiv \prod_{i<j} |\lambda_i - \lambda_j|^\beta. \qquad (11.265)$$

The potential, which is assumed invariant under unitary transformations of Φ can be rewritten in terms of the eigenvalues as Tr $V(\Phi) = \sum_i V(\lambda_i)$. The kinetic energy follows from the Laplacian [25]

$$\sum_i \frac{\partial^2}{\partial \Phi_{ii}^2} + \frac{1}{2} \sum_{i<j} \Big[\frac{\partial^2}{\partial (\mathrm{Re}\Phi_{ij})^2} + \frac{\partial^2}{\partial (\mathrm{Im}\Phi_{ij})^2} \Big] = \qquad (11.266)$$

$$\sum_i \frac{1}{J(\lambda_i)} \frac{\partial}{\partial \lambda_i} J(\lambda_i) \frac{\partial}{\partial \lambda_i} + Y(\Omega, \lambda_i), \qquad (11.267)$$

where $Y(\Omega, \lambda_i)$ represents the term dependent on $\Omega(\tau)$. For open boundary conditions we are free to focus on the singlet sector in which $Y = 0$. Commuting the Jastrow product $\sqrt{J(\lambda_i)}$ through each derivative generates two and three-body interactions of the eigenvalues. The Jastrow form of the metric in Eq. (11.265) leads to cancellation of the three-body terms [137]. Assimilating the factor of $\sqrt{J(\lambda_i)}$ into the definition of the wavefunction, we obtain the Calogero model

$$H_C = -\sum_i \frac{\partial^2}{\partial \lambda_i^2} + \beta \Big(\frac{\beta}{2} - 1 \Big) \sum_{i<j} \frac{1}{(\lambda_i - \lambda_j)^2} + \sum_i V(\lambda_i), \qquad (11.268)$$

describing the motion of N fermions interacting through an inverse square pairwise interaction in the presence of a harmonic background potential $V(\lambda_i)$. Calogero [137] has shown the model to be completely separable, and the spectrum integrable. A Jordan-Wigner transformation can be used to assign arbitrary statistics to the particles. Since we propose to examine only density correlations the phase associated with the gauge transformation does not enter, and without loss of generality the statistics of the particles can be taken to be fermionic. The benefit of this representation over the matrix model is clear, particularly for unitary ensembles when the interaction term vanishes.

The ground state wavefunction of H_C [137]

$$|0\rangle \propto \sqrt{J(\lambda_i)} \exp \Big[-\frac{\omega_0}{2} \sum_i \lambda_i^2 \Big], \qquad (11.269)$$

generates a probability distribution which coincides with that of Gaussian random matrix ensembles [25]. The mean DoS corresponds to Wigner's semi-circular distribution with a mean-interparticle spacing at the origin of $\Delta = (\pi^2/4N\omega_0)^{1/2}$.

Since correlation functions decay on scale comparable to the average interparticle spacing, a range over which the average level density changes only by a factor of $\mathrm{O}(N^{-1})$, it is possible to remove the confining potential by constraining the particles to move on a ring. Properties of the resulting distribution coincide with the circular ensemble of Dyson unitary random matrices [25]. In other cases the potential smoothly regulates the DoS with particles filling the potential energy surface up to some Fermi energy. To order $1/N$ the local value of Δ is fixed and correlation functions again coincide with those of the circular ensemble. Formally the universality of the circular ensemble can be seen from renormalization group arguments as a flow to an attractive Gaussian fixed point of the potential [140].

As $N \to \infty$ correlation functions of H_C coincide with the periodic Sutherland Hamiltonian [136]

$$H_S = -\sum_i \frac{\partial^2}{\partial\lambda_i^2} + \beta\Big(\frac{\beta}{2} - 1\Big)\Big(\frac{\pi}{N}\Big)^2 \sum_{i<j} \frac{1}{\sin^2[\pi(\lambda_i - \lambda_j)/N]}, \quad (11.270)$$

where we have chosen $\Delta = 1$. This achieves our first goal of establishing a precise connection between the continuous random matrix model and the one-dimensional integrable quantum Hamiltonian H_S. Time-dependent correlation functions of the Sutherland Hamiltonian can therefore be represented by the path integral

$$\langle 0|\cdots|0\rangle \equiv \mathcal{Z}^{-1} \int \mathcal{D}\Phi(\tau)\cdots \mathrm{e}^{-S[\Phi(\tau)]}\,. \quad (11.271)$$

To complete the connection, we now consider dynamical correlation functions of H_S in the framework of the supersymmetry approach.

11.1. Supersymmetry Approach to the Matrix Field Theory

Let us now try to find an expression for the m-point correlator,

$$\big\langle 0\big|S_m(\{\lambda_\alpha, \tau_\alpha; \Sigma_\alpha\})\big|0\big\rangle = \Big\langle 0\Big|T\Big[\prod_{\alpha=1}^{m} \mathrm{Tr}\Big(\frac{1}{\lambda_\alpha + \mathrm{i}\Sigma_\alpha 0 - \Phi(\tau_\alpha)}\Big)\Big]\Big|0\Big\rangle. \quad (11.272)$$

For simplicity let us restrict attention to orthogonal ensemble of real symmetric matrices. Following our previous discussion, S_m can be presented as a functional integral in the form

$$S_m(\{\lambda_\alpha, \tau_\alpha; \Sigma_\alpha\}) = \left(\frac{\mathrm{i}}{2}\right)^m \int \mathrm{d}\Psi\, \mathrm{e}^{-L_0} \prod_\alpha \left[\Psi^\dagger P(\alpha, \mathrm{B})\Sigma_\alpha \Psi\right], \quad (11.273)$$

$$L_0 = -\frac{\mathrm{i}}{2}\bar{\Psi}[\hat{\lambda} + \mathrm{i}\hat{\Sigma}0]\Psi, \qquad L_1 = \frac{\mathrm{i}}{2}\bar{\Psi}\hat{\Phi}(\tau)\Psi, \quad (11.274)$$

where, as before, the different components form the elements of the block diagonal matrices $\hat{\lambda} = \mathrm{diag}(\lambda_1 \cdots \lambda_m)$, $\hat{\Phi}(\tau) = \mathrm{diag}(\Phi(\tau_1) \cdots \Phi(\tau_m))$.

The action is Gaussian in Φ and the path integral can be performed straightforwardly. As a result we generate the effective action from L_1,

$$L_{\mathrm{eff}} = -\frac{N\Delta^2}{4\pi^2} \sum_{\alpha,\beta} \mathrm{e}^{-2\kappa|\tau_\alpha - \tau_\beta|}\, \mathrm{STr} A_{\alpha\beta} A_{\beta\alpha}, \quad (11.275)$$

where $A = \sum_i^N \Psi_i \otimes \bar{\Psi}_i$, and $\kappa = \pi^2/4N\Delta^2$.

As before, the interaction can be decoupled by a Hubbard-Stratonovitch transformation that involves $4m \times 4m$ supermatrix fields Q. As a result

$$\langle 0|S_m|0\rangle = \left(\frac{\mathrm{i}}{2}\right)^m \int \mathrm{d}\Psi\, \mathrm{d}Q \exp\Big[-\frac{N}{4}\mathrm{STr}\, Q^2 - \frac{N\Delta}{2\pi}\sum_{\alpha\beta} \mathrm{e}^{-\kappa|\tau_\alpha - \tau_\beta|}\, \bar{\Psi}_\alpha^\dagger Q_{\alpha\beta} \Psi_\beta - L_0[\Psi]\Big]. \quad (11.276)$$

The Gaussian integration over Ψ can now be performed and yields,

$$\langle 0|S_m|0\rangle = \left(\frac{N}{2}\right)^m \int \mathrm{d}Q\ \ \mathrm{e}^{-F[Q]} \prod_\alpha \mathrm{STr}\ [\mathcal{G} P(\alpha, \mathrm{B})], \quad (11.277)$$

$$F[Q] = \frac{N}{4}\mathrm{STr}\ Q^2 - \frac{N}{2}\mathrm{STr} \ln \mathcal{G}^{-1}, \quad (11.278)$$

where $\mathcal{G}$ represents the supermatrix Green function (compare with Eq. (6.148))

$$[g(Q)^{-1}]_{\alpha\beta} = \frac{\mathrm{i}N\Delta}{\pi}\Big[\mathrm{e}^{-\kappa|\tau_\alpha - \tau_\beta|}\, Q_{\alpha\beta} - \mathrm{i}\frac{\pi}{N\Delta}\Big(\lambda_\alpha + \mathrm{i}\Sigma_\alpha\Big)\delta_{\alpha\beta}\Big]. \quad (11.279)$$

Taking $\lambda_\alpha/\Delta \sim \mathrm{O}(N^0)$ and $\tau_\alpha/\Delta^2 \sim \mathrm{O}(N^0)$ we can treat the integral within a conventional saddle-point approximation: The integration over Q restricted to the set of matrices satisfying the stationary condition $Q_{\mathrm{sp}}^2 = 1$ of Eq. (6.150). Expanding to leading order around the saddle-point we get

$$\langle 0|S_m|0\rangle = \left(\frac{\mathrm{i}\pi}{2\Delta}\right)^m \int \mathrm{d}Q\ \ \mathrm{e}^{-F[Q]} \prod_\alpha \mathrm{STr}[QP(\alpha, \mathrm{B})], \quad (11.280)$$

$$F[Q] = \mathrm{STr}\Big[\mathrm{i}\frac{\pi}{2\Delta}\sum_{\alpha} Q_{\alpha\alpha}\Big(\lambda_\alpha + \mathrm{i}\Sigma_\alpha 0\Big) \\ + \frac{\pi^2\beta}{8\Delta^2}\sum_{\alpha\beta}|\tau_\alpha - \tau_\beta|(Q_{\alpha\beta}Q_{\beta\alpha})\Big]. \tag{11.281}$$

Although the calculation was performed for orthogonal ensembles a similar approach can be applied to unitary and symplectic ensembles. To account for this we have included an appropriate factor of β into $F[Q]$.

With the exchange of variables,

$$\omega_\alpha \leftrightarrow \lambda_\alpha/\Delta, \qquad (x_\alpha - x_\beta)^2 \leftrightarrow 2|\tau_\alpha - \tau_\beta|/\Delta^2, \tag{11.282}$$

Eq. (11.281) coincides with Eq. (7.211) proving that the dynamical correlations of the ground state of the Sutherland Hamiltonian coincide with the statistical properties of RMT. However, Eq. (11.282) can not be considered as algebraic in that it is impossible to satisfy $x_\alpha = T_\alpha(\{\tau_\beta\})$ with a single choice of function $T_\alpha(\{\tau_\beta\})$ for $m > 2$.

To emphasize this correspondence let us consider the unitary ensemble. In this case the wavefunctions can be written as the Slater determinant of a set of non-interacting plain waves

$$|p\rangle = \frac{1}{N!}\det|\exp[\mathrm{i}p_i\lambda_j]|, \tag{11.283}$$

defined by the integral quantum numbers $\{n_i\}$ through the relation $p_i = 2\pi n_i/N$, and having energy equal to $E(p) = \sum_i p_i^2$. The ground state wavefunction, $|p_0\rangle$ defined by the set of quantum numbers which occupy the lowest N states has the form of a Vandermonde determinant allowing it to be written in the form of a Jastrow function

$$|0\rangle = \frac{1}{(N!N^N)^{1/2}}\prod_{i<j}|\,\mathrm{e}^{2\pi\mathrm{i}\lambda_i/N} - \mathrm{e}^{2\pi\mathrm{i}\lambda_j/N}\,|. \tag{11.284}$$

Inserting a complete set of states into the expression for the two-point density correlator we obtain

$$k(\lambda,\tau) = \frac{1}{N^2}\sum_{p\neq p_0} e^{-\tau(E(p)-E(p_0))} \\ \times \sum_{ij}\langle 0|\delta(\lambda-\lambda_i)|p\rangle\,\langle p|\delta(\lambda_j)|0\rangle. \tag{11.285}$$

Only states with a single particle excited above the Fermi surface contribute to the sum. The action of the density operator is to change the momentum of one of the particles. We therefore obtain the expression

$$k(\lambda,\tau)=\frac{2}{N^2}\sum_{|p|\leqslant p_F}\sum_{|p_1|>p_F}\exp[-\tau(p_1^2-p^2)+\mathrm{i}(p_1-p)\lambda], \tag{11.286}$$

where the Fermi momentum $p_F=\pi$. In the thermodynamic limit, $N\to\infty$ the rescaling $\lambda=p/p_F$, and $\lambda_1=p_1/p_F$ leads to the universal expression in Eq. (7.195).

A closed expression for the excited state wavefunctions at a non-vanishing value of the coupling constant is unknown. This makes a proof for the other symmetry classes less accessible. However, since the original publication [88] the results for the orthogonal and symplectic cases have been reproduced by Ha [141] using Jack Polynomials.

Since the Sutherland model displays a gapless linear low energy excitation spectrum it belongs to the universality class of Luttinger liquids [142, 143]. The $1/\tau$ asymptotic can therefore be determined by the method of bosonization [144, 145] when we obtain,

$$k(\lambda,\tau)=-\frac{1}{2\pi^2\beta}\sum_{\sigma=\pm1}\frac{1}{(\lambda+\mathrm{i}\sigma v_s\tau)^2}, \tag{11.287}$$

where the sum is over right and left movers, and the sound-wave velocity of the density fluctuations is given by $v_s=\pi\beta$ [136]. Comparing this to the large ω asymptotics of Eqs. (7.195), (7.208), and (7.209) given by

$$k(\omega,x)=\frac{1}{\beta\pi^2}\mathrm{Re}\frac{1}{(\mathrm{i}\omega+\pi\beta x^2/2)^2}, \tag{11.288}$$

and using Eq. (11.282) the correspondence is verified.

We have shown that the problem of level statistics in quantum chaotic systems and the ground state properties of H_S are related through the σ-model. We remark that the Schrödinger equation for the Sutherland Hamiltonian is also interpreted as a Fokker-Planck equation. Indeed, as recognized by Sutherland [136] it is in fact equivalent to Dyson's Brownian motion model [124] of level correlations in random matrix ensembles. The results above give physical meaning to the "fictitious" dynamics of the particles showing the friction coefficient to be related directly to the generalized conductance $C(0)$.

The connection of the Sutherland Hamiltonian to the matrix field theory can be exploited to determine an analytical expression for the m-point correlator of DoS

$$r(\{\epsilon\};\{x\})=\Delta^m\Big\langle\prod_{\alpha=1}^{m}\nu(\epsilon_i,x_i)\Big\rangle, \tag{11.289}$$

where $\{\epsilon\} \equiv \epsilon_1, \cdots \epsilon_m$, and $\{x\} = x_1, \cdots x_m$. Expanding Eq. (11.289) in terms of constituent Green functions an expression for r can be found through the generating function. The correspondence implied by Eq. (11.282) suggests that we can make use of a different approach to determine r. In particular, for unitary ensembles, the equivalent dynamical system describes non-interacting fermions and the correlation can be determined straightforwardly. Following Ref. [146] the m-point correlator for the impenetrable Bose gas at zero temperature is equal to the determinant of an $m \times m$ matrix

$$r(\{\theta\}; \{\tau\}) = \det M, \tag{11.290}$$

where the matrix M is constructed as follows:

$$M_{\alpha\beta} = \begin{cases} 1 & \alpha = \beta, \\ \frac{1}{2} \int_i d\lambda \ \ \mathrm{e}^{\pi^2|\tau_\alpha - \tau_\beta|\lambda^2 - \mathrm{i}\pi(\theta_\alpha - \theta_\beta)\lambda} & \alpha < \beta, \\ -\frac{1}{2} \int_o d\lambda_1 \ \ \mathrm{e}^{-\pi^2|\tau_\alpha - \tau_\beta|\lambda_1^2 + \mathrm{i}\pi(\theta_\alpha - \theta_\beta)\lambda_1} & \alpha > \beta, \end{cases} \tag{11.291}$$

with the momentum integrations λ and λ_1 defined on the range inside (i) and outside (o) the Fermi surface $[-1, 1]$ respectively.

In this symmetrized form Eq. (11.282) can be applied unambiguously and an expression for the universal m-point correlator $r(\{\epsilon\}; \{x\})$ deduced. Setting $m = 2$ we obtain the expression for the two-point density correlation function in Eq. (7.195). Moreover, setting all parameters, x_α to zero we obtain the expression for the "static" m-point correlator derived from RMT [25].

Switching emphasis, the approach based on the σ-model provided for the first time analytical expressions for the dynamic structure factor of a strongly interacting system of quantum particles. Soon after this result was reported, Haldane guessed the form of the dynamical correlator for coupling constant $\beta = 2 \times p/q$ [147], a result later confirmed explicitly by Ha [141]. The answer, which covers almost a page [141], was interpreted in terms of the properties of particles obeying fractional statistics in which the usual particle-hole excitation of the non-interacting Fermi gas is exchanged by a q-quasiparticle-p-quasihole excitation. For example, with $\beta = 2 \times 2/1$ the dynamic structure factor is obtained from the symplectic density correlator presented in Eq. (7.209) (see fig. 27). The double integral over the compact fermion-fermion sector reflects the two-quasihole excitations [148]. It is a surprising fact that the structure of the low energy excitations of the Sutherland model have a remarkably simple form. As yet, no connection between the generalized coupling constant, the non-linear σ-model, and a matrix field theory has been drawn but remains the subject of investigation. It is a still more intriguing prospect to wonder whether non-Hermitian

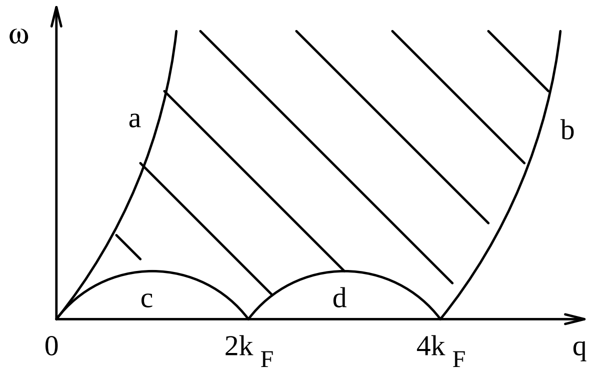

Fig. 27. Schematic diagram showing the regions of which the dynamic structure factor is non-vanishing for $\beta = 4$. The spectra weight is bounded by the (a) $q(q+4k_F)$, (b) $q(q-4k_F)$, (c) $2q(2k_F-q)$, and (d) $2(q-2k_F)(4k_F-q)$. A singularity at $2k_F$ signals the tendency of the system to form a charge density wave as a result of the repulsive interaction of the particles.

matrix models can provide a description of a strongly interacting system of two-dimensional quantum particles. However, these issues take us far from the original scope of this review and offer a good place to close.

12. Discussion

In these lectures we have steered a course through the properties of weakly disordered conductors to random matrix theory and quantum chaos. In covering such a broad field our choice of material has, by necessity, been undemocratic. In the first half of the course we have focussed on a general description of the phenomena of weak and strong localization. In doing so we have considered the manifestation of quantum coherence through magnetoresistance and universal conductance fluctuations, as well as examining the role of electron-electron interactions. Instead of attempting to present a comprehensive review (many excellent ones already exist in the literature [2, 8, 11–16, 30, 36, 37, 58, 149]) we have tried to emphasize the universality offered by the statistical description.

The concept of diffusion modes has been developed both through a diagrammatic perturbation theory and a non-perturbative field theory. We have discussed the insight offered by the latter into the nature of the localization transition. The same model provided a bridge between the statistical properties of disordered conductors and RMT which finds its origin in quantum chaos. We have described different universal properties which characterize quantum chaos.

Amongst the important related topics which have been omitted from this review include the statistical properties of scattering and transmission matrices. An account of recent developments can be found in the review by Mello in this volume (see also Refs. [150–152]).

Another very important field that we have not even touched upon is the theory of the metal-insulator transition in the presence of electron-electron interactions. (Some aspects of this problem are discussed in the courses by Schultz and Devoret in this volume.) In our view, the existing attempts (see, for example, Refs. [153, 154]) to extend the scaling approach to the strongly correlated disordered systems, while interesting, have not solved the problem and it remains one of the outstanding issues in condensed matter theory.

Many important areas in the field of quantum chaos remain only partially explored. Amongst these, perhaps the most compelling concerns the transition to chaos from either a regular (or integrable) state, or from a localized uncorrelated state. For the latter, recent studies of level statistics in disordered conductors in the vicinity of the mobility edge suggest the existence of a new universality class [155]. Over a wide interval, level repulsion is neither Wigner-Dyson nor Poisson. Instead, there is an intermediate regime in which the spectral rigidity of the $\Delta_3(E)$ statistic scales as a power law. Whether this is a generic feature of a wider class of systems remains a subject of debate. A related area of interest concerns the importance of $1/g$ corrections to universal level statistics [156, 157].

The connection between quantum chaos and the Sutherland-Calogero-Moser quantum models is also not completely understood. In particular, do rational values of β have any meaning in quantum chaos? Are there quantum models that correspond to the crossover regime? What is the effect of finite conductance on spectral statistics?

References

[1] P. W. Anderson, Phys. Rev. 109 (1958) 1492.
[2] B. Kramer and A. MacKinnon, Rep. Prog. Phys. 56 (1993) 1469.
[3] N. F. Mott, Metal-Insulator Transitions (Taylor and Francis, London, 1974).
[4] I. M. Lifshitz, Sov. Phys. Usp. 7 (1965) 549.
[5] J. Zittarz and J. S. Langer, Phys. Rev. 148 (1966) 741.
[6] P. A. Lee and A. D. Stone, Phys. Rev. Lett. 55 (1985) 1622.
[7] B. L. Altshuler, JETP Lett. 41 (1985) 648.

[8] R. A. Webb, S. Washburn, C. P. Umbach, and R. B. Laibowitz, Phys. Rev. Lett 54 (1985) 2696; R. A. Webb et al., in: Physics and Technology of Submicron Structures, eds., H. Heinrich, G. Bauer, and F. Kuchar (Springer, Berlin, 1988), Vol. 83, p. 98.
[9] D. Y. Sharvin and Y. V. Sharvin, JETP Lett. 34 (1981) 272.
[10] D. E. Khmelnitskii, Physica B+C 126 (1984) 235.
[11] G. Bergmann, Phys. Rep. 107 (1984) 1.
[12] P. A. Lee and T. V. Ramakrishnan, Rev. Mod. Phys. 57 (1985) 287.
[13] S. Chakravarty and A. Schmid, Phys. Rep. 140 (1986) 193.
[14] A. G. Aronov and Y. V. Sharvin, Rev. Mod. Phys. 59 (1987) 755.
[15] B. L. Altshuler, A. G. Aronov, M. E. Gershenson, and Y. V. Sharvin, in: Physics Reviews, ed., I. M. Khalatnikov (Harwood Academic Publishers, Switzerland, 1987), p. 225.
[16] B. L. Altshuler and P. A. Lee, Physics Today 41 (1988) 36.
[17] P. Sheng, Scattering and Localization of Classical Waves in Random Media (World-Scientific, Singapore, 1990).
[18] B. L. Altshuler, A. G. Aronov, and B. Z. Spivak, JETP Lett. 33 (1981) 94.
[19] B. L. Altshuler and B. Z. Spivak, JETP Lett. 42 (1985) 446.
[20] S. Feng, P. A. Lee, and A. D. Stone, Phys. Rev. Lett. 56 (1986) 1960.
[21] S. J. Klepper et al., Phys. Rev. B 44 (1991) 8380.
[22] E. M. Lifshitz and L. P. Pitaevskii, Physical Kinetics (Pergammon Press, Oxford, 1981).
[23] J. T. Edwards and D. J. Thouless, J. Phys. C 5 (1972) 807.
[24] D. J. Thouless, Phys. Rep. 13 (1974) 93.
[25] M. L. Mehta, Random Matrices (Academic Press, New York, 1991).
[26] D. J. Thouless, in: Ill Condensed Matter, eds., R. Balian, R. Maynard, and G. Toulous, Les Houches, Session XXXI (North-Holland, Amsterdam, 1978), p. 1.
[27] E. Abrahams, P. W. Anderson, D. C. Licciardello, and T. V. Ramakrishnan, Phys. Rev. Lett. 42 (1979) 673.
[28] N. F. Mott and W. D. Twose, Adv. Phys. 10 (1961) 107.
[29] V. L. Berezinskii, Sov. Phys. JETP 38 (1974) 620.
[30] T. V. Ramakrishnan, in: Chance and Matter, eds., J. Souletie, J. Vannimenus, and R. Stora, Les Houches, Session XLVI 1986 (North-Holland, Amsterdam, 1987), p. 213.
[31] A. A. Abrikosov, L. P. Gor'kov, and I. E. Dzhyaloshinskii, Methods of Quantum Field Theory in Statistical Physics (Prentice-Hall, Englewood Cliffs, NJ, 1963).
[32] S. F. Edwards, Philos. Mag. 3 (1958) 1020.
[33] J. S. Langer and T. Neal, Phys. Rev. Lett. 16 (1966) 1984.
[34] L. P. Gor'kov, A. I. Larkin, and D. E. Khmelnitskii, JETP Lett. 30 (1979) 228.
[35] P. W. Anderson, E. Abrahams, and T. V. Ramakrishnan, Phys. Rev. Lett. 43 (1979) 718.
[36] B. L. Altshuler, A. G. Aronov, D. E. Khmelnitskii, and A. I. Larkin, in: Quantum Theory of Solids, ed., I. M. Lifshits (Mir Publishers, Moscow, 1982), p. 130.
[37] B. L. Altshuler and A. G. Aronov, in: Electron-Electron Interactions in Disordered Systems, eds., A. L. Efros and M. Pollak (North-Holland, Amsterdam, 1985), p. 1.
[38] P. A. Lee, J. Noncrystall. Solids 35 (1980) 21.
[39] S. Hikami, A. I. Larkin, and Y. Nagaoka, Prog. Theor. Phys. 63 (1980) 707.
[40] A. Kawabata, Solid State Commun. 34 (1980) 431; J. Phys. Soc. Jpn. 49 (1980)

628.
[41] B. L. Altshuler, A. G. Aronov, and D. E. Khmelnitskii, Sol. State Commun. 39 (1981) 619.
[42] P. M. Echternach et al., Phys. Rev. B 48 (1993) 11516; Phys. Rev. B 50 (1994) 5748.
[43] B. L. Altshuler, A. G. Aronov, and D. E. Khmelnitskii, J. Phys. C 15 (1982) 7367.
[44] B. L. Altshuler and A. G. Aronov, Solid State Commun. 39 (1979) 115.
[45] R. C. Dynes and J. P. Garno, Phys. Rev. Lett. 46 (1981) 137.
[46] B. Z. Spivak, unpublished; L. Levitov, unpublished.
[47] B. L. Altshuler and B. I. Shklovskii, Sov. Phys. JETP 64 (1986) 127.
[48] B. L. Altshuler and D. E. Khmelnitskii, JETP Lett. 42 (1985) 359.
[49] S. Washburn and R. A. Webb, Adv. Phys. 35 (1986) 375.
[50] F. J. Wegner, Z. Phys. B 35 (1979) 207.
[51] L. Schäfer and F. J. Wegner, Z. Phys. B 38 (1980) 113.
[52] K. B. Efetov, A. I. Larkin, and D. E. Khmelnitskii, Sov. Phys. JETP 52 (1980) 568.
[53] A. Houghton, A. Jevicky, R. D. Kenway, and A. M. M. Pruisken, Phys. Rev. Lett. 45 (1980) 394.
[54] K. Junglich and R. Oppermann, Z. Phys. B 38 (1980) 93.
[55] S. Hikami, Phys. Rev. B 24 (1981) 2671.
[56] A. J. MaKane and M. Stone, Ann. Phys. (NY) 131 (1981) 36.
[57] K. B. Efetov, Sov. Phys. JETP 82 (1982) 872.
[58] K. B. Efetov, Adv. Phys. 32 (1983) 53.
[59] S. F. Edwards and P. W. Anderson, J. Phys. F 5 (1975) 965.
[60] V. J. Emery, Phys. Rev. B 11 (1975) 239.
[61] J. J. M. Verbaarschot and M. R. Zirnbauer, J. Phys. A 17 (1985) 1093.
[62] J. J. M. Verbaarschot, H. A. Weidenmüller, and M. R. Zirnbauer, Phys. Rep. 129 (1985) 367.
[63] Y. V. Fyodorov, these proceedings .
[64] F. A. Berezin, Introduction to Superanalysis (Reidel, Dodrecht, 1987).
[65] A. Altland, S. Iida, and K. B. Efetov, J. Phys. A 26 (1993) 3545.
[66] V. N. Prigodin, B. L. Altshuler, K. B. Efetov, and S. Iida, Phys. Rev. Lett. 72 (1994) 546.
[67] N. Taniguchi, B. D. Simons, and B. L. Altshuler, preprint .
[68] A. M. M. Pruisken, Nucl. Phys. B 235 (1984) 277; H. Levine, S. Libby, and A. A. M. Pruisken, Nucl. Phys. B 240 (1985) 30, 49, 71.
[69] H. A. Weidenmüller, Nucl. Phys. B 290 (1987) 87; H. A. Weidenmüller and M. R. Zirnbauer, Nucl. Phys. B 305 (1988) 339.
[70] D. E. Khmelnitskii, JETP Lett. 38 (1983) 552.
[71] A. M. Polyakov, Phys. Lett. B 59 (1975) 79.
[72] E. Brezin and J. Zinn-Justin, Phys. Rev. B 14 (1976) 3110.
[73] F. J. Wegner, Nucl. Phys. B 316 (1989) 663.
[74] S. Hikami, Prog. Theor. Phys. 107 (1992) 213.
[75] J. T. Chayes, L. Chayes, D. S. Fisher, and T. Spencer, Phys. Rev. Lett. 57 (1986) 299.
[76] A. MacKinnon and B. Kramer, Z. Phys. B 53 (1983) 1.
[77] V. E. Kravtsov, I. V. Lerner, and V. I. Yudson, Sov. Phys. JETP 94 (1988) 259; Phys. Lett. A 134 (1989) 245.
[78] B. L. Altshuler, V. E. Kravtsov, and I. V. Lerner, in: Mesoscopic Phenomena in

Solids, eds., B. L. Altshuler, P. A. Lee, and R. A. Webb (North-Holland, Amsterdam, 1991), p. 449.
[79] M. A. Kastner, Rev. Mod. Phys. 64 (1992) 849; Physics Today 46 (1993) 24
[80] L. P. Gor'kov and G. M. Eliashberg, Sov. Phys. JETP 21 (1965) 940.
[81] B. D. Simons and B. L. Altshuler, Phys. Rev. Lett. 70 (1993) 4063.
[82] M. R. Zirnbauer, Nucl. Phys. B[FS] 265 (1986) 375.
[83] V. E. Kravtsov and M. R. Zirnbauer, Phys. Rev. B 46 (1992) 4332.
[84] E. Akkermans and G. Montambaux, Phys. Rev. Lett. 68 (1992) 642.
[85] O. Bohigas, in: Chaos and Quantum Physics, eds., M. -J. Gianonni, A. Voros, and J. Zinn-Justin, Les Houches, Session LII 1989 (North-Holland, Amsterdam, 1991), p. 91.
[86] E. P. Wegner, Ann. Math. 53 (1953) 36.
[87] B. D. Simons, P. A. Lee, and B. L. Altshuler, Phys. Rev. Lett. 70 (1993) 4122.
[88] B. D. Simons, P. A. Lee, and B. L. Altshuler, Nucl. Phys. B 409 (1993) 487.
[89] F. Haake, Signatures of Quantum Chaos (Springer, Berlin, 1991).
[90] U. Smilansky, these proceedings .
[91] Y. G. Sinai, Funct. Anal. Appl. 2 (1968) 61,245; Russ. Math. Surveys 25 (1970) 137.
[92] B. D. Simons and B. L. Altshuler, Phys. Rev. B 48 (1993) 5422.
[93] M. Faas, B. D. Simons, X. Zotos, and B. L. Altshuler, Phys. Rev. B 48 (1993) 5439.
[94] J. Zakrzewski and D. Delande, Phys. Rev. E 47 (1993) 1650.
[95] B. D. Simons et al., Phys. Rev. Lett. 71 (1993) 2899.
[96] A. D. Stone, these proceedings .
[97] A. Szafer and B. L. Altshuler, Phys. Rev. Lett. 70 (1993) 587.
[98] M. C. Gutzwiller, Chaos in Classical and Quantum Mechanics (Springer-Verlag, New York, 1990).
[99] M. V. Berry, in: Chaos and Quantum Physics, eds., M. -J. Gianonni, A. Voros, and J. Zinn-Justin, Les Houches, Session LII 1989 (North-Holland, Amsterdam, 1991), p. 251.
[100] J. Keating, these proceedings .
[101] M. V. Berry and J. P. Keating, J. Phys. A 27 (1994) 6167.
[102] J. H. Hannay and A. M. O. de Almeida, J. Phys. A 17 (1984) 3429.
[103] M. V. Berry and M. Robnik, J. Phys. A 19 (1986) 649, 669.
[104] A. Pandey and M. L. Mehta, Commun. Math. Phys. 16 (1983) 2655; M. L. Mehta and A. Pandey, J. Phys. A 16 (1983) 2655,L601.
[105] N. Taniguchi, A. Hasimoto, B. D. Simons, and B. L. Altshuler, Europhys. Lett. 27 (1994) 335.
[106] U. Sivan and F. P. Milliken and K. Milkove and S. Rishton and Y. Lee and J. M. Hong and V. Boegli and D. Kern and M. de Franza, Europhys. Lett. 25 (1994) 605.
[107] A. Kamenev and D. Braun, J. Phys. I (France) 4 (1994) 1049.
[108] N. Taniguchi, A. V. Andreev, and B. L. Altshuler, Europhys. Lett. in press.
[109] N. Taniguchi and B. L. Altshuler, Phys. Rev. Lett. 71 (1993) 4031.
[110] M. V. Berry, in: Chaotic Behavior of Deterministic Systems, eds., G. Looss, R. Helleman, and R. Stora (North-Holland, New York, 1983), p. 171
[111] P. O'Conner, J. Gehlen, and E. J. Heller, Phys. Rev. Lett. 58 (1987) 1296
[112] B. I. Shklovskii, JETP Lett. 36 (1982) 352.
[113] A. Kamenev and Y. Gefen, Phys. Rev. Lett. 70 (1993) 1976; Phys. Rev. B 49

(1994) 14474; A. Kamenev, B. Reulet, H. Bouchiat, and Y. Gefen, Europhys. Lett. in press; B. Reulet and H. Bouchiat, Phys. Rev. B in press.
[114] B. Spivak, F. Zhou, and T. M. Beal-Monod, Phys. Rev. B in press.
[115] M. Wilkinson, J. Phys. A 21 (1988) 4021.
[116] N. Taniguchi and B. L. Altshuler, unpublished .
[117] R. Jalabert, A. D. Stone, and Y. Alhassid, Phys. Rev. Lett. 68 (1992) 3468.
[118] V. N. Prigodin, K. B. Efetov, and S. Iida, Phys. Rev. Lett. 71 (1993) 1230.
[119] K. B. Efetov, Phys. Rev. Lett. 70 (1993) 1315.
[120] V. I. Fal'ko and K. B. Efetov, Preprint (1994).
[121] V. N. Prigodin, Preprint (1994).
[122] A. Kudrolli, V. Kidambi, and S. Shridar, Preprint (1994).
[123] V. N. Prigodin, N. Taniguchi, A. Kudrolli, V. Kidambi, and S. Shridar, Preprint (1995).
[124] F. J. Dyson, J. Math. Phys. 3 (1962) 140, 157, 166; F. J. Dyson and M. L. Mehta, J. Math. Phys. 4 (1963) 701.
[125] P. Pechukas, Phys. Rev. Lett. 51 (1983) 943.
[126] T. Yukawa, Phys. Rev. Lett. 54 (1985) 1883.
[127] P. Gaspard, S. A. Rice, and K. Nakamura, Phys. Rev. Lett. 63 (1989) 930.
[128] P. Gaspard, S. A. Rice, H. J. Mikeska, and K. Nakamura, Phys. Rev. A 42 (1990) 4015.
[129] D. Saher, P. Gaspard, and P. Gaspard, Phys. Rev. A 44 (1991) 7841.
[130] E. Austin and M. Wilkinson, Nonlinearity 5 (1992) 1137.
[131] T. Takami and H. Hasegawa, Phys. Rev. Lett. 68 (1992) 419.
[132] C. W. J. Beenakker, Phys. Rev. Lett. 70 (1993) 4126.
[133] O. Narayan and B. S. Shastry, Phys. Rev. Lett. 71 (1993) 2106.
[134] K. Nakamura and M. Lakshamanan, Phys. Rev. Lett. 57 (1986) 1661.
[135] E. Brezin, C. Itzykson, G. Parisi, and J. Zuber, Commun. Math. Phys. 59 (1978) 35.
[136] B. Sutherland, J. Math. Phys. 12 (1971) 246, 251; Phys. Rev. A 4 (1971) 2019, Phys. Rev. A 5 (1972) 1372.
[137] F. Calogero, J. Math. Phys. 10 (1969) 2191, 2197.
[138] F. David, Nucl. Phys. B 257 (1985) 45,543.
[139] V. A. Kazakov, Phys. Lett. B 150 (1985) 282.
[140] E. Brezin and A. Zee, Nucl. Phys. B [FS] 402 (1993) 613.
[141] Z. Ha, Phys. Rev. Lett 73 (1994) 1574.
[142] J. M. Luttinger, J. Math. Phys. 15 (1963) 609.
[143] E. H. Lieb and D. C. Mattis, Mathematical Physics in One-Dimension (Academic, New York, 1966).
[144] K. B. Efetov and A. I. Larkin, Sov. Phys. JETP 42 (1975) 390.
[145] F. D. M. Haldane, Phys. Rev. Lett. 47 (1981) 1840.
[146] A. R. Its, A. G. Izergin, V. E. Korepin, and N. A. Slavnov, Int. J. Mod. Phys. B 4 (1990) 1003.
[147] F. D. M. Haldane, in: Proceedings of the International Colloquium in Modern Field Theory (Tata Institute, Bombay, India, 1994).
[148] E. R. Mucciolo, B. S. Shastry, B. D. Simons, and B. L. Altshuler, Phys. Rev. B 49 (1994) 15197.
[149] Y. Imry, Introduction to Mesoscopic Systems; these proceedings
[150] A. D. Stone and P. A. Mello and K. A. Muttalib and J. -L. Pichard, in: Mesoscopic Phenomena in Solids, eds., B. L. Altshuler, P. A. Lee, and R. A. Webb (North-

Holland, Amsterdam, 1991), p. 369.
[151] C. W. J. Beenakker and H. Van Houten, Quantum Transport in Semiconducting Nanostructures, Solid State Physics (Academic Press, New York) 44 (1991) p. 1
[152] J. B. Pendry, Adv. Phys. in press
[153] A. M. Finkelshtein, Sov. Sci. Rev. A Phys. 14 (1990) 1.
[154] D. Belitz and T. R. Kirkpatrick, Rev. Mod. Phys. 66 (1994) 261.
[155] V. E. Kravtsov, I. V. Lerner, B. L. Altshuler, and A. G. Aronov, Phys. Rev. Lett. 72 (1994) 888; A. G. Aronov, V. E. Kravtsov, and I. V. Lerner, JETP Lett. 59 (1994) 40.
[156] V. E. Kravtsov and A. D. Mirlin, Preprint .
[157] Y. Fyodorov and A. D. Mirlin, Preprint .